AFRL-RH-WP-TR-2008-0066

Wavelet-Based Signal Processing for Monitoring Discomfort and Fatigue

Cristhian Potes
Ricardo von Borries
Cristiano Jacques Miosso

University of Texas at El Paso
500 W University Ave
El Paso TX 79968-0001

June 2008
Final Report for September 2006 to May 2008

Air Force Research Laboratory
Human Effectiveness Directorate
Biosciences and Protection Division
Biomechanics Branch
Wright-Patterson AFB OH 45433-7947

NOTICE AND SIGNATURE PAGE

Using Government drawings, specifications, or other data included in this document for any purpose other than Government procurement does not in any way obligate the U.S. Government. The fact that the Government formulated or supplied the drawings, specifications, or other data does not license the holder or any other person or corporation; or convey any rights or permission to manufacture, use, or sell any patented invention that may relate to them.

This report was cleared for public release by the 88th ABW Public Affairs Office and is available to the general public, including foreign nationals. Copies may be obtained from the Defense Technical Information Center (DTIC) (http://www.dtic.mil).

THIS REPORT HAS BEEN REVIEWED AND IS APPROVED FOR PUBLICATION IN ACCORDANCE WITH ASSIGNED DISTRIBUTION STATEMENT.

AFRL-RH-WP-TR-2008-0066

_____//signed//_____
Nathan Wright, Work Unit Manager
Biomechanics Branch

_____//signed//_____
MARK M. HOFFMAN, Deputy Chief
Biosciences and Protection Division
Human Effectiveness Directorate
Air Force Research Laboratory

This report is published in the interest of scientific and technical information exchange, and its publication does not constitute the Government's approval or disapproval of its ideas or findings.

REPORT DOCUMENTATION PAGE

Form Approved
OMB No. 074-0188

PLEASE DO NOT RETURN YOUR FORM TO THE ABOVE ADDRESS.

1. REPORT DATE (DD-MMM-YYYY)	2. REPORT TYPE	3. DATES COVERED (From – To)
June 2008	Final Report	September 2006 – May 2008

4. TITLE AND SUBTITLE

Wavelet-Based Signal Processing for Monitoring Discomfort and Fatigue

5a. CONTRACT NUMBER
FA8650-06-1-6748

5b. GRANT NUMBER

5c. PROGRAM ELEMENT NUMBER
62202F

6. AUTHOR(S)

Cristhian Potes
Ricardo von Borries
Cristiano Jacques Miosso

5d. PROJECT NUMBER
7184

5e. TASK NUMBER
02

5f. WORKUNIT NUMBER
71840219

7. PERFORMING ORGANIZATION NAME(S) AND ADDRESS(ES)
University of Texas at El Paso
500 W University Ave
El Paso TX 79968-0001

8. PERFORMING ORGANIZATION REPORT NUMBER

9. SPONSORING / MONITORING AGENCY NAME(S) AND ADDRESS(ES)
Air Force Materiel Command
Air Force Research Laboratory
Human Effectiveness Directorate
Biosciences and Protection Division
Biomechanics Branch
Wright-Patterson AFB OH 45433-7947

10. SPONSOR / MONITOR'S ACRONYM
AFRL/RHPA

11. SPONSOR/MONITOR'S REPORT NUMBER(S)
AFRL-RH-WP-TR-2008-0066

12. DISTRIBUTION / AVAILABILITY STATEMENT
Approved for public release; distribution is unlimited.

13. SUPPLEMENTARY NOTES
88ABW/PA cleared 4Aug08, WPAFB-08-4987.

14. ABSTRACT
Muscle fatigue involves both a decrease in the frequency and increase in the amplitude of a surface electromyographic (SEMG) signal. Muscle fatigue is also related to a decrease of the force impeding to reach the same initial level of the maximum voluntary contraction (MVC). To determine indices of muscle fatigue, a method is proposed to estimate both the instantaneous frequency (IF) and the instantaneous amplitude (IA) by decomposing the SEMG signal using a filter bank. A linear regression model was adopted to compute the IF and IA slopes. These slopes were then classified in muscle increase force, recovery, muscle decrease force and fatigue by using a joint analysis of frequency and amplitude. SEMG signals were recorded from 26 normal human subjects when doing an exertion of 70% and 100% of their MVC during a session of eight hours. It was found that slopes derived from the proposed filter bank are equivalent to those slopes derived from the spectrogram and the smoothed pseudo Wigner-Ville distribution. Furthermore, slopes derived from the filter bank indicated that they can be used as indices to determine muscle fatigue. These results were confirmed by correlating indices of muscle fatigue with perceived levels of discomfort reported by the subjects after performing an exertion of 70% MVC in hours two, four, and six.

15. SUBJECT TERMS

16. SECURITY CLASSIFICATION OF:			17. LIMITATION OF ABSTRACT	18. NUMBER OF PAGES	19a. NAME OF RESPONSIBLE PERSON:
a. REPORT	b. ABSTRACT	c. THIS PAGE			Nathan Wright
U	U	U	SAR	96	19b. TELEPHONE NUMBER *(Include area code)*

Standard Form 298 (Rev. 8/98)
Prescribed by ANSI Std. Z39-18

THIS PAGE IS INTENTIONALLY LEFT BLANK

Contents

List of Figures

List of Tables

Preface

The authors would like to acknowledge the Air Force Research Laboratory, Human Effectiveness Directorate, for supporting this research (contract number FA8650-06-1-6748). In particular, the authors would like to acknowledge personnel in the Wright-Patterson Air Force Base, Drs. Zhiging Cheng and Ted Knox for helping with the electromyographic data set and providing important feedback along the project. A special thank you also goes to Mr. Nathan Wright, the Contract Monitor for this project. Mr. Wright's suggestions and constant supervision were essential for the successful conclusion of this project. This AFRL project opened new areas of research for students and faculty from the University of Texas at El Paso, UTEP.

THIS PAGE IS INTENTIONALLY LEFT BLANK

1

Theoretical Background

1.1 Introduction

A method for computing indices of muscle fatigue is introduced by decomposing the surface electromyographic (SEMG) signal using a filter bank and estimating from the subbands of the filter bank both by the instantaneous frequency (IF) and the instantaneous amplitude (IA). These time dependent parameters are then used to compute indices of muscle increase force, recovery, decrease force and fatigue.

Surface electromyographic signals have been proposed as a potential tool to detect and measure muscle fatigue [8], [11], [13], [3]. Specifically, muscle fatigue involves a decrease in the maximum force and a measurable shift in the power spectrum of the SEMG signal, which is commonly reported to occur toward lower frequencies [15], [20], [16], although there are fewer reports of increased frequencies [16]. Consequently, the mean frequency, median frequency, and IF have been extensively used in the assessment of muscle fatigue as indicators of how the frequency of the SEMG signal changes over time [20], [25], [30], [19]. Additionally, muscle fatigue also involves an increase in the SEMG signal's amplitude [15], [20], [32], [9]. The root mean square, the average rectified value, and a recent technique introduced by Merletti [21], [15], [19], [27] have been proposed as amplitude estimators of the SEMG signal, that can then be used as an additional input to the analysis of muscle fatigue.

When considering changes in the frequency and amplitude of the SEMG signal to investigate muscle fatigue, the level of stationarity of the signal should be considered. Different analysis techniques have been found appropriate for assessment of muscle fatigue, but they are dependent on the level of stationarity [9], [12], [25], [11]. The SEMG signal is considered wide-sense stationary when recorded during isometric constant force contractions over time intervals lasting from one to two seconds [21]. In contrast the SEMG signal is considered non-stationary when recorded during dynamic contractions. Non-stationarities of the SEMG signal can be classified as slow or fast [4].

Time-frequency (TF) distributions from the Cohen class and wavelets have demonstrated to be useful approaches in the analysis of SEMG signals with static and dynamic muscle contractions [8], [12], [25], [11], [4], [13], [3]. The spectrogram is an example of TF distributions that has been used in the analysis of static and dynamic muscle contractions with low to medium non-stationarities [32], [9]. The objective of TF distributions and wavelets in this context is to provide information about how the energy of the signal is distributed over time and frequency. In

most cases, they have been used to estimate the frequency but not the amplitude. An exception is the work by Luttman [20], [19], which introduces a joint analysis of spectrum and amplitude (JASA) of SEMG signals. During this research, JASA is referred as a joint analysis of frequency and amplitude.
In order to assess muscle fatigue, the IF and the IA from the subband components of SEMG signals are estimated and decomposed with a 32-channel cosine modulated filter bank. The SEMG signals provided by the Air Force Research Laboratory (AFRL) were recorded from 26 healthy human subjects during prolonged wear of weighted flight helmets. A linear regression model is adopted to compute the slopes from the IF and IA estimates. The slopes derived from the filter bank are then compared with the slopes derived from the spectrogram and the smoothed pseudo Wigner-Ville distribution (SPWVD). Finally, the slopes are used as indices of muscle increase force, recovery, decrease force and fatigue, and are correlated to perceived levels of discomfort reported by the subjects.

1.2 Overview

An extensive search of the literature shows that, according to most researchers, in muscle fatigue there is a shift of the total power spectrum of the SEMG signal toward lower frequencies because the conduction velocity of the motor actions potentials on the muscle membrane decreases. Spectral variables such as the mean frequency (MNF), the median frequency (MF) and the instantaneous frequency (IF) have been extensively proposed to measure this shift in the power spectrum. However, it is still unclear which spectral variable is the best in terms of detecting this shift. For instance some authors state that the MF is preferred since it is less sensitive to noise. Rather, others state that the MNF is more stable and sensitive to changes in the underlying spectrum [20]. Also, it has been proposed that in the assessment of muscle fatigue one should analyze changes in both the power spectrum and the amplitude of the SEMG signal [15], [20], [16], [19], [32] [9].
In the literature different techniques are found to estimate spectral variables (MNF, MF and IF) and the amplitude of the SEMG signal. A classical method for estimating the MNF and the MF is explained in [15], [20], [19], [32], [9]. First, the SEMG signal is divided into equal segments (epochs) with a duration of 500 ms or 1 s. If the signal is non-stationary, then the SEMG signal is divided into epochs of 250 ms or 500 ms [9]. On the other hand, if the signal is highly non-stationary, then the signal is divided into epochs shorter than 125 ms. Some authors suggest an overlap in the epochs of 50% to reduce the variance [20]. However, epoch overlapping is not recommended since it increases the computational time without providing significant improvement of the quality of the estimates [9].
After the SEMG signal is divided into different epochs, the power spectral density (PSD) of the

epoch is then estimated by applying the absolute value squared of the fast Fourier transform (FFT). The MNF and the MF of a SEMG signal can be estimated as

$$MNF = \frac{\int_{-\infty}^{\infty} f(S(f))^2 df}{\int_{-\infty}^{\infty} (S(f))^2 df}, \tag{1.1}$$

$$MF = \frac{1}{2} \int_{0}^{\infty} (S(f))^2 df, \tag{1.2}$$

where $S(f)$ is the estimated PSD of the SEMG signal $s(t)$, and f is the frequency variable. Finally, the amplitude of the SEMG signal can be estimated from each epoch as

$$RMS = \sqrt{\frac{1}{T} \int_{\frac{-T}{2}}^{\frac{T}{2}} s(t)^2 dt}, \tag{1.3}$$

$$ARV = \frac{1}{T} \int_{\frac{-T}{2}}^{\frac{T}{2}} |s(t)| dt, \tag{1.4}$$

where T is the length of the interval where the SEMG signal $s(t)$ is analyzed [15], [19], [32] [9]. Another technique in the literature regarding the estimation of spectral variables (MNF, MF, and amplitude) is the use of time-varying autoregressive models (TVAR). SEMG signals can be represented using an autoregressive (AR) model with parameters changing with time. Thus, the time-varying spectrum can be estimated from the time-varying model parameters, and the IF of the non-stationary signal can be extracted [31], [33]. Furthermore, the selection of the model order for an AR is not critical, and an order of 10 seems to be appropriate for epochs of 125ms, 250ms, 500ms, and 1s [9]. TVAR can be used to monitor the muscle fatigue development during isometric contraction [33], [31].

Some authors propose to estimate the IF by computing the first derivative of the phase of the Hilbert transform of a signal [10]. However, other authors point out that the IF derived from this method is meaningful just for monocomponent signals. In the case of multicomponent signals such as the SEMG signals, one would obtain at some points negative frequencies and frequencies outside the bandwidth of the signal [30]. As a result this method is not suggested to estimate the IF of SEMG signals. An alternative solution to this issue is proposed in [30] and [10]. In [30], a technique known as the Hilbert-Huang transform (HHT) is proposed. The HHT is based on decomposing the SEMG signal into a set of intrinsic mode functions in such a way that they may be Hilbert transformed. It is concluded that the HHT is the best choice in the analysis of muscle fatigue, and that wavelets are lowest in performance after a comparison of the slopes derived from HHT, TVAR, and wavelets. The other solution given in [10] proposes to extract the IF from an adaptive TF distribution of the signal. This adaptive TF distribution is obtained by decomposing the signal into components with good TF localizations and combining the Wigner distribution of

the components. Hence, the proposed TF distribution is free of cross terms, positive, and with good TF localization.

Recently, TF analysis has been adopted in the analysis of both stationary and non-stationary electromyographic signals. The fact that spectral variables can be extracted from a TF distribution makes this an interesting distribution in the assessment of muscle fatigue. In the literature different approaches to estimate a TF distribution is found. Included among them are the Wigner-Ville distribution (WVD), the short-time Fourier transform (STFT) or spectrogram, the Choi-Williams distribution (CWD), the smoothed pseudo Wigner-Ville distribution (SPWVD), and wavelets. A comparison of the WVD, spectrogram, SPWVD and CWD is attained in [4], [3], [8] and [1]. The results show that the WVD is an efficient tool in the analysis of monocomponent signals; however, its performance in the analysis of multi-component signals is negatively affected by cross terms in the estimates of the spectral variables. The spectrogram is restricted by the fact that a good localization in time leads to a poor localization in frequency and vice-versa; furthermore, it assumes the analyzed signal to be stationary inside each considered fixed time window, which is not true in the case of dynamic contractions. Regarding the SPWVD, it destroys components of the signal in the rejection of the cross terms and also employs fixed time and frequency windows. Finally, the CWD seems to be very effective in decreasing the effects of cross terms and in retaining most of the useful properties of a TF distribution; however, it does not dramatically improve the results with respect to the SPWVD in terms of better peak tracking capabilities.

Wavelet and Wavelet packets (WP) have been recently introduced in the analysis of muscle fatigue [18], [14], [12], [25], [29], [11], [13], [27]. For instance it may be possible to assess muscle fatigue by determining the wavelet decomposition of the signal with the wavelets Sym4 or Sym5 and eight or nine levels of iterations in the decomposition [18]. In addition, some authors have proposed to estimate the MNF of a SEMG signal by using WP. By comparing (1) MNF curves derived from WP with (2) MNF curves obtained from STFT, it is inferred that both (1) and (2) exhibit qualitatively similar shapes and trends [25]. WP does not show cross terms as does the WVD and has the advantage, compared to the traditional TF distributions, of being the only one that allows selecting the frequency range of interest [29].

A comparison of the STFT, the CWD, the WVD, and the continuous wavelet transform (CWT) is performed in [11] and [13]. In this comparison it is inferred that the STFT is affected in time or in frequency resolution by the choice of the time window. It is also concluded that the WVD is disturbed by cross terms affecting the estimation of the frequency. Moreover, the CWD is the most suitable method to represent non-stationary SEMG signals; however, its use requires careful selection of the parameters in the kernel which should be adapted to each specific signal. Finally, the CWT is very reliable for the analysis of non-stationary signals, the IF estimates based on the CWT are less noisy than the other techniques, and the CWT does not require any smoothing

function. The main drawback of the CWT is that it is computationally expensive and requires large storage requirements. Discrete wavelet transform (DWT) is proposed to overcome this issue [18], [14], [12], [25], [29].
All the analyzed papers regarding the assessment of muscle fatigue by using wavelets and WP have focused in analyzing just changes in the frequency of the SEMG signal over time, yet the amplitude of the SEMG signal has been disregarded.
One of the characteristics of muscle fatigue is a decrease in the frequency and an increase in the amplitude of the SEMG signal. By using a linear regression model, slopes can be computed to measure the decrease or increase rate of the estimated frequency and amplitude over time [15], [20], [30], [19], [27], [32], [9]. A joint analysis of frequency and amplitude is proposed to classify the slopes into four stages: (1) increase force when both the frequency and the amplitude slopes increase over time, (2) recovery when the frequency slopes increase and the amplitude slopes decrease, (3) decrease force when both the frequency and the amplitude slopes decrease over time, or (4) fatigue when the frequency slopes decrease and the amplitude slopes increase [20], [19]. Although a joint analysis of frequency and amplitude seems to be suitable to identify muscle fatigue, a relationship is not yet known between the decrease rate of the frequency and the increase rate of the amplitude, and the intensity of fatigue that is felt by the subject. Additionally, the time interval to compute the slopes is also unknown. Some papers compute the slopes from the whole set of the estimated IF and IA while others compute the slopes on segments of 20s, 40s or 50s of the estimated IF and IA [30], [19], [27], [32], [9].

1.3 Desired Characteristics of a Time-Frequency (TF) Distribution in the Analysis of SEMG Signals

Time-Frequency analysis is an important tool in the development of indices of muscle fatigue since the frequency and the amplitude of the SEMG signal can be extracted from a TF distribution. The analyzed papers have focused on the estimation of the frequency, yet they have disregarded the evolving of the amplitude over time. In this research both the frequency and amplitude are extracted from the spectrogram, the CWD, and the SPWVD. The evaluation of these techniques is based on the desired characteristics of a TF distribution mentioned below.

1.3.1 Time and Frequency Marginals

The time and frequency marginals of a joint TF distribution $P(t, \omega)$ of a signal $x(t)$ are respectively given by

$$P(t) = \int_{-\infty}^{\infty} P(t, \omega) df = |x(t)|^2 \tag{1.5}$$

and

$$P(\omega) = \int_{-\infty}^{\infty} P(t,\omega)dt = |X(\omega)|^2 = \left| \int_{-\infty}^{\infty} x(t)e^{-j\omega t}dt \right|^2, \tag{1.6}$$

where $X(\omega)$ is the Fourier transform of the signal $x(t)$, $P(t)$ is the time marginal, and $P(\omega)$ is the frequency marginal of the signal $x(t)$. If the TF distribution satisfies the time and frequency marginals, then according to (1.1) and (1.2) the time and frequency marginals must be, respectively, the instantaneous energy and the energy density spectrum of the analyzed signal.

1.3.2 Time and Frequency Finite Support

If a signal $x(t)$ is zero inside the time interval $[t_1, t_2]$, then a TF distribution satisfying $P(t,\omega) = 0$ for $t \in [t_1, t_2]$ is expected. Similarly, if the spectrum of a signal $x(t)$ is zero inside the frequency interval $[\omega_1.\omega_2]$, then a TF distribution satisfying $P(t,\omega) = 0$ for $\omega \in [\omega_1.\omega_2]$ is expected [6], [23].

1.3.3 Time and Frequency Localization

The time localization of a signal $x(t)$ at time t_0 is given by

$$x(t) = \delta(t - t_0) \Rightarrow P(t,\omega) = \delta(t - t_0),$$

and the frequency localization at frequency ω_0 is given by

$$X(\omega) = \delta(\omega - \omega_0) \Rightarrow P(t,\omega) = \delta(\omega - \omega_0)$$

[23].

1.3.4 Positivity

Wigner demonstrated that any bilinear distribution that satisfies the time and frequency marginals cannot always be positive; it must have regions of negative values for any signal. However, Cohen showed that there exist TF distributions that are not bilinear but are positive and satisfy the marginals. One of the advantages of having a TF distribution that is positive and satisfies the marginals is that the distribution also satisfies the time and frequency finite support [6].

1.3.5 Suppression of Cross Terms

Cross terms are artifacts or interference terms that are undesirable in the analysis of muscle fatigue because they negatively affect the estimation of the IF. These cross terms are introduced

by the bilinearity of some distributions such as the Wigner-Ville distribution. For instance, let a signal $x(t)$ be expressed as the sum of two parts $x_1(t) + x_2(t)$. The WVD of $x(t)$ is then given by

$$WVD(t,\omega) = WVD_{11}(t,\omega) + WVD_{22}(t,\omega) + WVD_{12}(t,\omega) + WVD_{21}(t,\omega),$$

where $WVD_{12}(t,\omega)$ and $WVD_{21}(t,\omega)$ are the cross-WVD. Therefore, the WVD of the sum of two signals is not the sum of the WVD of each signal. It also adds cross terms interfering with the analysis of the distribution.

1.3.6 Window Independence

The aim of introducing a TF window is to reduce cross terms and better localize the quick changes of the SEMG signal. However, these windows destroy desirable properties of a distribution such as the time and frequency marginals and time and frequency support. Furthermore, the choice of the size of the TF windows play an important role in the assumption of the stationarity of the SEMG signal as well as in a TF localization trade-off. A TF localization trade-off implies that a good localization in time leads to a poor localization in frequency and vice-versa.

1.3.7 Energy Conservation

The total energy of an ideal joint TF distribution should be the total energy of the signal $x(t)$ [6]

$$E = \int_{-\infty}^{\infty}\int_{-\infty}^{\infty} P(t,\omega)d\omega dt = \int_{-\infty}^{\infty} |x(t)|^2 dt = \int_{-\infty}^{\infty} |X(\omega)|^2 d\omega.$$

1.3.8 Instantaneous Frequency

The first order moment of frequency for a given time defines the IF of a signal $x(t)$ as

$$\phi(t) = \frac{\int_{-\infty}^{\infty} \omega P(t,\omega)d\omega}{\int_{-\infty}^{\infty} P(t,\omega)d\omega}. \tag{1.7}$$

If the signal is written in terms of its phase φ and amplitude A,

$$x(t) = A(t)e^{j\varphi(t)},$$

then it is straightforward to show that

$$\phi(t) = \frac{1}{2\pi}\frac{d}{dt}\varphi(t). \tag{1.8}$$

1.4 TF distributions

The following TF distributions are the most widely used in the analysis of muscle fatigue.

1.4.1 The Short-Time Fourier Transform (STFT) and the Spectrogram

The linear STFT is defined as the Fourier transform of subsequences (short segments) of a signal windowed in the time domain. As a result the STFT is a function of the time t and the frequency ω depending of the size of the window $h(t)$.

$$STFT(t,\omega) = \int x(\tau)h(\tau - t)e^{-j2\pi\omega\tau}d\tau,$$

where t is the shift of the time window. A time Gaussian window of size 128 samples is used in this research.

The spectrogram (squared magnitude of the STFT) is always positive, real, and computationally fast. However, due to the time window introduced by the STFT, the spectrogram does not satisfy the marginals as well as the TF support and the TF localization. The spectrogram suffers from a TF localization trade-off and assumes stationarities of the signal in short intervals of time given by the size of the window $h(t)$. The previous assumption of stationarity is true for SEMG signals with static contractions.

1.4.2 The Wigner-Ville Distribution (WVD)

The bilinear WVD distribution is defined as:

$$W(t,\omega) = \frac{1}{2\pi}\int x^*\left(t - \frac{1}{2}\tau\right)x\left(t + \frac{1}{2}\tau\right)e^{-j\tau\omega}d\tau,$$

where $*$ denotes the complex conjugate of a function. This distribution differs from the spectrogram in that: (1) it is not always positive, (2) it holds the time and frequency marginals, (3) it generates considerable amount of cross terms in the analysis of multicomponent signals, and (4) it is non local. The WVD, like the spectrogram, does not satisfy the time and frequency finite support. In addition, the WVD has not been used in the analysis of muscle fatigue since cross terms introduce errors in the estimation of the IF.

A bidimensional smoothing function (kernel) can be designed to convolve with the WVD. The aim of introducing this kernel is to make the WVD more local and to reduce the cross terms. Additionally, desirable properties can be accomplished by constraining the kernel function. The CWD and the SPWVD define two different kernels to make the WVD suitable in the analysis of muscle fatigue.

1.4.3 The Choi-Williams distribution (CWD)

The kernel for the CWD is defined as

$$\phi(\nu,\tau) = e^{-\frac{(\pi\nu\tau)^2}{2\sigma^2}}. \tag{1.9}$$

It is noticed that for this distribution when $\sigma \to +\infty$, the WVD is obtained. Likewise, the cross terms are almost zero when $\sigma \to 0$. The CWD satisfies the time and frequency marginals and localization, but it is still non positive and it does not satisfy the time and frequency finite support. However, its efficiency strongly depends on the choice of a critical parameter which has to be adapted according to the nature of the SEMG signal. The parameter σ was set to 1, and time and frequency Gaussian windows were set to 128 and 64 samples, respectively, for this research.

1.4.4 The Smoothed Pseudo Wigner-Ville Distribution (SPWVD)

It was shown before that the spectrogram is dependent on a short-time window yielding to a TF localization trade-off. In order to make the smoothing function more independent in both time and frequency, the SPWVD introduces a separable kernel function defined as

$$\phi(\nu,\tau) = g(\tau)H(\nu),$$

where $H(\nu)$ is a frequency smoothing window with $H(0)$ being forced to 1, and $g(\tau)$ is a smoothing time window with $g(0)$ being forced to 1. However, because of the introduction of the kernel, the time and frequency marginals of the WVD are not satisfied. The SPWVD is still non positive and does not hold the time and frequency finite support. Time and frequency Gaussian windows of lengths 128 and 64 samples, respectively, are used for this research.

1.5 Evaluation of the Time-Frequency (TF) Distributions

In this section a comparison of the spectrogram, WVD, CWD and SPWVD is made by estimating known parameters, the IF, and the IA of synthesized signals. Matlab functions from the TF toolbox downloaded from tftb.nongnu.org. are used to compute each TF distribution.

1.5.1 Tests with Known signals

The following eight experiments use known signals whose IF and IA values can be theoretically computed. These theoretical IF and IA values are compared with those values estimated from the Spectrogram, the WVD, the CWD, and the SPWVD. Based on these comparisons, the techniques that better estimate the IF and IA of known signals are selected to estimate the IF and IA of SEMG signals. The results of each experiment are shown at the end of this Chapter.

Experiment 1

Two sinusoids of different frequencies modulated in amplitude

Consider a signal which is the sum of two sinusoids of different frequencies and is modulated in amplitude by multiplying it by a ramp signal.

$$s(t) = At(\sin(2\pi f_1 t + \sin(2\pi f_2 t)) \tag{1.10}$$

where A is equal to 1, $f_1 = 100$ Hz and $f_2 = 150$ Hz. Knowing the frequency components of $s(t)$ is easy to compute the IF as $\hat{f} = \frac{f_1+f_2}{2} = 125$ Hz. The expected IA is a ramp function. See Figs. 1.1 and 1.2. The Matlab code to generate this signal is shown below.

```
Fs=1024; %sampling frequency
f1=100; % frequency of the first sinusoid
f2=150; % frequency of the second sinusoid
n=0:1/(Fs-1):1; % number of samples
s1=sin(2*pi*f1*n); % first sinosoid
s2=sin(2*pi*f2*n); % second sinusoid
s3=(s1+s2).*n; % sum of two sinusoids modulated in amplitude
```

Experiment 2

Two parallel chirp signals increasing in frequency and modulated in amplitude

A chirp signal is characterized by its frequency content changing with time and therefore, it is a non-stationary signal which is very important to analyze. Using the command `chirp` in Matlab, a composed signal is generated by adding two chirp signals. The first chirp signal has an IF going from 100 Hz to 150 Hz, and the second chirp signal has an IF going from 125 Hz to 175 Hz, both with 1024 samples. The expected instantaneous frequency of the added signals starts at 112.5 Hz and ends at 162.5 Hz. This signal is modulated in amplitude by multiplying it by a Gaussian signal. See Figs. 1.3 and 1.4. The Matlab code to generate this signal is shown below.

```
Fs=1024; % sampling frequency
n=0:1/(Fs-1):1; % number of samples
amp=amgauss(1024,512,256); % Gaussian signal centralized at
time sample 512
s1=chirp(n,100,1,150); % first chirp signal
s2=chirp(n,125,1,175); % second chirp signal
s=(s1+s2).*amp; % sum of two chirp signals modulated in amplitude
```

Experiment 3

Two crossed chirp signals increasing and decreasing in frequency, and modulated in amplitude

Using the command `chirp` in Matlab, a composed signal is generated adding two chirp signals. The first chirp signal has an IF going from 100 Hz to 300 Hz and the second chirp signal has an IF going from 300 Hz to 100 Hz, both with 1024 samples. The expected IF of the composed signal is a constant with a value of 200 Hz. This signal is modulated in amplitude by multiplying it by a Gaussian signal. See Figs. 1.5 and 1.6. The Matlab code to generate this signal is shown below.

```
Fs=1024; % sampling frequency
n=0:1/(Fs-1):1; % number of samples
amp=amgauss(1024,512,256); % Gaussian signal centralized at
time sample 512
s1=chirp(n,100,1,300); % first chirp signal
s2=chirp(n,300,1,100); % second chirp signal
s=(s1+s2).*amp; % sum of two chirp signals modulated in amplitude
```

Experiment 4

Chirp signal with increasing frequencies followed by a sinusoid and a Chirp signal with decreasing frequencies

Another chirp signal is computed with the following characteristics: (1) constant amplitude and linear frequency modulation varying from 100 Hz to 400 Hz in the interval $[0, 384]$ samples, (2) constant amplitude and constant frequency of 400 Hz in the interval $[385, 640]$ samples, and (3) constant amplitude and linear frequency modulation varying from 400 Hz to 100 Hz in the interval $[641, 1024]$ samples. See Figs. 1.7 and 1.8. The Matlab code to generate this signal is shown below.

```
Fs=1024; % sampling frequency
n=0:1/(Fs-1):1; % number of samples
s1=fmlin(384,0.1,0.4); % first signal linearly modulated in frequency
s2=fmlin(256,0.4,0.4); % second signal linearly modulated in frequency
s3=fmlin(384,0.4,0.1); % third signal linearly modulated in frequency
s=[s1;s2;s3]; % three signals modulated in frequency
```

Experiment 5

Four successive chirp signals increasing in frequency

Consider a signal with constant amplitude and linear frequency modulation varying from 100 Hz to 400 Hz in four time intervals of 256 samples each one. See Figs. 1.9 and 1.10. The Matlab code to generate this signal is shown below.

```
Fs=1024; % sampling frequency
n=0:1/(Fs-1):1; % number of samples
s1=fmlin(256,0.1,0.4); % first signal linearly modulated in frequency
s2=fmlin(256,0.1,0.4); % second signal linearly modulated in frequency
s3=fmlin(256,0.1,0.4); % third signal linearly modulated in frequency
s4=fmlin(256,0.1,0.4); % fourth signal linearly modulated in frequency
s=[s1;s2;s3;s4]; % four signals modulated in frequency
```

Experiment 6

Three atoms localized in frequency and time

An atom is an elementary waveform localized at a certain time and frequency over the TF plane. A linear combination of elementary atoms using the Matlab function `atoms` from the time-frequency toolbox downloaded from tftb.nongnu.org is generated. This experiment uses three atoms centralized in time and frequency according to: (1) atom 1 is centralized in time in the sample 64 with a duration of 100 samples and in frequency 200 Hz, (2) atom 2 is centralized in time in the sample 320 with a duration of 100 samples and in frequency 400 Hz, and finally (3) atom 3 is centralized in time in the sample 640 with a duration of 100 samples and in frequency 250 Hz. See Table 1.1 and Figs. 1.12 and 1.13. The ideal TF distribution of these three atoms is represented in the TF plane shown in Fig. 1.11.

Table 1.1 Description of the time-frequency localization of three atoms used in Experiment 6.

	Coordinates		
Atoms	**Time (samples)**	**Frequency (Hz)**	**Duration (samples)**
1	64	200	100
2	320	400	100
3	640	250	100

The Matlab code to generate this signal is shown below.

```
s=atoms(1024, [64,0.2,100,1;320,0.4,100,1;640,0.25,100,1]);
```

Experiment 7

Four atoms localized in frequency and time

This experiment uses four atoms centralized in time and frequency according to: (1) atom 1 is centralized in time in the sample 200 with a duration of 100 samples and in frequency 110 Hz, (2) atom 2 is centralized in time in the sample 200 with a duration of 100 samples and in frequency 330 Hz, (3) atom 3 is centralized in time in the sample 200 with a duration of 100 samples and in frequency 420 Hz, and finally (4) atom 4 is centralized in time in the sample 512 with a duration of 200 samples and in frequency 200 Hz. See Table 1.2 and Figs. 1.15 and 1.16. The ideal TF distribution of these four atoms is represented in the TF plane shown in Fig. 1.14.

The Matlab code to generate this signal is shown below.

```
s=atoms(1024,[200,0.11,100,1;200,0.33,100,1;200,0.42,100,1;
512,0.2,200,1]);
```

Table 1.2 Description of the time-frequency localization of four atoms used in Experiment 7.

	Coordinates		
Atoms	**Time (samples)**	**Frequency (Hz)**	**Duration (samples)**
1	200	110	100
2	200	330	100
3	200	420	100
4	512	200	200

Experiment 8

Five atoms localized in frequency and time

This experiment uses five atoms centralized in time and frequency according to: (1) atom 1 is centralized in time in the sample 200 with a duration of 100 samples and in frequency 110 Hz, (2) atom 2 is centralized in time in the sample 200 with a duration of 100 samples and in frequency 330 Hz, (3) atom 3 is centralized in time in the sample 200 with a duration of 100 samples and in frequency 420 Hz, (4) atom 4 is centralized in time in the sample 512 with a duration of 200 samples and in frequency 200 Hz, and finally (5) atom 5 is centralized in time in the sample 615 with a duration of 25 samples and in frequency 450 Hz. See Table 1.3 and Figs. 1.18 and 1.19. The ideal TF distribution of theses five atoms is represented in the TF plane shown in Fig. 1.17.

Table 1.3 Description of the time-frequency localization of five atoms used in Experiment 8.

	Coordinates		
Atoms	**Time (samples)**	**Frequency (Hz)**	**Duration (samples)**
1	200	110	100
2	200	330	100
3	200	420	100
4	512	200	200
5	615	450	25

The Matlab code to generate this signal is shown below.

```
s=atoms(1024,[200,0.11,100,1;200,0.33,100,1;200,0.42,100,1;
512,0.2,200,1]);
```

1.6 Evaluation of the Time-Frequency (TF) Distributions

This section presents the results after having compared the IF and IA values computed theoretically from the known signals with those IF and IA values estimated from the Spectrogram, the WVD, the CWD, and the SPWVD. According to Figs. 1.1, 1.3, 1.5, 1.7, 1.9, 1.12, 1.15, and 1.18 the WVD is not window dependent and gives the best TF resolution, but strongly presents cross terms. The spectrogram is time-window dependent and gives the worst TF resolutions but with negligible cross terms. Also, the SPWVD is window independent but allows to choose the best compromise between resolution and cross terms. In the theoretical experiments, it is shown in Figs. 1.2, 1.4, 1.6, 1.8, 1.10, 1.13, 1.16, and 1.19 that although the spectrogram and the SPWVD are window dependent and do not satisfy the TF finite support, they can give good estimations of the IF and the IA. In contrast the WVD and the CWD provide negative frequencies and assume frequencies that are outside the bandwidth of the analyzed signal. Table 1.4 summarizes the strengths and shortcomings of each evaluated TF distribution (spectrogram, WVD, CWD, SPWVD).

Table 1.4 Summary of strengths and shortcomings of the evaluated techniques.

Spectrogram	WVD	CWD	SPWVD
Advantages			
Fast to compute	Energy conservation	Energy conservation	Reduces cross terms
Positive	TF marginals	TF marginals	More local
	TF localization	TF localization	
	Finite time support	Reduces cross terms	
	Non-local	More local	
Disadvantages			
TF localization trade-off	Non-positive	Non-positive	Non-positive
Not satisfy TF marginals	Cross terms	Not satisfy TF support	TF localization trade-off
Not satisfy TF support	Negative IF	Negative IF	Not satisfy TF marginals
Assumes signal stationary			Not satisfy TF support

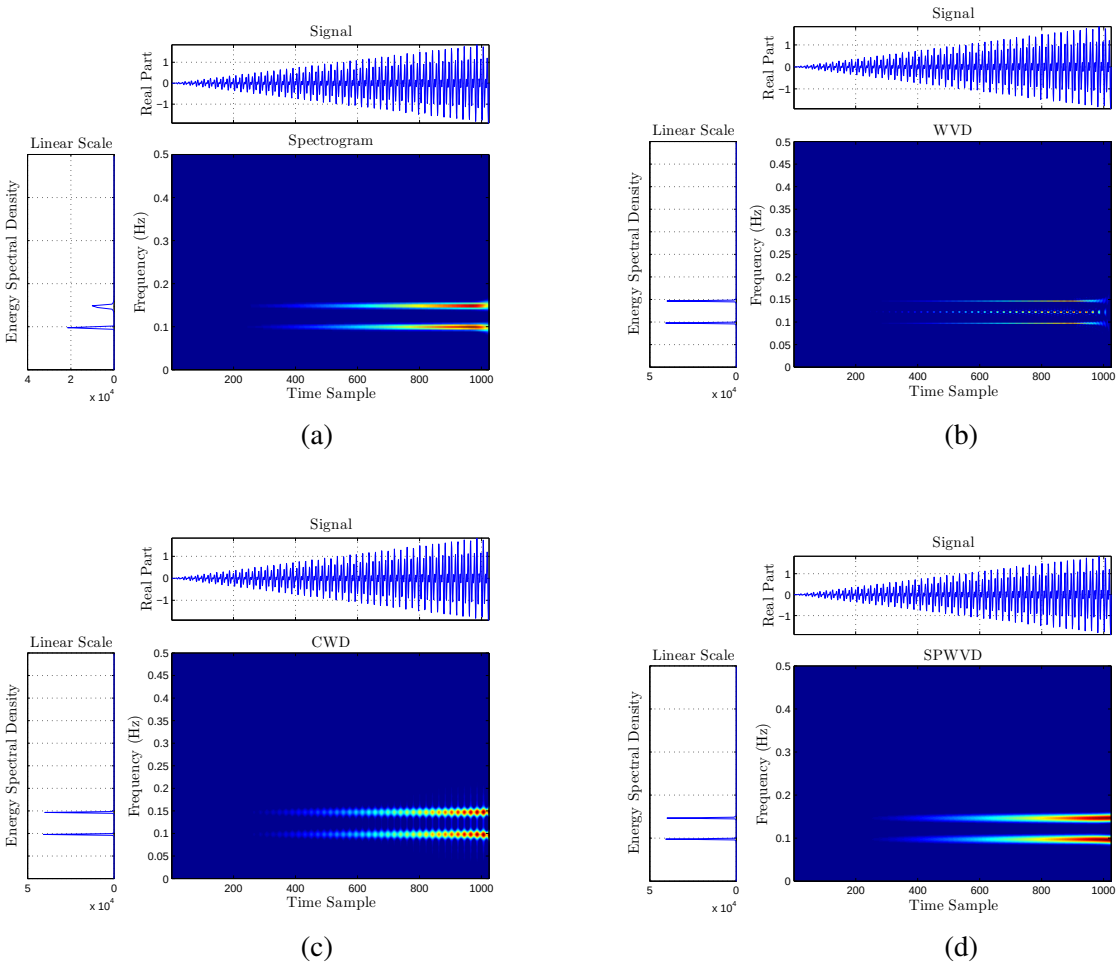

Figure 1.1 TF distributions of the signal in Experiment 1. Each TF distribution has a normalized frequency from 0 to 0.5. (a) Spectrogram with a time Gaussian window of length 128 samples. (b) WVD. It gives the best TF resolution but is affected by cross terms. (c) CWD with a time Gaussian window of length 128 samples, a frequency Gaussian window of length 64 samples, and parameter $\sigma = 1$, as defined in (1.9). (d) SPWVD with a time Gaussian window of length 128 samples and frequency Gaussian window of length 64 samples.

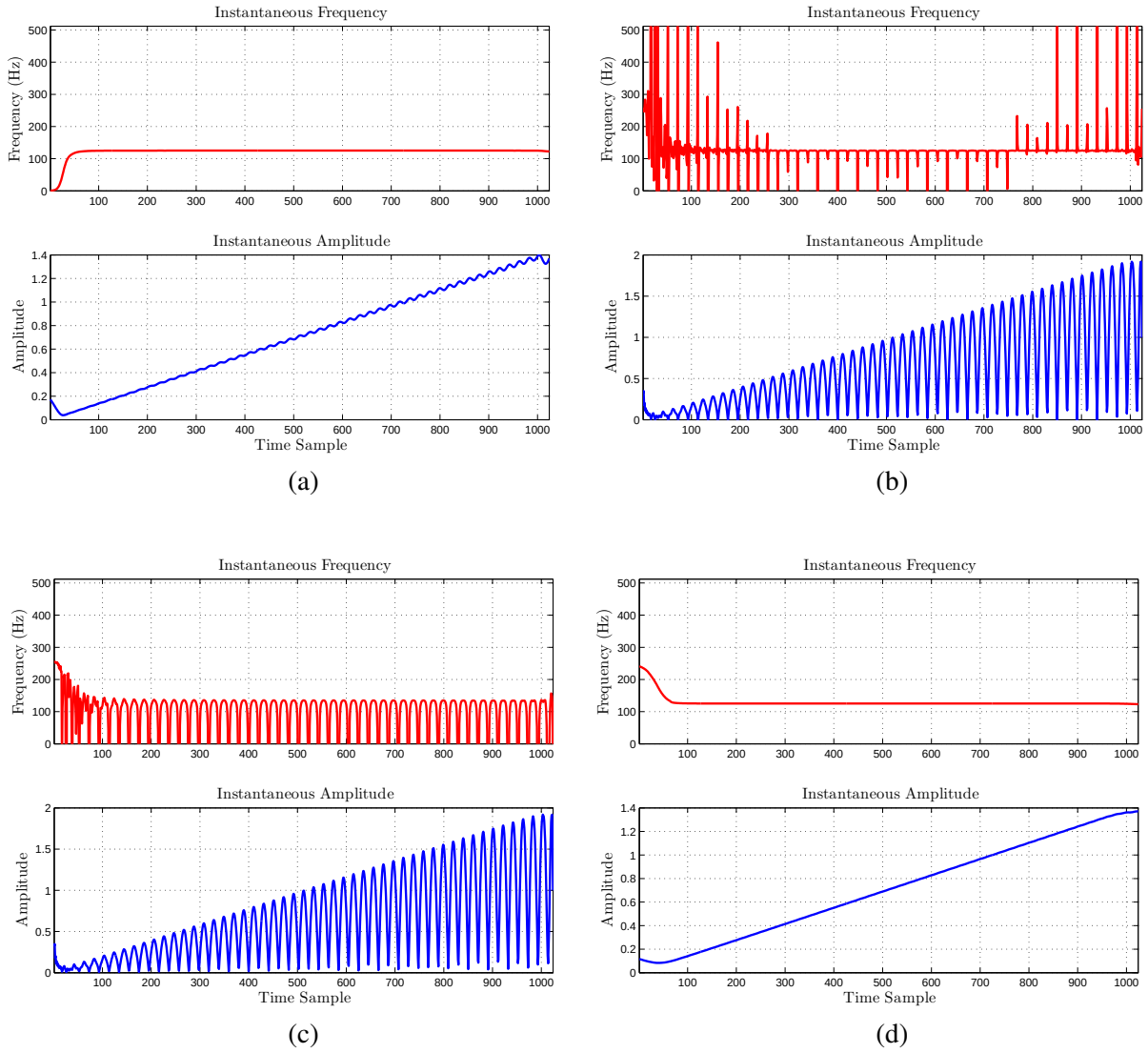

Figure 1.2 Computed IF and IA for Experiment 1. The expected IF is 125 Hz, and the expected IA is a ramp function. The WVD and the CWD provide negative IF and frequencies outside the bandwidth of the signal. (a) The spectrogram gives a good estimation of the IF and the IA. (b) The WVD gives a wrong estimation of the IF and a good estimation of the IA. (c) The CWD gives a wrong estimation of the IF and a good estimation of the IA. (d) The SPWVD gives a good estimation of the IF and the IA.

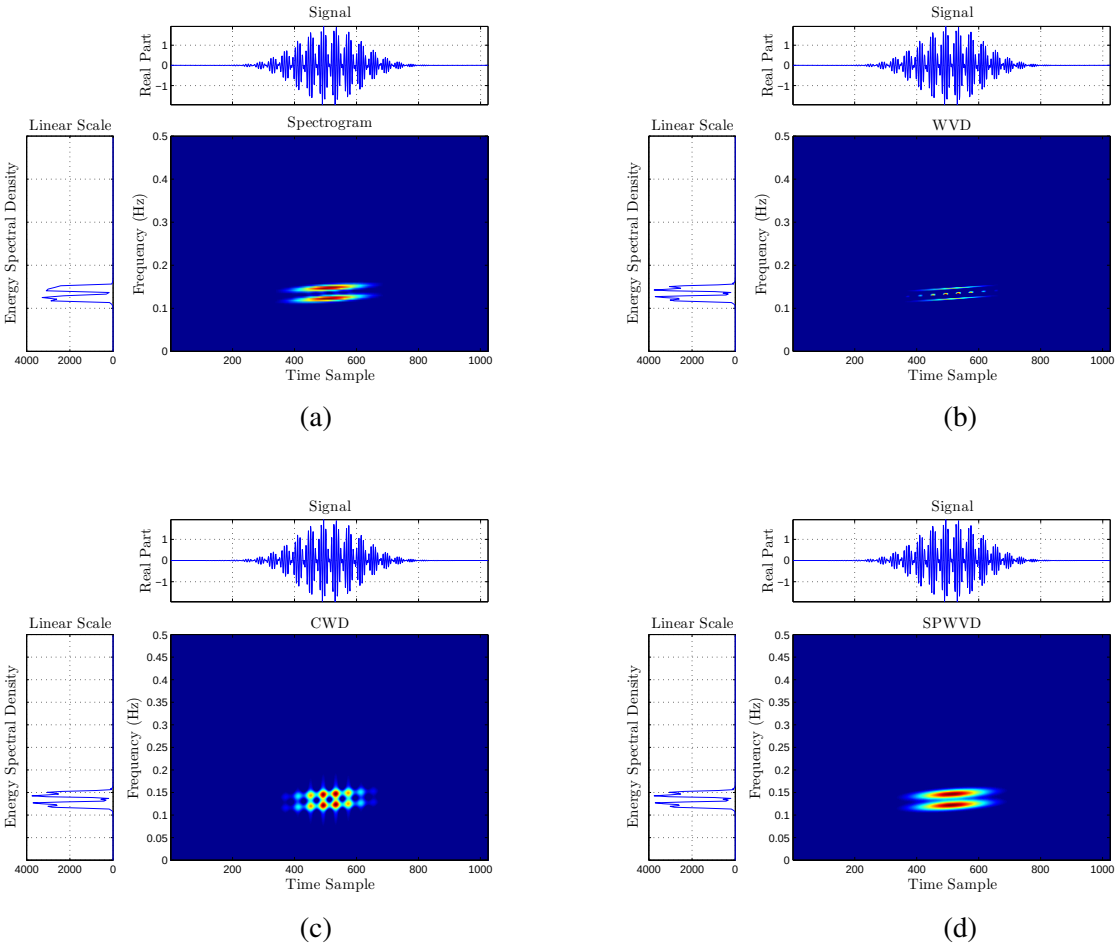

Figure 1.3 TF distributions of the signal in Experiment 2. Each TF distribution has a normalized frequency from 0 to 0.5. The region of support of the composed signal is in the time sample $[384, 640]$. (a) Spectrogram with a time Gaussian window of length 128 samples. (b) WVD. It gives the best TF resolution but is affected by cross terms. (c) CWD with a time Gaussian window of length 128 samples, frequency Gaussian window of length 64 samples, and parameter $\sigma = 1$, as defined in (1.9). (d) SPWVD with a time Gaussian window of length 128 samples and frequency Gaussian window of length 64 samples).

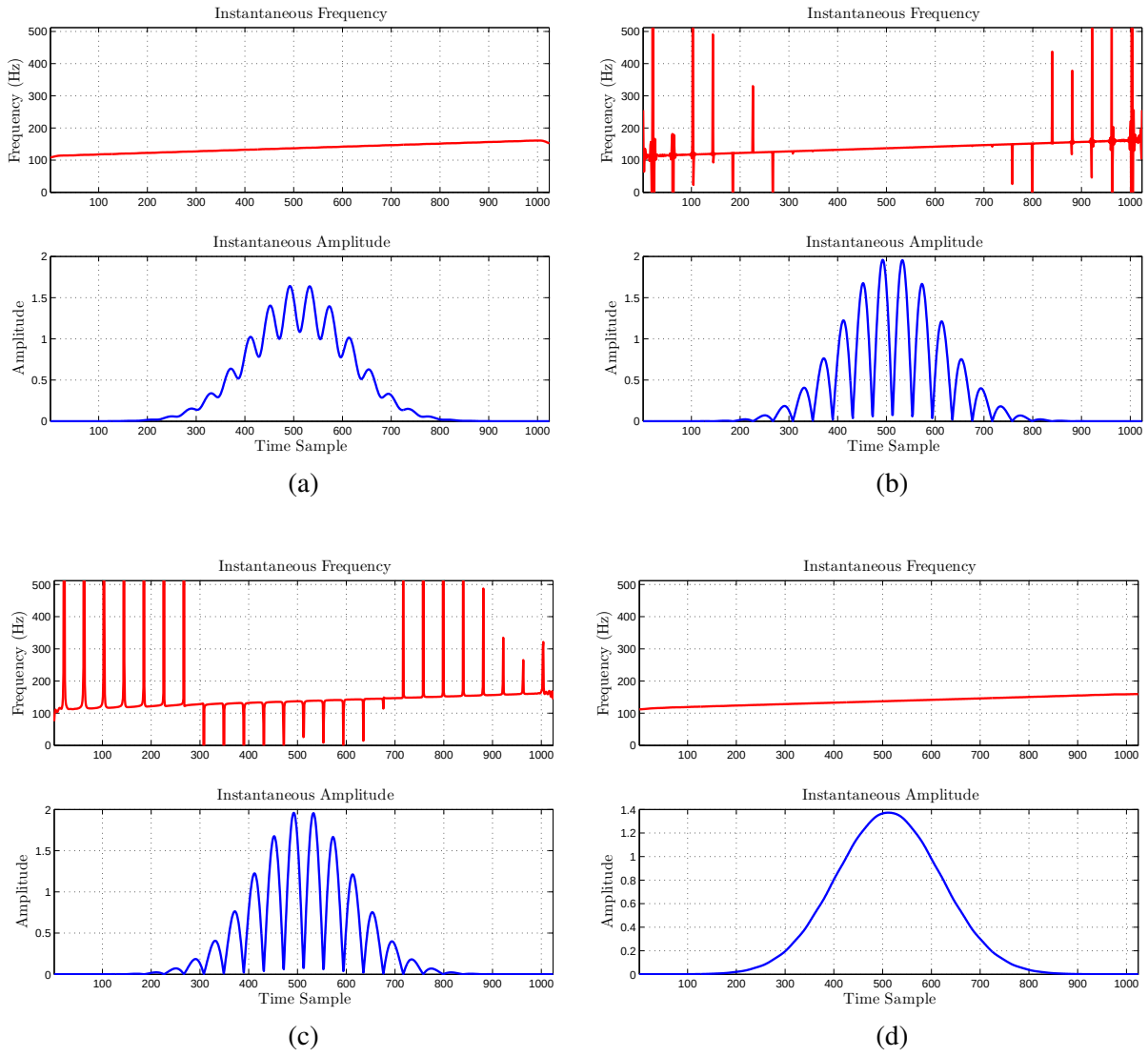

Figure 1.4 Computed IF and IA for Experiment 2. The expected IF is 112.5 Hz at time sample 1 and 162.5 Hz at time sample 1024, and the expected IA is a Gaussian function centered at time sample 512 with duration 256 samples. The WVD and the CWD provide negative IF and frequencies outside the bandwidth of the signal. Any of the evaluated TF distributions satisfy the TF support since all of them show IF outside the region of support. (a) The spectrogram gives a good estimation of the IF and the IA. (b) The WVD gives a wrong estimation of the IF and a good estimation of the IA. (c) The CWD gives a wrong estimation of the IF and a good estimation of the IA. (d) The SPWVD gives a good estimation of the IF and the IA.

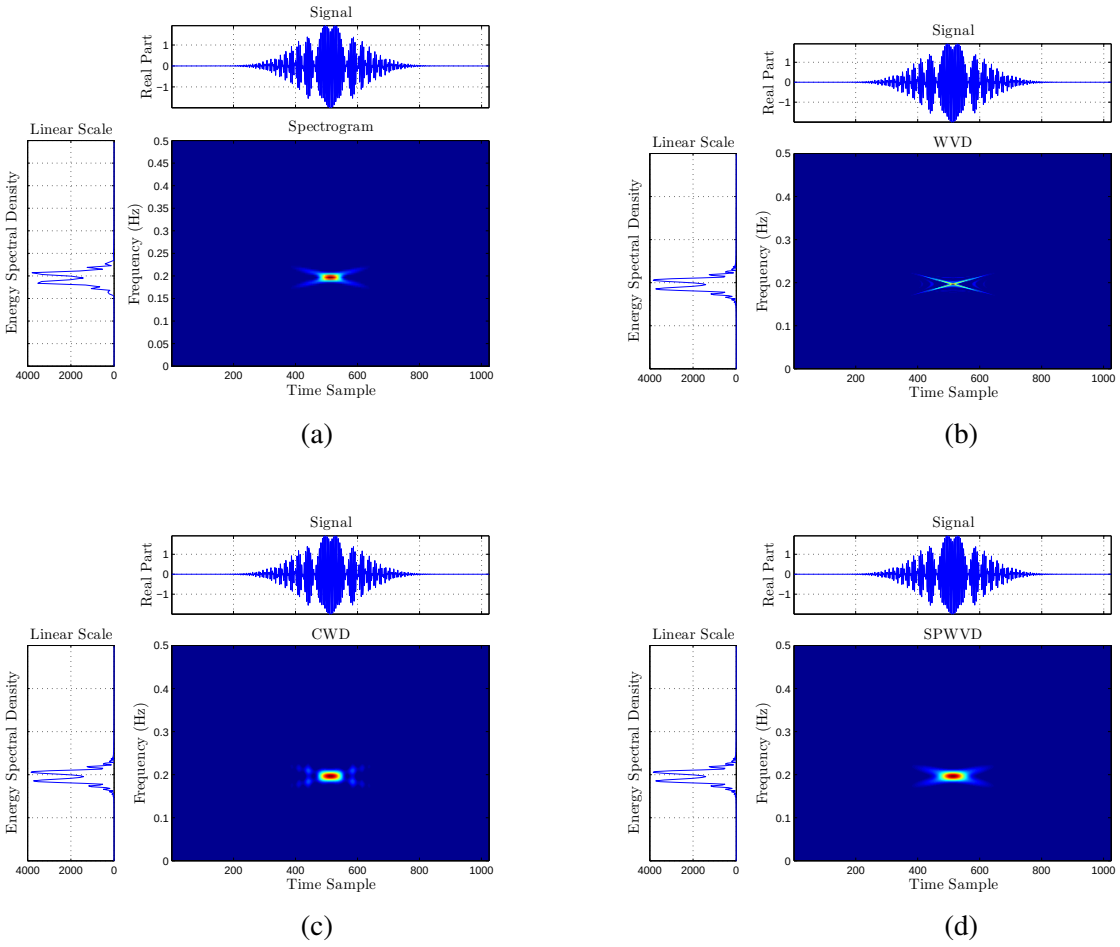

Figure 1.5 TF distributions of the signal in Experiment 3. Each TF distribution has a normalized frequency from 0 to 0.5. The region of support of the composed signal is in the time sample $[384, 640]$. (a) Spectrogram with a time Gaussian window of length 128 samples. (b) WVD. It gives the best TF resolution but is affected by cross terms. (c) CWD with a time Gaussian window of length 128 samples, frequency Gaussian window of length 64 samples, and parameter $\sigma = 1$, as defined in (1.9). (d) SPWVD with a time Gaussian window of length 128 samples and frequency Gaussian window of length 64 samples.

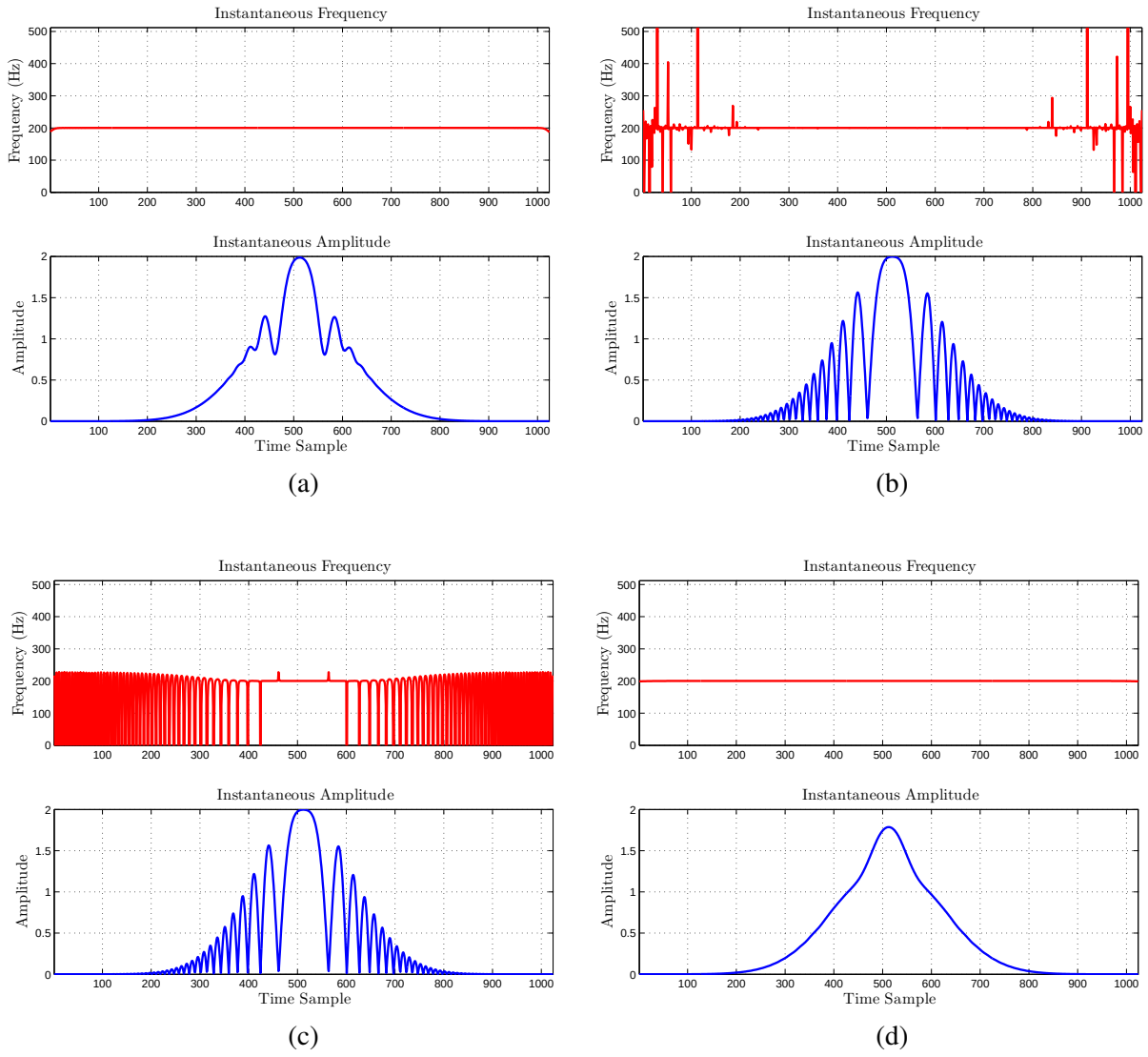

Figure 1.6 Computed IF and IA for Experiment 3. The expected IF is a constant frequency of 200 Hz along the time, and the expected IA is a Gaussian function centered at time sample 512 with duration 256 samples. The WVD and the CWD provide negative IF and frequencies outside the bandwidth of the signal. Any of the evaluated TF distributions satisfy the TF support since all of them show IF outside the region of support. (a) The spectrogram gives a good estimation of the IF and the IA. (b) The WVD gives a wrong estimation of the IF and a good estimation of the IA. (c) The CWD gives a wrong estimation of the IF and a good estimation of the IA. (d) The SPWVD gives a good estimation of the IF and the IA.

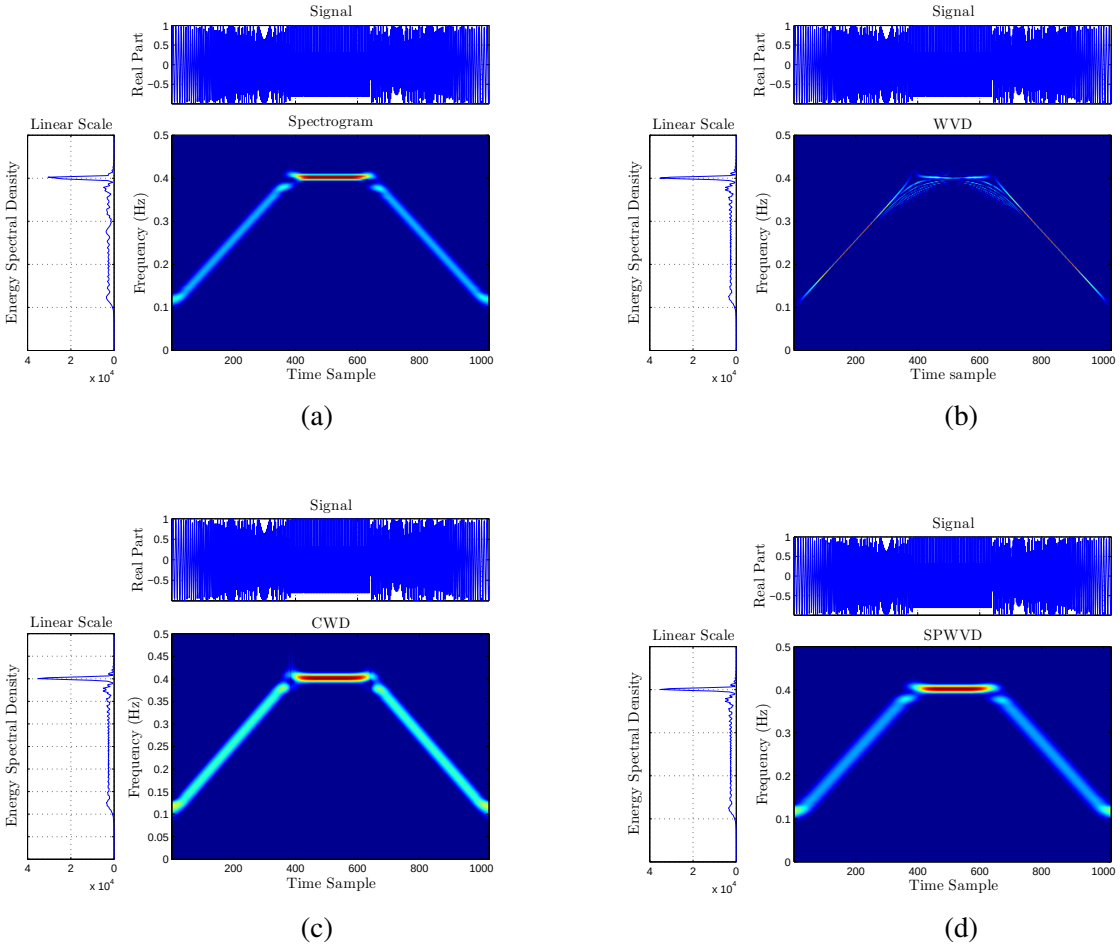

Figure 1.7 TF distributions of the signal in Experiment 4. Each TF distribution has a normalized frequency from 0 to 0.5. (a) Spectrogram with a time Gaussian window of length 128 samples. (b) WVD. It gives the best TF resolution but is affected by cross terms. (c) CWD with a time Gaussian window of length 128 samples, frequency Gaussian window of length 64 samples, and parameter $\sigma = 1$, as defined in (1.9). (d) SPWVD with a time Gaussian window of length 128 samples and frequency Gaussian window of length 64 samples.

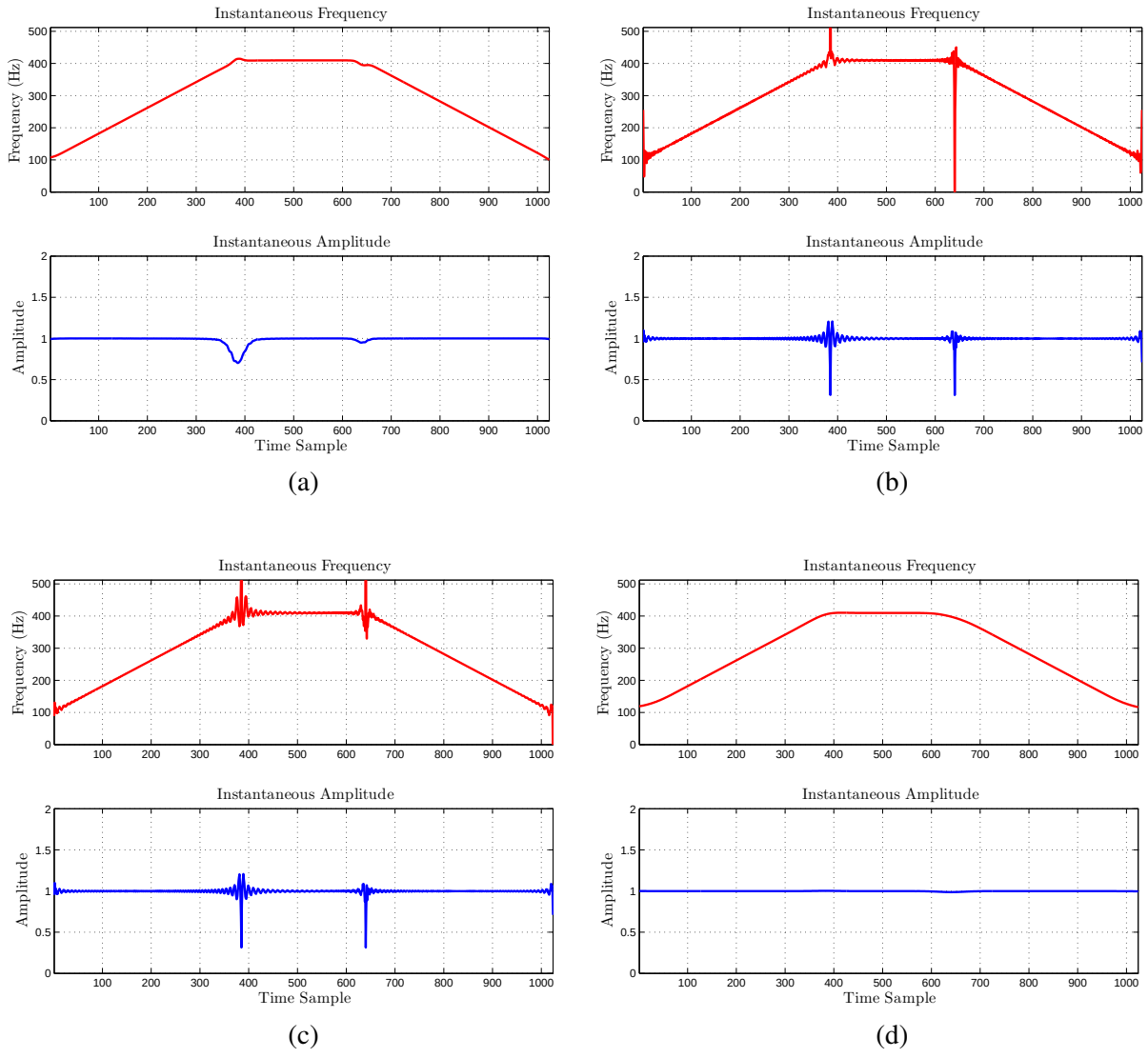

Figure 1.8 Computed IF and IA for Experiment 4. First, the expected IF increases linearly from 100 Hz to 400 Hz at time sample $[0, 384]$. Second, the expected IF is a constant of 400 Hz at time sample $[385, 640]$. Finally, the expected IF decreases linearly from 400 Hz to 100 Hz at time sample $[641, 1024]$. The expected IA is a constant value. The WVD and the CWD provide frequencies outside the bandwidth of the signal. All the evaluated TF distributions show transitions in the discontinuities of the analyzed signal giving a wrong estimation of the IA. These abrupt changes of the signal are not presented in SEMG signals. (a) The spectrogram gives a good estimation of the IF. (b) The WVD gives a wrong estimation of the IF. (c) The CWD gives a wrong estimation of the IF. (d) The SPWVD gives a good estimation of the IF.

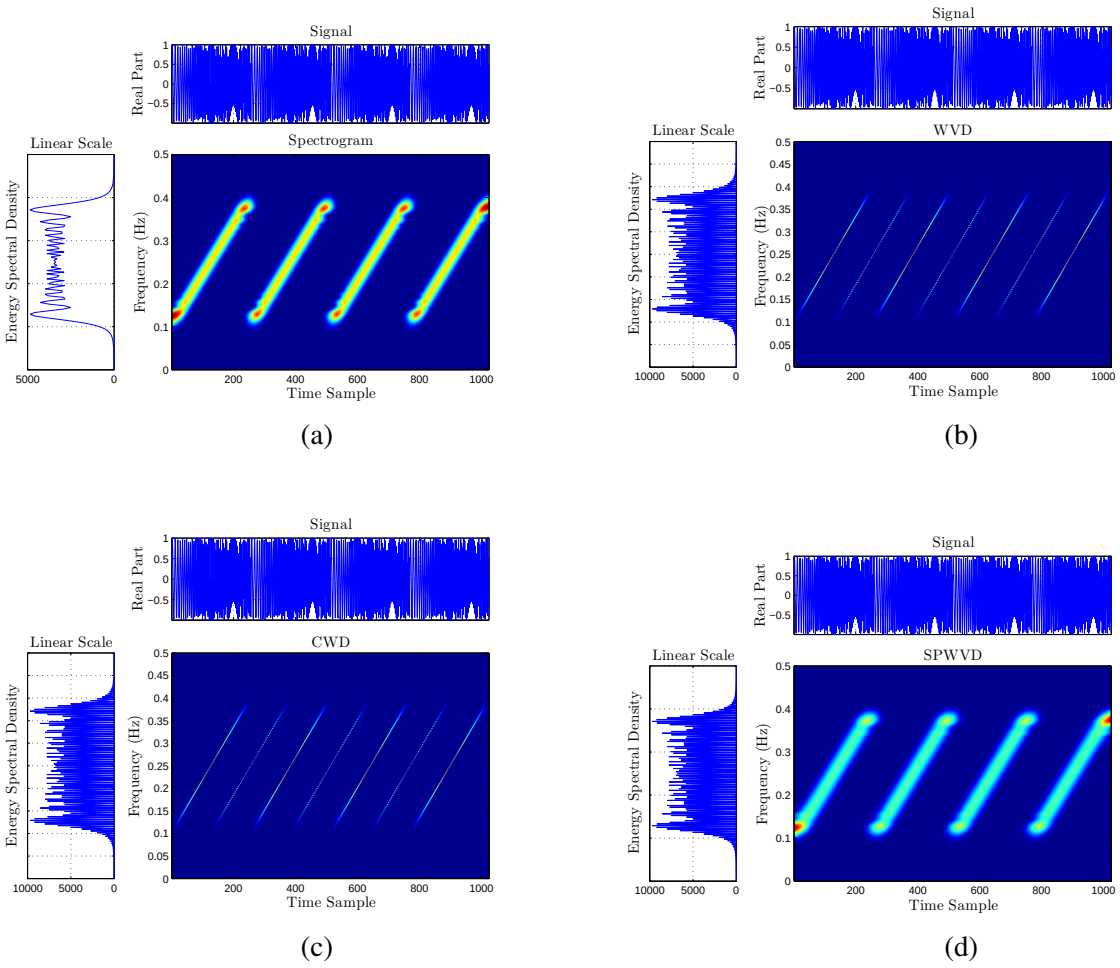

Figure 1.9 TF distributions of the signal in Experiment 5. Each TF distribution has a normalized frequency from 0 to 0.5. (a) Spectrogram with a time Gaussian window of length 128 samples. (b) WVD. It gives the best TF resolution but is affected by cross terms. (c) CWD with a time Gaussian window of length 128 samples, frequency Gaussian window of length 64 samples, and parameter $\sigma = 1$, as defined in (1.9). (d) SPWVD with a time Gaussian window of length 128 samples and frequency Gaussian window of length 64 samples.

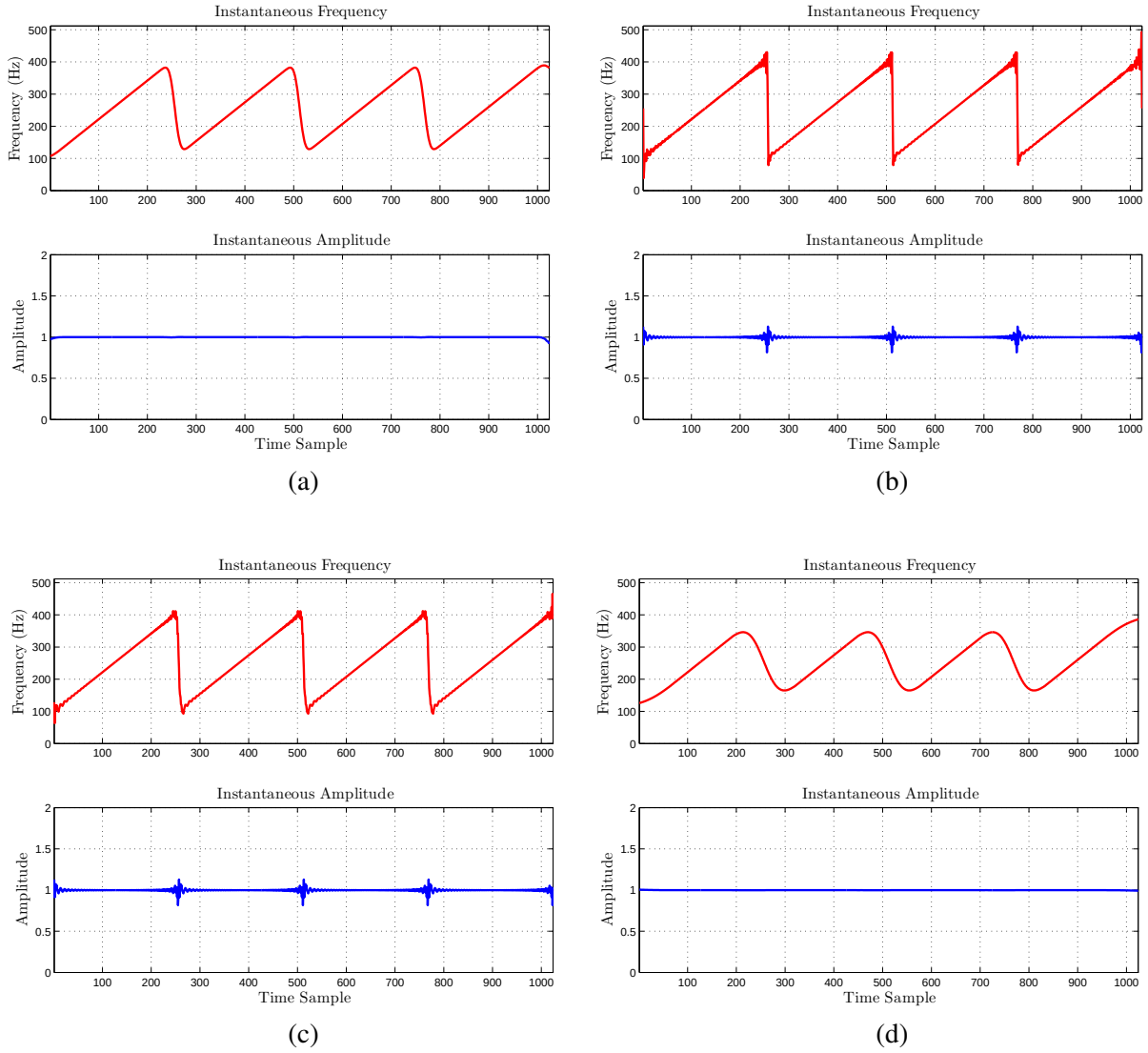

Figure 1.10 Computed IF and IA for Experiment 5. The expected IF increases linearly from 100 Hz to 400 Hz in four time intervals of 256 samples. The expected IA is a constant value. The spectrogram and the SPWVD are less susceptible to the discontinuities of the signal giving a smooth IA. (a) The computed IF from the spectrogram does not reach the maximum frequency of 400 Hz. (b) The WVD gives a good estimation of the IF. (c) The CWD gives a good estimation of the IF. (d) The computed IF from SPWVD also does not reach the maximum frequency of 400 Hz.

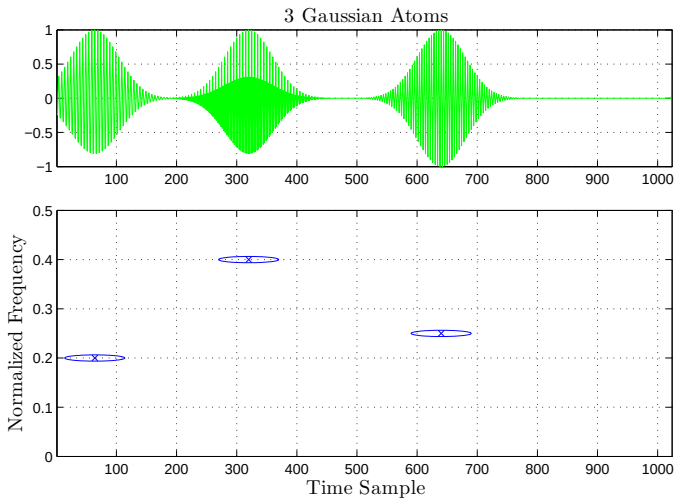

Figure 1.11 Ideal TF distribution of the signal in Experiment 6 with a normalized frequency from 0 to 0.5.

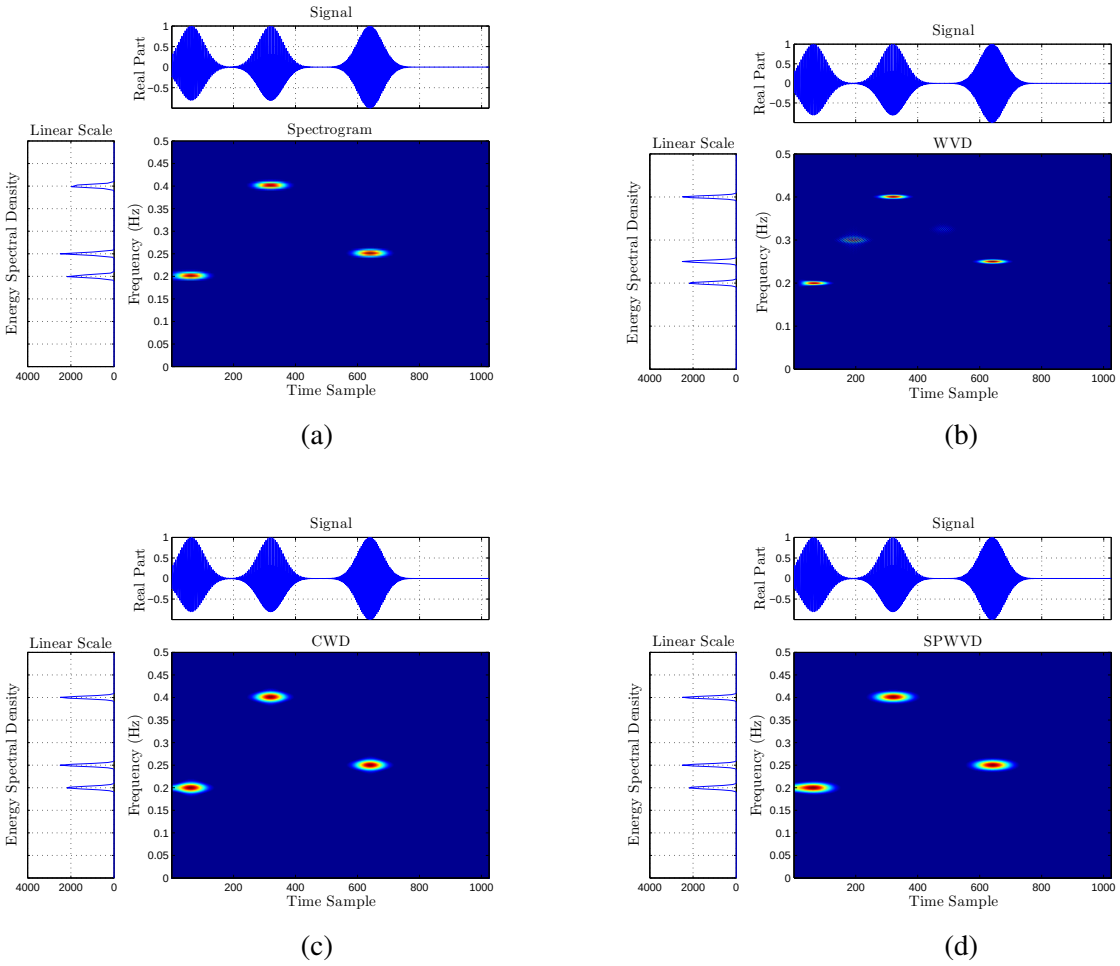

Figure 1.12 TF distributions of the signal in Experiment 6. Each TF distribution has a normalized frequency from 0 to 0.5. (a) Spectrogram with a time Gaussian window of length 128 samples. (b) WVD. It gives the best TF resolution but is affected by cross terms. (c) CWD with a time Gaussian window of length 128 samples, frequency Gaussian window of length 64 samples, and parameter $\sigma = 1$, as defined in (1.9). (d) SPWVD with a time Gaussian window of length 128 samples and frequency Gaussian window of length 64 samples.

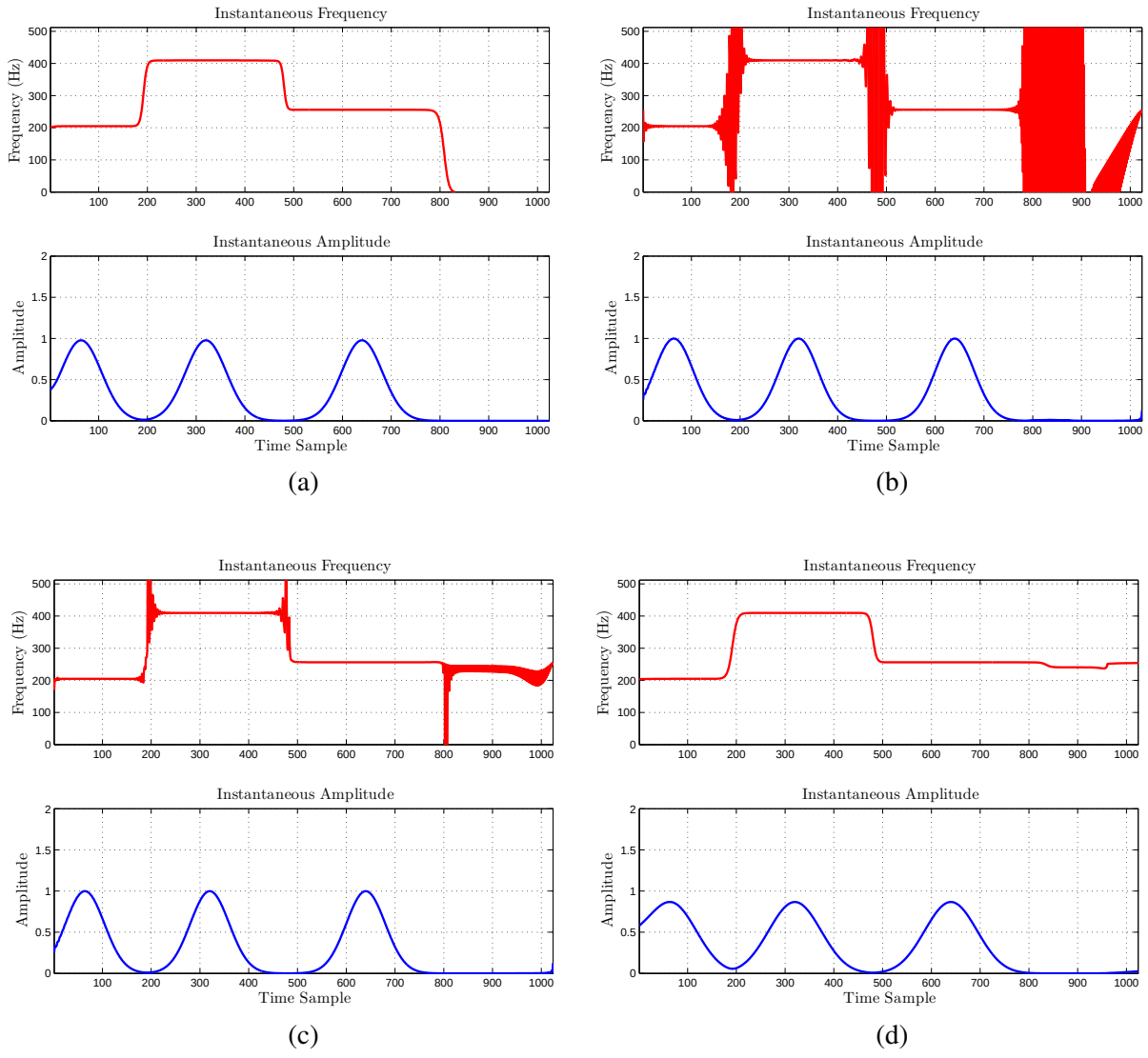

Figure 1.13 Computed IF and IA for Experiment 6. Three Gaussian atoms in the TF plane. One atom is located at time sample 64 with an expected IF of 200 Hz, a second atom is located at time sample 320 with an expected IF of 400 Hz, and a third atom is located in sample 640 with an IF of 250 Hz. The expected IA for the three atoms is three Gaussian functions centered at time samples 64, 320 and 640. (a) The spectrogram gives a good estimation of the IF and the IA. The spectrogram is the only one that shows an IF of zero when the signal is zero. In this case the time support property is satisfied. (b) The WVD gives a wrong estimation of the IF and a good estimation of the IA. (c) The CWD gives a wrong estimation of the IF and a good estimation of the IA. (d) The SPWVD gives a good estimation of the IF and the IA.

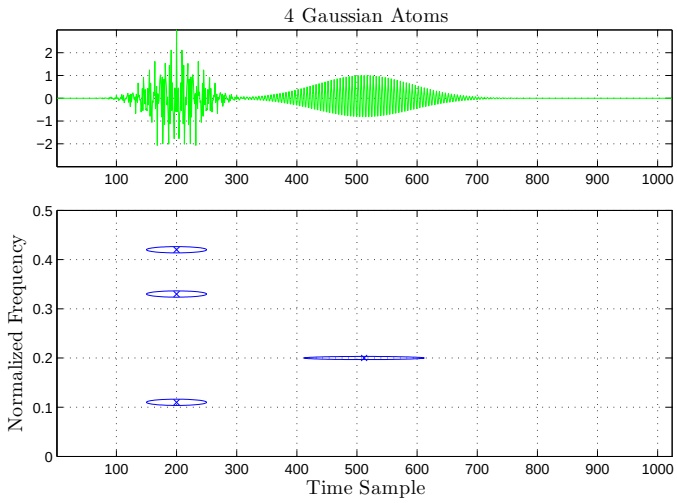

Figure 1.14 Ideal TF distribution of the signal in Experiment 7 with a normalized frequency from 0 to 0.5.

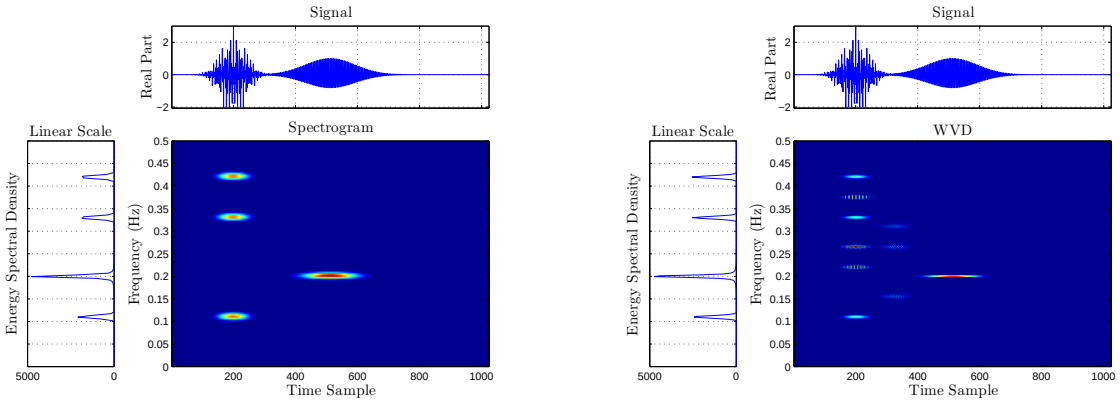

(a)

(b)

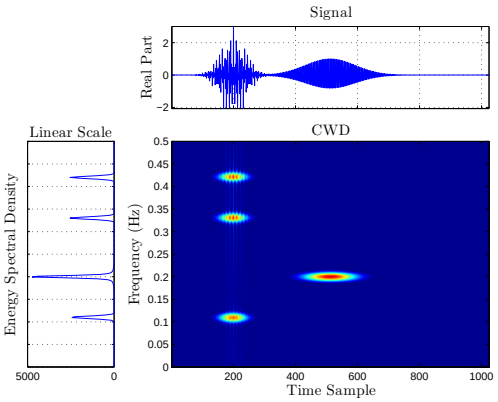

(c)

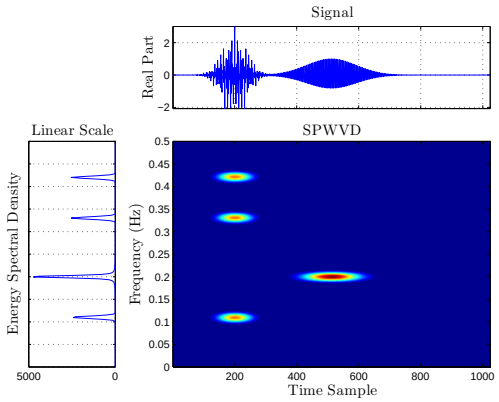

(d)

Figure 1.15 TF distributions of the signal in Experiment 7. Each TF distribution has a normalized frequency from 0 to 0.5. (a) Spectrogram with a time Gaussian window of length 128 samples. (b) WVD. It gives the best TF resolution but is affected by cross terms. (c) CWD with a time Gaussian window of length 128 samples, frequency Gaussian window of length 64 samples, and parameter $\sigma = 1$, as defined in (1.9). (d) SPWVD with a time Gaussian window of length 128 samples and frequency Gaussian window of length 64 samples.

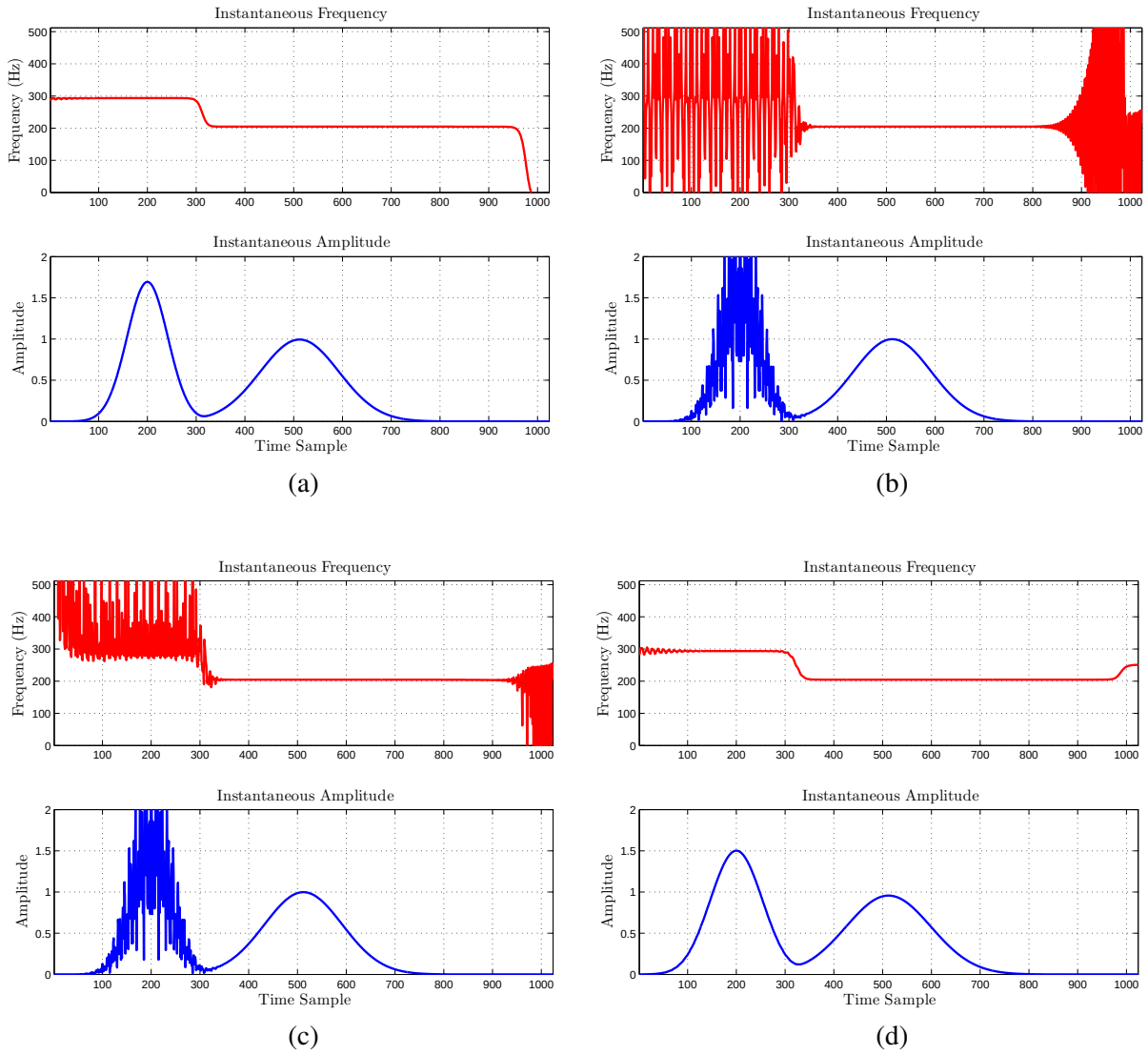

Figure 1.16 Computed IF and IA for Experiment 7. Four Gaussian atoms in the TF plane. The expected IF is 287 Hz at time sample $[100, 300]$ and 200 Hz at time sample $[312, 711]$. The expected IA for the four atoms is two Gaussian functions centered at time sample 200 and 512. (a) The spectrogram gives a good estimation of the IF and the IA. (b) The WVD gives a wrong estimation of the IF and a good estimation of the IA. (c) The CWD gives a wrong estimation of the IF and a good estimation of the IA. (d) The SPWVD gives a good estimation of the IF and the IA.

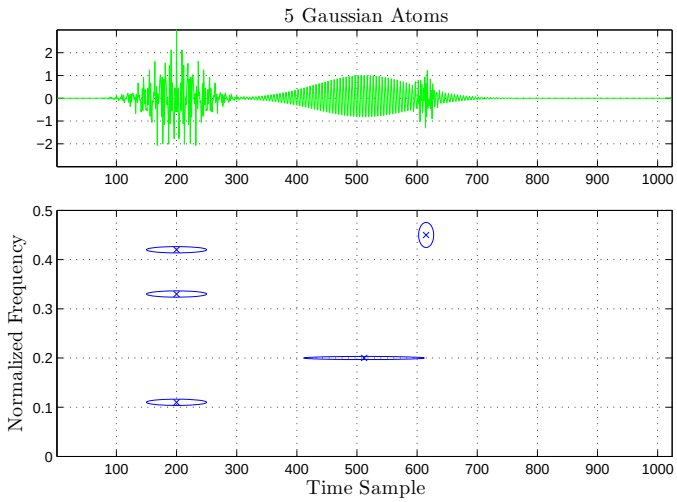

Figure 1.17 Ideal TF distribution of the signal in Experiment 8 with a normalized frequency from 0 to 0.5.

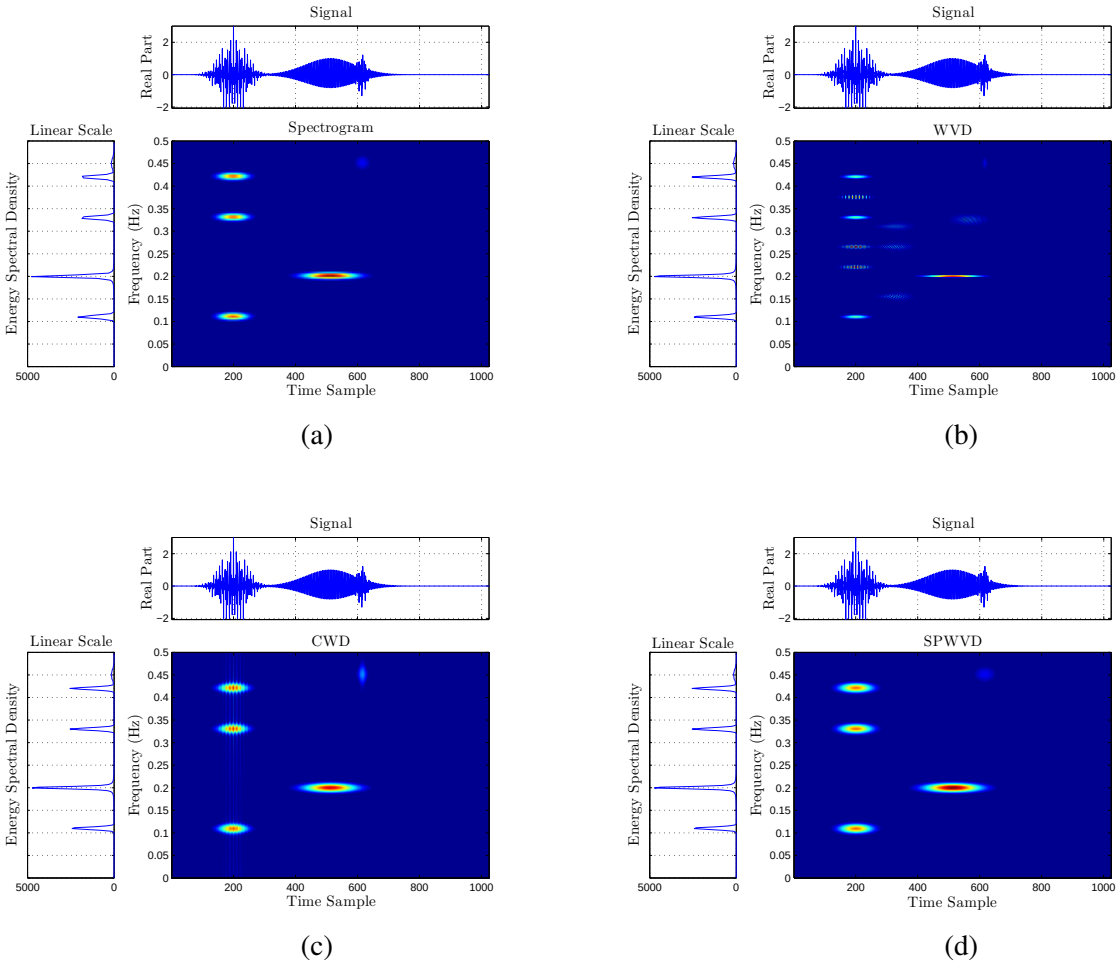

Figure 1.18 TF distributions of the signal in Experiment 8. Each TF distribution has a normalized frequency from 0 to 0.5. (a) Spectrogram with a time Gaussian window of length 128 samples. (b) WVD. It gives the best TF resolution but is affected by cross terms. (c) CWD with a time Gaussian window of length 128 samples, frequency Gaussian window of length 64 samples, and parameter $\sigma = 1$, as defined in (1.9). (d) SPWVD with a time Gaussian window of length 128 samples and frequency Gaussian window of length 64 samples.

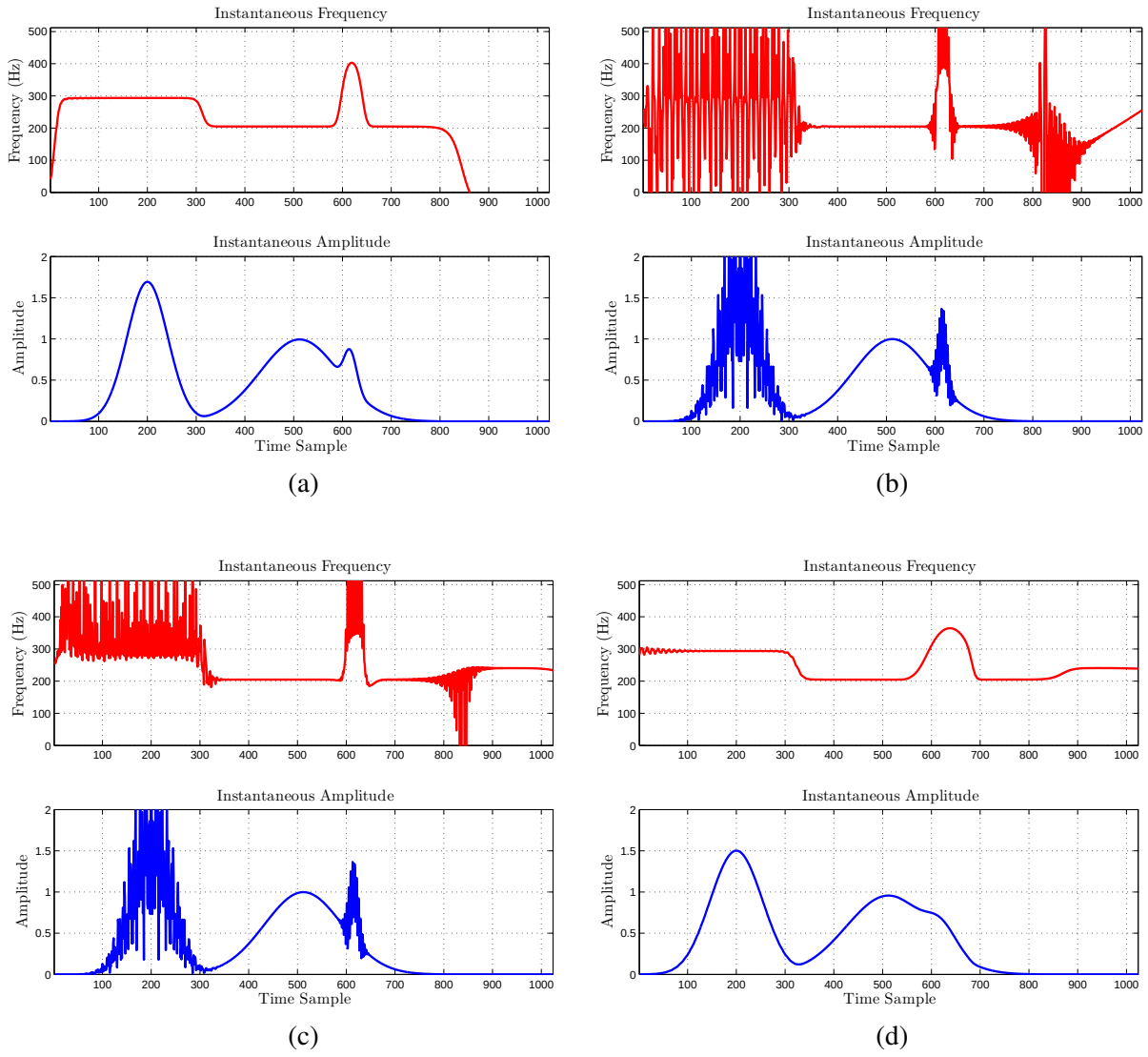

Figure 1.19 Computed IF and IA for Experiment 8. Five Gaussian atoms in the TF plane. The expected IF is 287 Hz at time sample $[100, 300]$, 200 Hz at time sample $[312, 711]$, and 450 Hz at time sample $[590, 639]$. The expected IA for the five atoms is three Gaussian functions centered at time sample 200, 512, and 615. In general any of the analyzed TF distributions could not reach the maximum frequency of 450 Hz. The WVD and the CWD still provide negative IF and frequencies outside the bandwidth of the signal. The spectrogram and the SPWVD provide adequate estimations of the IF and IA. (a) Spectrogram. (b) WVD. (c) CWD. (d) SPWVD.

2

Materials and Method

2.1 Materials

Muscle fatigue was evaluated from SEMG signals recorded from 26 normal human subjects, 11 females and 15 males. The females had an average age of 23 years, weight of 146 pounds and height of 163 cm; the males had an average age of 27 years, weight of 184 pounds and height of 177 cm. The SEMG signals were acquired at a sampling frequency of 1024 Hz from six neck muscles: trapezius, splenius capitis and sternocleidomastoid, from both left and right sides.
A Delsys Bagnoli-8 EMG system with DE-2.1 standard differential EMG electrodes was used for the collection of the myoelectric data. Prior to entrance into the study, basic anthropometry measurements (age, weight, height) were collected from each subject to ensure that they fulfilled the requirements of the study.

2.2 Study Design

For this research 3480 SEMG recorded signals provided by the Air Force Research Laboratory are analyzed in the evaluation of muscle fatigue. The objective of this analysis is to present indices to measure neck muscle fatigue during prolonged wear of weighted flight helmets. These indices are useful in the development of guidelines to guarantee good performance and safety to the pilots. In this study each subject was exposed to five sessions of eight hours with a minimum waiting period of 48 hours between them. In each session the subject wore a different weighted flight helmet as shown in Table 2.1. They also performed a 100% maximum voluntary contraction (MVC) before and after the eight-hour session, and a 70% MVC at the end of every hour (first hour to seventh hour). The 70% MVC was held until the subject could no longer maintain the exertion for a maximum time of three minutes. A dynamometer was used to monitor the strength given by the subject's neck muscle during the 70% and 100% MVC exertion. During this strength monitoring, SEMG data were recorded to measure the change in muscular activity and to analyze muscle fatigue. During each session of eight hours, the subjects completed a comfort survey before the initial 100% MVC, after hours two, four and seven, and after the final 100% MVC. After collection of the data, the SEMG signal of each subject was normalized to his 100% MVC as suggested by Merletti [21].

Table 2.1 Helmet configurations (Air Force Research Laboratory).

Cell	Weight (Lb)	Helmet Center of Gravity (CG)
A	3.0	Baseline
B	4.5	Near head
C	4.5	Forward head
D	6.0	Near head
E	6.0	Forward head

2.3 Method

The idea of using wavelets in the analysis of muscle fatigue arises as an alternative solution to the TF resolution issue (Heisenberg uncertainty principle) introduced by the STFT and SPWVD. Wavelets suggest that this resolution problem can be solved by defining short time windows for high frequencies and long time windows for low frequencies. Additionally, wavelets have demonstrated to be a reliable method in the analysis of nonstationary biological signals with the advantage of being independent of any smoothing function, in contrast to the spectrogram, SPWVD, and CWD, which are dependent of a smoothing function.

The proposed technique (see Appendix A) to assess muscle fatigue starts by filtering the recorded SEMG signal with a cosine modulated filter bank. In the SEMG tool box, a cosine modulated filter bank with 16 and 32 channels is provided. The outputs of the 16 or 32 channels are the subband coefficients which are then squared and arranged in a time subband representation. The IF was estimated from Equation 1.7 as the first order moment of the time subband representation at a certain point in time. To estimate the IA from the time subband representation, the following sequential stages are proposed: (1) define a rectangular window for each subband with a length that is inversely proportional to the central frequency of the subband; (2) find in each subband the maximum coefficient inside the window; (3) finally, add all the corresponding maximum values to obtain an estimate of the IA. The estimate of the IA for the next point in time is computed by shifting the rectangular window one sample to the right and then steps (1) to (3) are repeated until the IA is estimated along all the signal. Table 2.2 summarizes the strengths and shortcomings of using a filter bank as a TF distribution in the analysis of muscle fatigue.

After the IF and the IA are estimated from the signal, IF and IA slopes are computed by applying a first order linear regression model to the estimated IF and IA for one minute intervals every one second. The aim of these slopes is to measure the decrease or increase rate of the IF and IA, thus providing an index to measure the intensity of muscle increase force, recovery, muscle decrease force or fatigue. However, it was not found in the literature any suggestion about the decrease or increase rate of the slopes where muscle increase force, recovery, muscle decrease force and

Table 2.2 Strengths and shortcomings of using a filter bank as a TF distribution.

Advantages
Positivity
Good IF estimation
Good IA estimation
Reduced cross terms
Window independent
Allow to select the frequency range of interest
Local in time and frequency
Fast to compute
Disadvantages
TF marginals not satisfied
TF support not satisfied
No energy conservation

fatigue should be considered. Likewise, it was not found any suggestion about either the time interval to be used in the first order linear regression model or the time shift between two consecutive slopes (see Fig. 2.1).

The IF and the IA variables estimated from the filter bank are compared with the IF and the IA variables estimated from two well known TF distributions used in the analysis of biomedical signals, namely, spectrogram, and SPWVD. First, the SEMG signal is Hilbert transformed and then any of the mentioned TF distributions is computed. Second, the IF parameter is estimated by computing the first order moment of the frequency distribution at a certain point in time as shown in (1.7) [15], [21]. Finally, the IA parameter is estimated by computing the square root of the time marginal of the employed TF distribution. To compute the IF and the IA slopes, a first order linear regression model is applied to the estimated IF and IA with the same time intervals and time shift between slopes used in the filter bank.

The IF and IA slopes derived from the spectrogram and the SPWVD are compared and correlated to those slopes derived from the filter bank by using a relative quadratic difference and Pearson's correlation coefficient [27]. The IF and the IA of the SEMG signal are not estimated by using the CWD because as it was shown in Section 1.5 the CWD provides an IF with negative frequencies and frequencies outside the bandwidth of the signal.

A joint analysis of frequency and amplitude is adopted in this research to analyze both the decrease or increase rate of the IF and the decrease or increase rate of the IA. By using a joint analysis of frequency and amplitude, as shown in Fig 2.2, the IF and IA slopes are classified into four stages: (1) increase force when both the IF slopes and the IA slopes increase over time, (2)

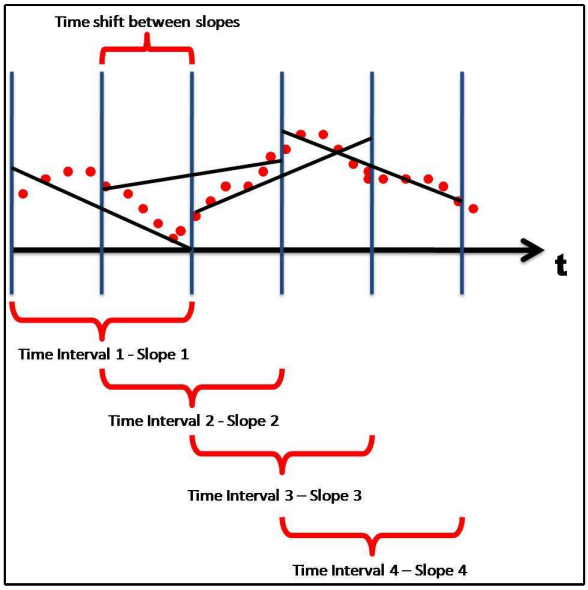

Figure 2.1 The time interval to be used in the first order linear regression and the time shift between slopes are unknown in the literature.

recovery from previous muscle fatigue when there is an increase in the IF slopes and a decrease in the IA slopes, (3) decrease force when both the IF slopes and the IA slopes decrease over the time, (4) muscle fatigue when there is a decrease in the IF slopes and an increase in the IA slopes. A common procedure in the joint analysis of frequency and amplitude is to count the number of points in each stage (increase force, recovery, decrease force and fatigue) [20], [19]. However, in this research, instead of counting the number of points, it is proposed in each stage to add the square of the distance of the points to the origin of the IA $\times$ IF plane as a measure of the energy of the point in that stage. The aim of this procedure is to determine whether the level of fatigue reported by the subject is directly related to the rates of IF decrease and IA increase.

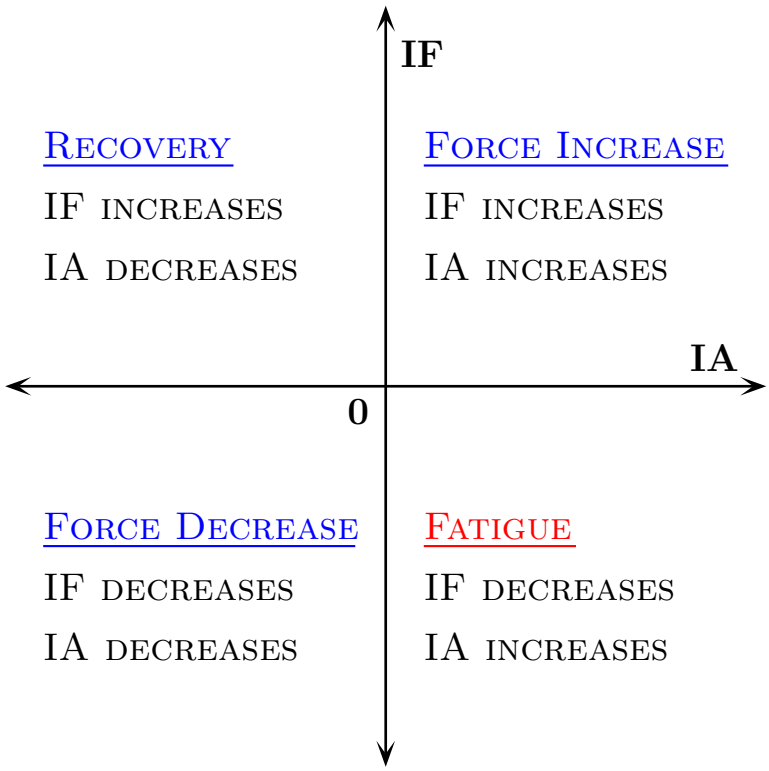

Figure 2.2 Classification of the IF and IA slopes using a joint analysis of frequency and amplitude.

3

Results

This chapter describes the experimental results obtained by applying the filter bank decomposition proposed in this research to different SEMG signals provided by the AFRL. These results are compared with those given by the standard techniques, namely the spectrogram and the SPWVD. Section 3.1 compares the IF and IA slopes estimated using the filter bank decomposition with the slopes given by the spectrogram and the SPWVD; this comparison is based on the computation of Pearson's correlation coefficient and the relative quadratic difference. Note that the IF and IA slopes are the indices used to assess muscle fatigue, which is the object of study in this research. Using these slopes, the method of joint analysis of frequency and amplitude classifies the muscle activity in each hour into the following stages: increase force, recovery, decrease force, or fatigue. The results of these classifications are presented in Section 3.2.
Finally, the energy of the IF and IA slopes for each stage is proposed as a measure of the intensity level of increase force, recovery, decrease force, or fatigue. The correlation between the measured energy in the fatigue stage and the perceived levels of discomfort reported by the subjects is then evaluated in Section 3.2.

3.1 Comparison of IF and IA Slopes

This section compares the IF and IA slopes as computed by the proposed filter bank decomposition with those given by the spectrogram and the SPWVD for three kinds of muscle: splenius capitis, sterno, and trapezius (see Fig. 3.4). As mentioned in Section 2.3, the method developed in this project has the advantage of being computationally faster and improves cross terms supression. However, it is still important to verify if the obtained slopes have the same trend as those given by the standard spectrogram and SPWVD techniques as the following examples show.
Example 1 below illustrates the extraction of the IF and IA slopes of a typical SEMG signal recorded from the right trapezius after hour 2 when the subject was performing an exertion of 70% MVC. Figure 3.1(a) shows the signal samples corresponding to 3 minutes at the end of hour 2, while Fig. 3.1(b) shows the corresponding IF and IA slopes obtained using the three methods (spectrogram, SPWVD, and filter bank decomposition). Observe in the top of Fig. 3.1(b) that the IF slopes computed using the three methods are, most of the time, very close. Although the IA slopes, shown in the bottom of Fig. 3.1(b), are clearly different in the peak region, the three methods provide the same trend of slopes, meaning that when the results of one of the methods is

increasing or decreasing with time the same happens to the other two methods. In this way, in terms of providing valid indices for fatigue assessment, the three methods can be considered equivalent in this example, but the proposed filter bank decomposition method has the advantage of being faster and window-independent.

A second example is shown in Fig. 3.2. Figure 3.2(a) shows the signal samples extracted from the right splenius during the last 3 minutes of hour 6 when the subject was performing 70% MVC. The corresponding IF and IA slopes are shown in Fig. 3.2(b). As observed in Example 1 illustrated in Fig. 3.1, the IF slopes obtained from the filter bank decomposition are equivalent to those provided by the spectrogram and the SPWVD, while the IA slopes, which differ in the peak regions, present always the same trends. Again it is noted that the IF and IA slopes given by the proposed method are satisfactory for the assessment of muscle fatigue with less computational time and with window-independence.

The behavior verified in Figs. 3.1 and 3.2 for the proposed method, characterized by IA and IF slopes trends close to those given by the spectrogram and the SPWVD, was typical of all the simulations, provided that the analyzed signal does not have high and localized peaks. These peaks appear in some cases, probably due to poor placement of the electrodes or bad contact of the electrodes with the subject's skin. The consequences of these wrong signal acquisitions are illustrated in Example 3, in Fig. 3.3. First, Fig. 3.3(a) shows the samples from the signal acquired from the left splenius at the 3 minutes at the end of the hour 7. Note the high peaks around minutes 0.3, 1.6, and 2.4. In this case, as it is shown in the top of Fig. 3.3(b), the IF slopes differ for all the three evaluated techniques (spectrogram, SPWVD, and filter bank decomposition). The IA slopes, shown in the bottom of Fig. 3.3(b), are still very similar in trend (for all three methods, they increase or decrease in the same time regions). However, the conclusion is that the peaks observed in Fig. 3.3(a) make the IF slopes inappropriate as indices of muscle fatigue, as they are due to wrong measurements.

Example 1

Subject information

Subj ID: NF F-1

Test # : NFF0002

Cell: B

Muscle: Right Trapezius

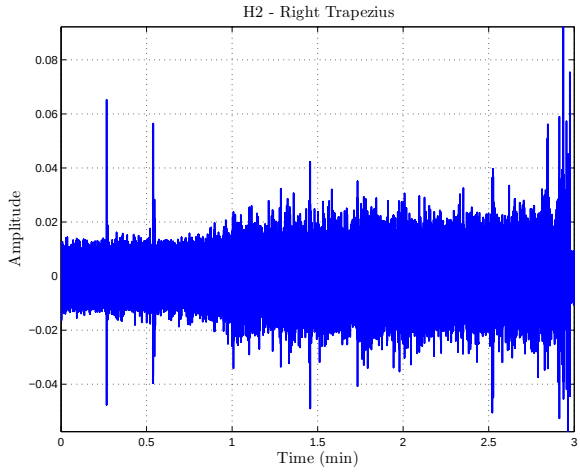

(a)

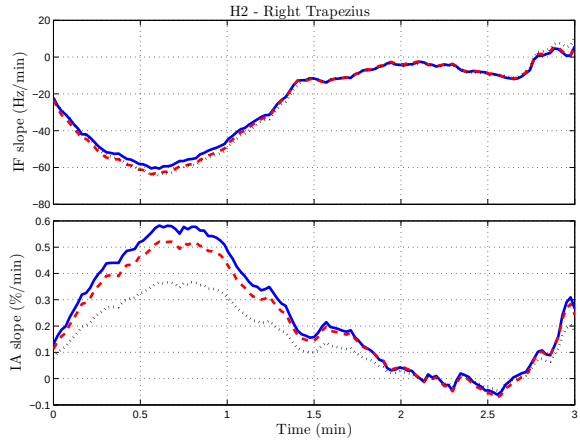

(b)

Figure 3.1 Correct SEMG signal and correct estimation of its IF and IA. (a) SEMG signal recorded from the right trapezius at the end of the second hour. (b) Computed slopes from the IF and the IA using three different methods – spectrogram (dashed red line), SPWVD (dotted black line), and filter bank (continuous blue line). The IF and IA estimates from the three methods show similar trends.

Example 2

Subject information

Subj ID: NF F-1

Test # : NFF0060

Cell: E

Muscle: Right Splenius

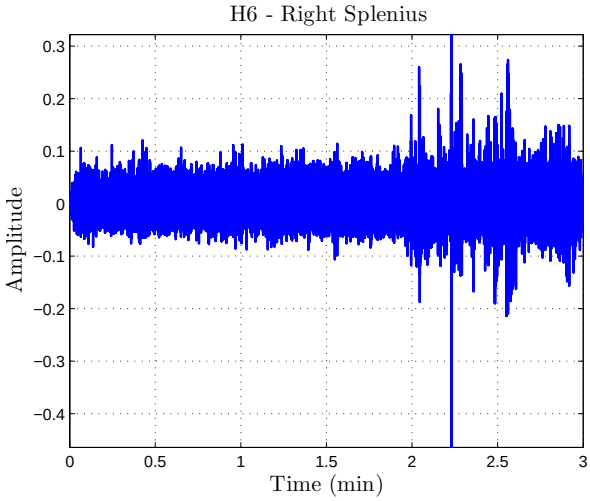

(a)

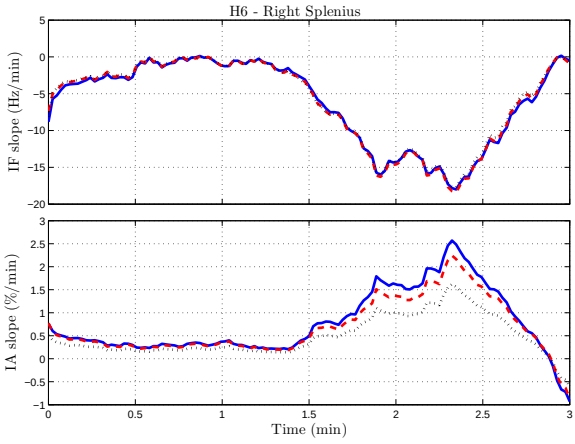

(b)

Figure 3.2 Correct SEMG signal and correct estimation of its IF and IA. (a) SEMG signal recorded from the right splenius at the end of the sixth hour. (b) Computed slopes from the IF and the IA using three different methods – spectrogram (dashed red line), SPWVD (dotted black line), and filter bank (continuous blue line). The IF and IA estimates from the three methods show similar trends.

Example 3

Subject information

Subj ID: NF F-1

Test # : NFF00060

Cell: E

Muscle: Left Splenius

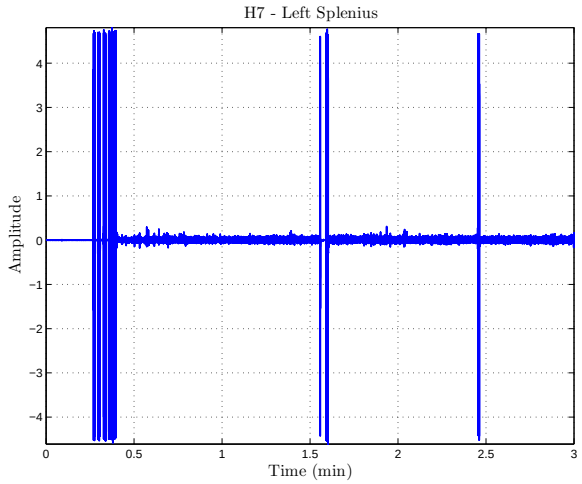

(a)

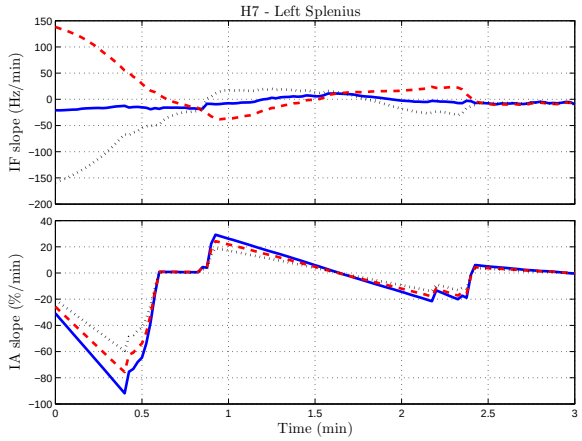

(b)

Figure 3.3 Wrong SEMG signal and wrong estimation of its IF and IA. (a) SEMG signal recorded from the left splenius at the end of the seventh hour. This signal shows high peaks and small amplitude values at certain time. This noise seems to be caused by a bad contact of the electrodes with the skin of the subject or with the EMG equipment. (b) Computed slopes from the IF and the IA using three different methods – spectrogram (dashed red line), SPWVD (dotted black line), and filter bank (continuous blue line). The IF estimated from the three methods show different values.

Two figures of merit were used to quantify the comparison between the slopes computed from the subbands of the filter bank with the slopes computed from either the spectrogram or SPWVD. The first figure of merit was the relative quadratic difference defined as

$$\alpha = \frac{\sum_{n=1}^{L}(s_{fb}[n] - s_{tf}[n])^2}{\sum_{n=1}^{L}(s_{fb}[n])^2} \times 100, \tag{3.1}$$

where $s_{fb}[n]$ is either the IF slope or the IA slope at time n estimated from the filter bank, and $s_{tf}[n]$ is either the IF slope or the IA slope at time n estimated from either the spectrogram or the SPWVD.

The second figure of merit was the Pearson's correlation coefficients defined as

$$\rho = \frac{1}{L\,\sigma_{fb}\,\sigma_{tf}} \sum_{n=1}^{L} \left(s_{fb}[n] - \overline{s}_{fb}\right)\left(s_{tf}[n] - \overline{s}_{tf}\right), \tag{3.2}$$

where σ_{fb}, and $\overline{s}_{fb}$ are the standard deviations and the sample means, respectively, of either the IF or IA slopes computed from the filter bank. The parameters σ_{tf}, and $\overline{s}_{tf}$ are the standard deviations and the sample means, respectively, of either the IF or IA slopes computed from either the spectrogram or the SPWVD. The relative quadratic difference is computed for $n = 0, 1, 2, \ldots, L$, where L is the number of slopes that were computed over an interval of the estimated IF or IA. The results for the relative quadratic difference computed for 3480 SEMG signals provided by the AFRL are summarized in Table 3.1. In the case of the IF slopes computed with the filter bank, 96% had differences not greater than 0.5% with respect to those slopes given by the spectrogram, and 90% had differences not greater than 0.5% with respect to those slopes given by the SPWVD. In the case of the IA slopes computed with the filter bank, 99% had differences not greater than 0.5% with respect to those slopes given by the spectrogram, and 100% had differences not greater than 0.5% with respect to those slopes given by the SPWVD.

The results for the Pearson's correlation coefficients computed for 3480 SEMG signals provided by the AFRL are summarized in Table 3.2. Note that a correlation coefficient of 1 means that the slopes derived from the spectrogram and the SPWVD follow the same trend as the slopes derived from the filter bank. In the case of the IF slopes computed with the filter bank, 94% had correlation coefficients greater than 0.9 with respect to those slopes given by the spectrogram, and 88% had correlation coefficients greater than 0.9 with respect to those slopes given by the SPWVD. In the case of the IA slopes computed with the filter bank, 97% had correlation coefficients greater than 0.9 with respect to those slopes given by the spectrogram, and 100% had correlation coefficients greater than 0.9 with respect to those slopes given by the SPWVD.

Cohen has limited the use of wavelets and filter bank in the TF analysis since physical quantities derived from the TF distribution such as the moments are meaningless or sometimes they do not exist [7]. However, from the results of the filter bank proposed in this research, it is inferred that

slopes derived from the spectrogram and the SPWVD show not only identical trends but also similar values to those slopes derived from the filter bank. For a few number of slopes, 3% of the results, neither the filter bank, the spectrogram, or the SPWVD show equivalent slopes. This is because a wrong acquisition of the signal causes high localized peaks in some samples, which can lead to invalid indices mainly in the case of the IF, as shown in Fig. 3.3.

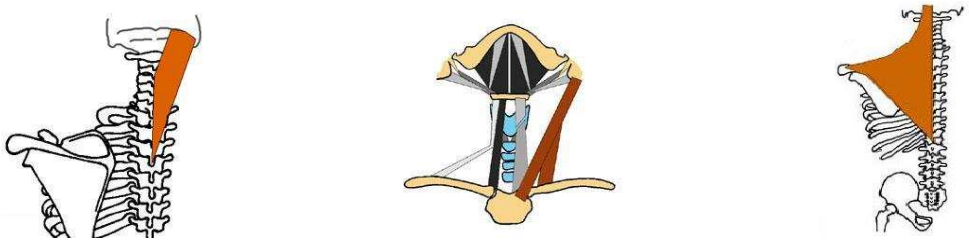

(a) (b) (c)

Figure 3.4 Neck muscles involved in the analysis of muscle fatigue. (a) Muscle – Splenius capitis; Action – Extends and rotates cervical spine. (b) Muscle – Sterno; Action – Flexes and laterally rotates cervical spine. Extends neck when neck is already partially extended; (c) Muscle – Trapezius. Action – Stabilizes, elevates, retracts, and rotates scapula (source – AFRL).

Table 3.1 Relative quadratic difference α of the IF and IA slopes obtained from the spectrogram, SPWVD, and filter bank during the analysis of 3480 SEMG signals.

Method	$\%$ of IF slopes with $\alpha \leq 0.5\%$	$\%$ of IA slopes with $\alpha \leq 0.5\%$
Spectrogram $\times$ Filter Bank	96	99
SPWVD $\times$ Filter Bank	90	100

Table 3.2 Pearson's correlation coefficient ρ of the IF and IA slopes obtained from the spectrogram, SPWVD, and filter bank during the analysis of 3480 SEMG signals.

Method	$\%$ of IF slopes with $\rho > 0.9$	$\%$ of IA slopes with $\rho > 0.9$
Spectrogram $\times$ Filter Bank	94	97
SPWVD $\times$ Filter Bank	88	100

3.2 Joint Analysis of Frequency and Amplitude

This section describes the results obtained for the classification of the muscle activity as stages of increase force, recovery, decrease force, or fatigue. This classification is based on the IF and IA slopes, which were obtained for a subject during the eight-hour session. Also, the energy of the IF and IA slopes is proposed as a measure of the intensity level of muscle activity at each stage. To evaluate the effectiveness of this measure, the correlation between the measured energy in the fatigue stage and the perceived levels of discomfort reported by the subjects is evaluated.
The results of the classification of the muscle activity stage for a female subject performing an exertion of 70% MVC while using different weighted flight helmets A (3.0 Lb baseline CG), B (4.5 Lb near head CG), C (4.5 Lb forward head CG), and E (6.0 Lb forward head CG) are plotted respectively in Figs. 3.5, 3.7, 3.9, and 3.11 (helmet D with 4.5 Lb near head CG was not considered because there was no signal to analyze). In each figure, items (a) to (g) corresponding to each hour, present the classified slopes derived from the filter bank decomposition in an IA $\times$ IF plane, in which each quadrant corresponds to a different stage (increase force, recovery, decrease force, and fatigue). In this way, the muscle activity is classified as: (1) increase force when both the IF slopes and the IA slopes increase over time, (2) recovery from previous muscle fatigue when there is an increase in the IF slopes and a decrease in the IA slopes, (3) decrease force when both the IF slopes and the IA slopes decrease over time, (4) muscle fatigue when there is a decrease in the IF slopes and an increase in the IA slopes.
Also shown in Figs. 3.5, 3.7, 3.9, and 3.11 are the energy levels (in blue) that were computed from the slopes given by the filter bank decomposition. The correlation between these energy levels and the perceived levels of discomfort reported by the subjects is evaluated next.
It is inferred from Fig. 3.6 that in the fifth and sixth hour most of the energy is concentrated in muscle fatigue (28.72% in the fifth hour and 25.17% in the sixth hour); however, the first and second hour show less energy in the stage fatigue (3.55% in the first hour and 13% in the second hour). According to these results, the subject is expected to report more fatigue in the sixth hour than in the second hour. The previous assumption is confirmed with the perceived levels of discomfort reported by the subject when wearing helmet A. In the questionnaire the subject reported for the following regions (head, upper neck, lower neck, shoulders, upper back, lower back) in the second hour: (1) no discomfort in the upper back, upper neck, and lower neck; (2) no hot spots and no numbness in any region. In addition, the subject reported no headache, relaxed mental state, alert mental frame of mind, and attentive concentration level. In contrast, during the sixth hour the subject reported soreness and moderate hot spots in all the regions, but no numbness in any region. In addition, the subject reported minimal headache, slightly tense, tired mental frame of mind, and distracted concentration level.
Figure 3.8 shows the analysis of muscle fatigue when the subject wore helmet B. In this analysis,

the right splenius and right trapezius were the muscles most fatigued in the first, second, and fourth hour. In the sixth hour the right sterno is the only muscle showing a recovery from previous muscle fatigue. Most of the neck muscles present fatigue at the end of the fifth, sixth, and seventh hour. In the questionnaire the subject reported for the folowing regions (head, upper neck, lower neck, shoulders, upper back, lower back) in the second and fourth hour: (1) no discomfort in the head, upper neck, lower neck, shoulders, upper back, and lower back; (2) no hot spots and no numbness in any region. In addition, the subject reported no headache, relaxed mental state, alert mental frame of mind, and attentive concentration level. In contrast, during the sixth hour the subject reported: (1) soreness in the head, upper neck, lower neck, shoulders and upper back, and discomfort in the lower back; (2) moderate hot spots in all the regions, but no numbness in any region. In addition, the subject reported severe headache, slightly tense, tired mental frame of mind, and distracted concentration level.

In the case of helmet C , the results derived from the filter bank could not be correlated to the perceived levels of discomfort reported by the subject because these discomfort levels were not found in the data provided by the AFRL. However, from the analysis of helmet C, it can be inferred that the right splenius is, during most of the time except for the fourth hour, the most fatigued muscle. In addition, it can be concluded that the neck muscles in the seventh hour are more fatigued than in the previous hours.

For the analysis of muscle fatigue when the subject wore helmet E, it can be inferred from Fig. 3.12 that most of the energy related to fatigue is concentrated in the fifth hour and sixth hour (32.8% in the fifth hour and 32.5% in the sixth hour). The second and the fourth hour show less fatigue (8% in the second hour and 11% in the fourth hour). The right splenius is the most fatigued muscle during the fifth and sixth hour. In regard to the questionnaire, the subject reported for the following regions (head, upper neck, lower neck, shoulders, upper back, lower back) in the second hour: (1) discomfort in the head, upper neck, lower neck, shoulders and upper back, and no discomfort in the lower back; (2) moderate hot spots in the upper neck, lower neck, shoulders and upper back; (3) no numbness in any region. In addition, the subject reported minimal headache, slightly tense, tired mental frame of mind, and attentive concentration level. In the fourth hour the subject reported: (1) soreness in head, upper neck, lower neck, shoulders and upper back, and no discomfort in the lower back; (2) moderate hot spots in the head, upper neck, lower neck, shoulders and upper back, and no hot spots in the lower back; (3) no numbness in any region. In addition, the subject reported severe headache, slightly tense, tired mental frame of mind, and distracted concentration level. Finally, in the sixth hour the subject felt a stronger fatigue reporting: (1) pain in the head, upper neck, lower neck, shoulders and upper back, and discomfort in the lower back; (2) severe hot spots in the head, upper neck, lower neck, shoulders and upper back, and moderate hot spots in the lower back; (3) no numbness in any region. In addition, the subject reported severe headache, restless mental state, exhausted mental frame of

mind, and loss of focus in the concentration level. Pain reported by this subject correlates the results obtained from the filter bank.

During this analysis of muscle fatigue, it is noted that the energy levels of fatigue are not consistent for all the helmets. It was expected that a higher energy in the stage of fatigue would be obtained when the subject wore helmet E instead of A. In addition, if a set of muscles are fatigued in the fifth and the sixth hour, it was expected that the same set of muscles would be fatigued in hour 7. However, this did not occur in the analysis.

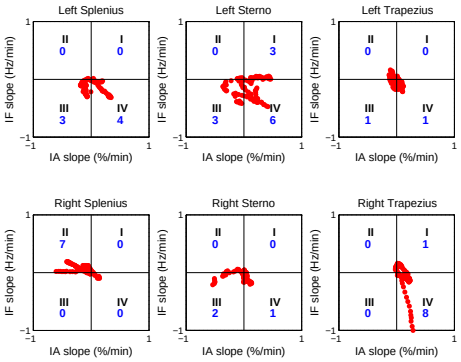

(a)

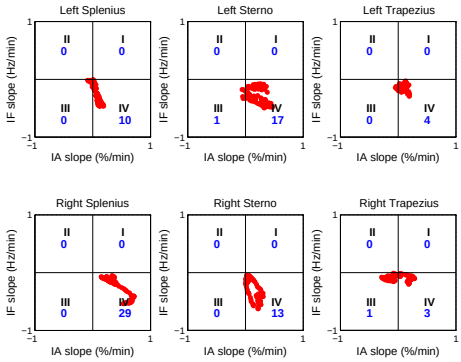

(b)

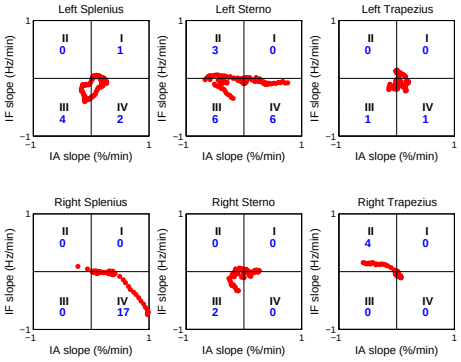

(c)

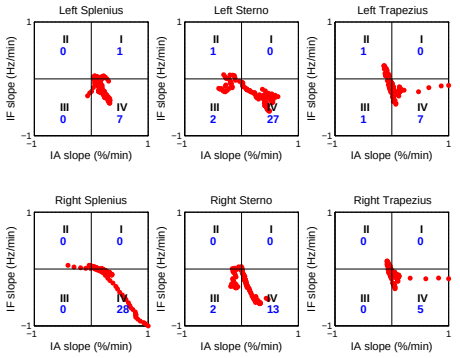

(d)

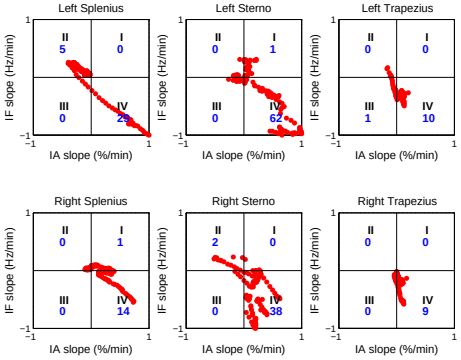

(e)

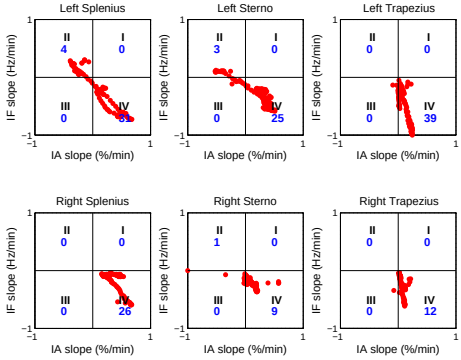

(f)

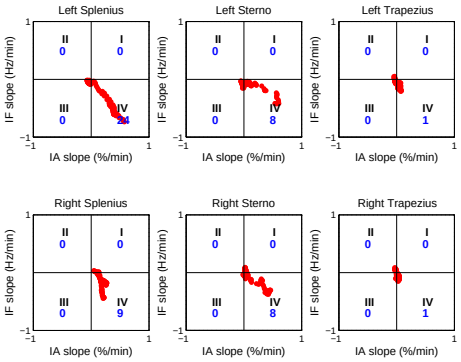

(g)

Figure 3.5 Joint analysis of frequency and amplitude for subject ID # NF F-1, test # NFF0001, cell A (3.0 Lb baseline CG). Stages (I) muscle increase force, (II) recovery, (III) muscle decrease force, (IV) fatigue. (a) hour 1, (b) hour 2, (c) hour 3, (d) hour 4, (e) hour 5, (f) hour 6, (g) hour 7. The numbers inside each quadrant (in blue) correspond to the energy of the slopes in that stage.

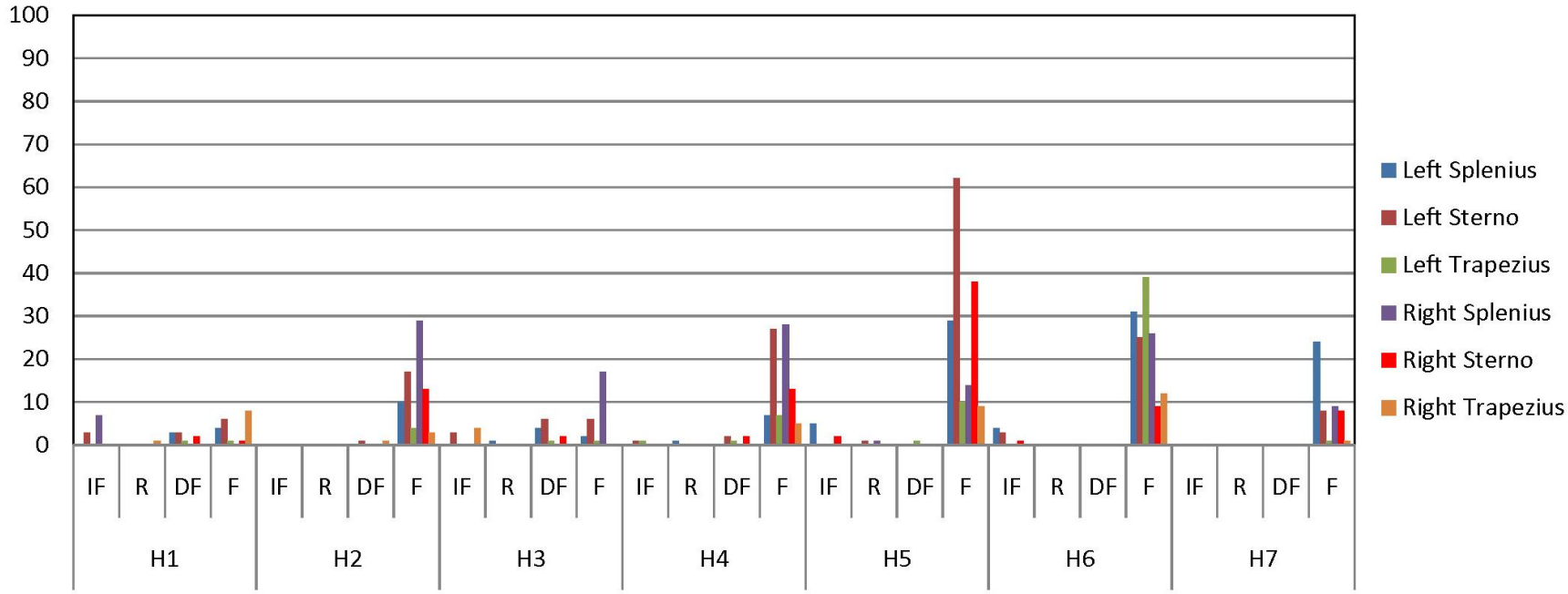

Figure 3.6 Analysis of muscle fatigue when the subject wore helmet A (3.0 Lb baseline CG). During the fifth and sixth hour, most of the energy is concentrated in muscle fatigue (28.72% in the fifth hour and 25.17% in the sixth hour). The first and second hour show less energy in the stage fatigue (3.55% in the first hour and 13% in the second hour). The left sterno is the most fatigued muscle during the eight hour session.

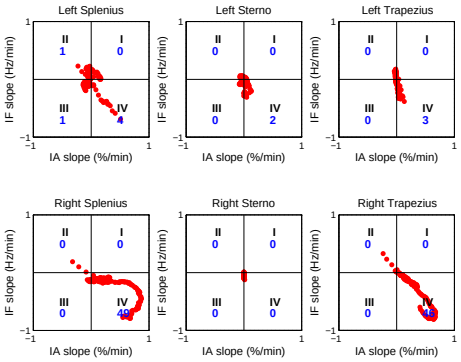

(a)

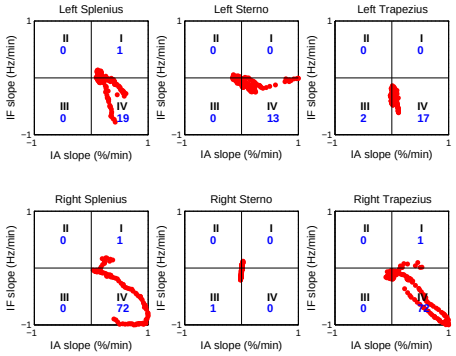

(b)

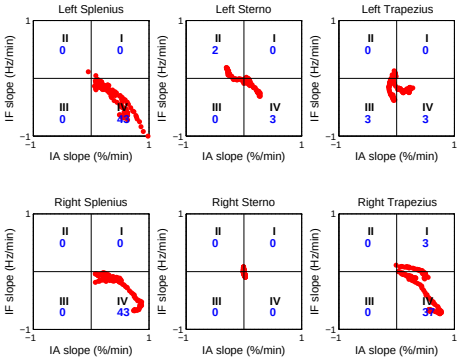

(c)

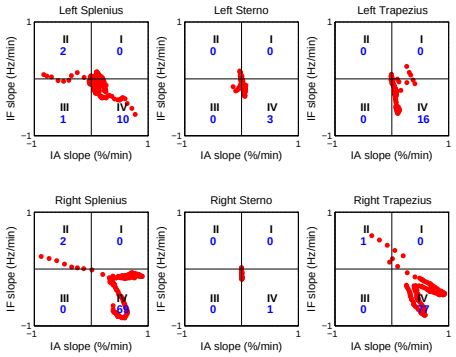

(d)

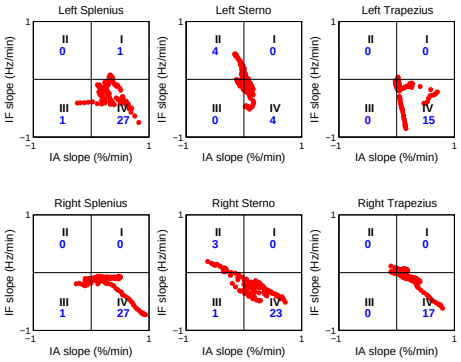

(e)

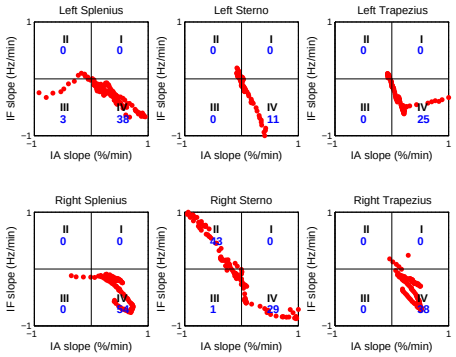

(f)

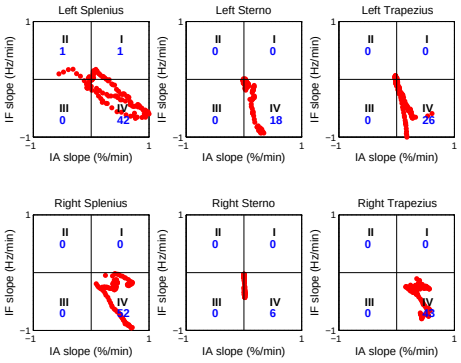

(g)

Figure 3.7 Joint analysis of frequency and amplitude for subject ID # NF F-1, test # NFF0002, cell B (4.5 Lb near head CG). Stages (I) muscle increase force, (II) recovery, (III) muscle decrease force, (IV) fatigue. (a) hour 1, (b) hour 2, (c) hour 3, (d) hour 4, (e) hour 5, (f) hour 6, (g) hour 7. The numbers inside each quadrant (in blue) correspond to the energy of the slopes in that stage.

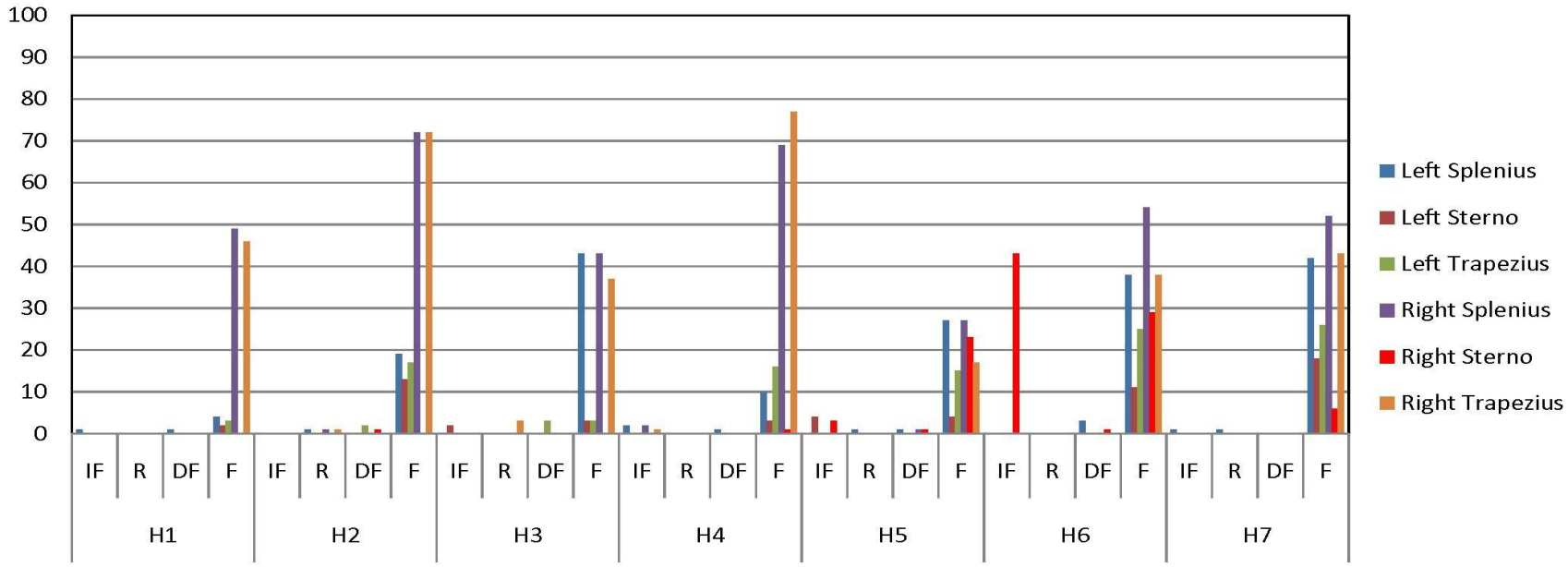

Figure 3.8 Analysis of muscle fatigue when the subject wore helmet B (4.5 Lb near head CG). The right splenius and right trapezius are the most fatigued muscles at the end of the first, second and fourth hour. The right sterno is the only muscle showing a recovery from previous muscle fatigue during the sixth hour. Most of the neck muscles present fatigue at the end of the fifth, sixth and seventh hour.

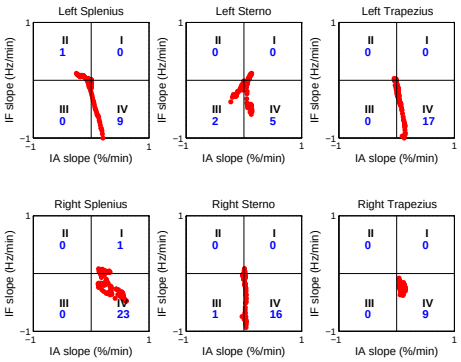

(a)

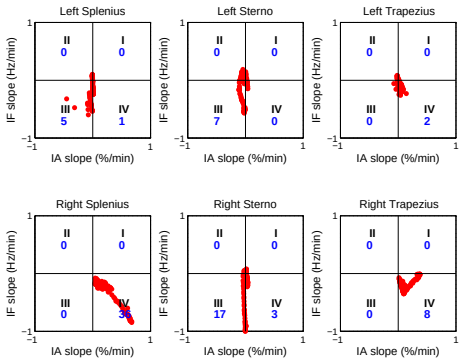

(b)

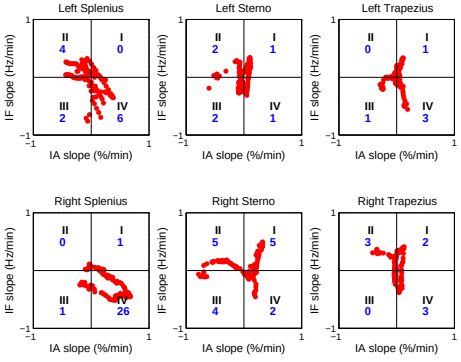

(c)

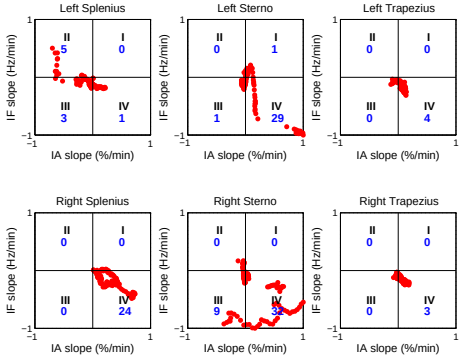

(d)

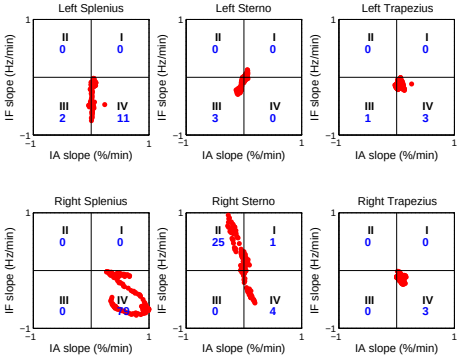

(e)

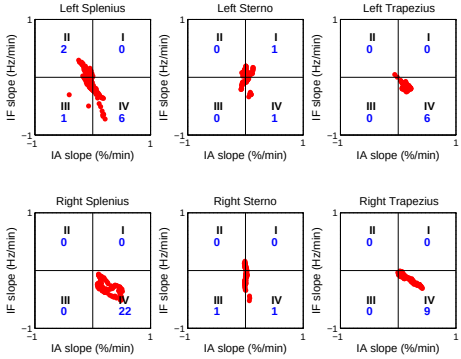

(f)

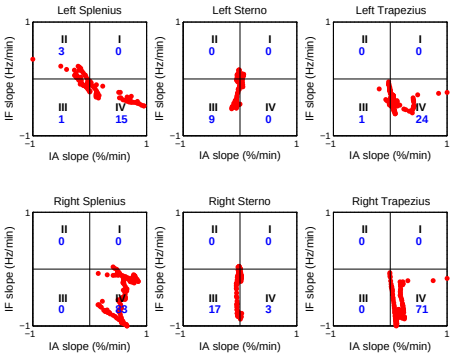

(g)

Figure 3.9 Joint analysis of frequency and amplitude for subject ID # NF F-1, test # NFF0024, cell C (4.5 Lb forward head CG). Stages (I) muscle increase force, (II) recovery, (III) muscle decrease force, (IV) fatigue. (a) hour 1, (b) hour 2, (c) hour 3, (d) hour 4, (e) hour 5, (f) hour 6, (g) hour 7. The numbers inside each quadrant (in blue) correspond to the energy of the slopes in that stage.

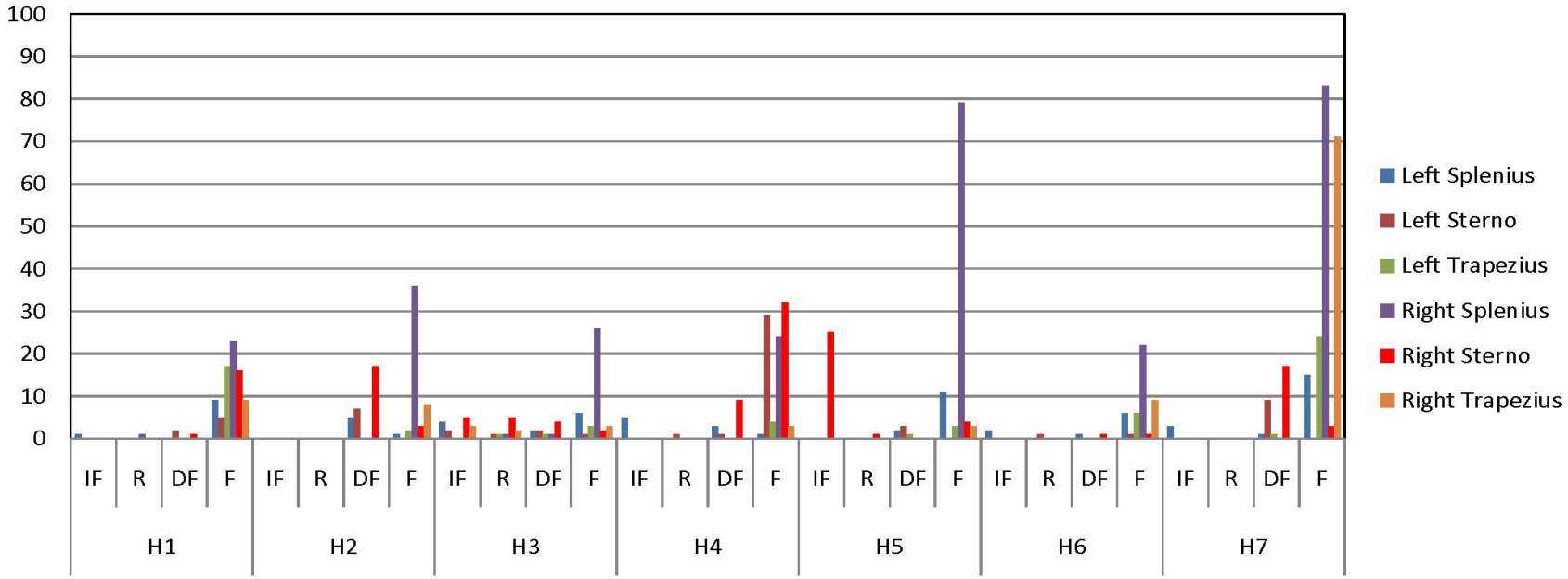

Figure 3.10 Analysis of muscle fatigue when the subject wore helmet C (4.5 Lb forward head CG). The right splenius is most of the time, except for the fourth hour, the most fatigued muscle.

Missing Data

(a)

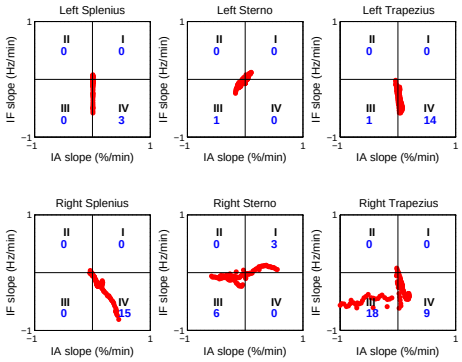

(b)

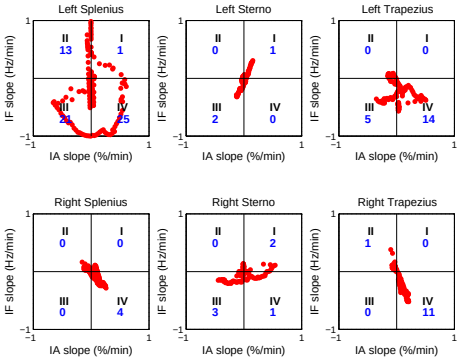

(c)

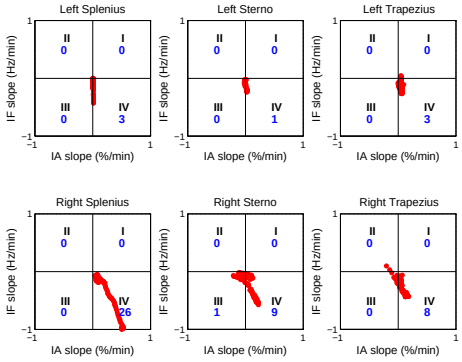

(d)

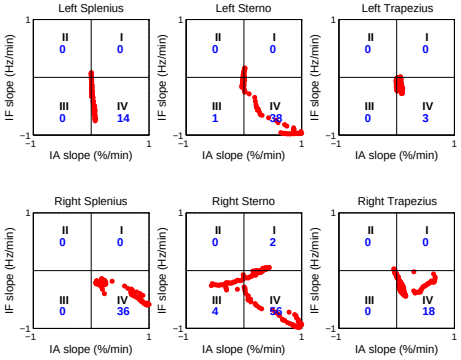

(e)

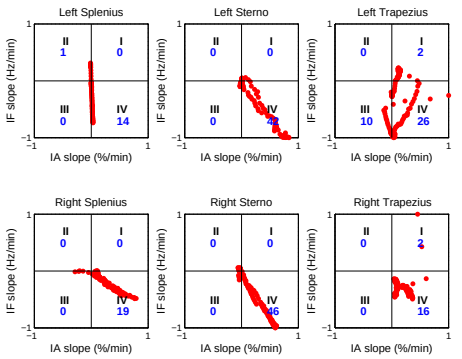

(f)

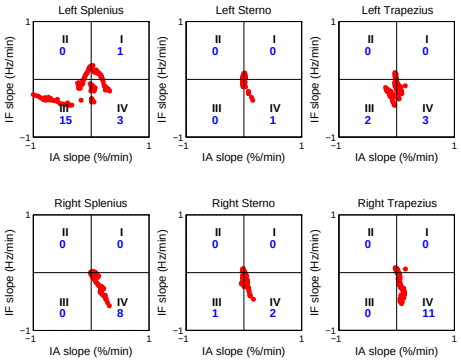

(g)

Figure 3.11 Joint analysis of frequency and amplitude for subject ID # NF F-1, test # NFF0060, cell E (6.0 Lb forward head CG). Stages (I) muscle increase force, (II) recovery, (III) muscle decrease force, (IV) fatigue. (a) hour 1, (b) hour 2, (c) hour 3, (d) hour 4, (e) hour 5, (f) hour 6, (g) hour 7. The numbers inside each quadrant (in blue) correspond to the energy of the slopes in that stage.

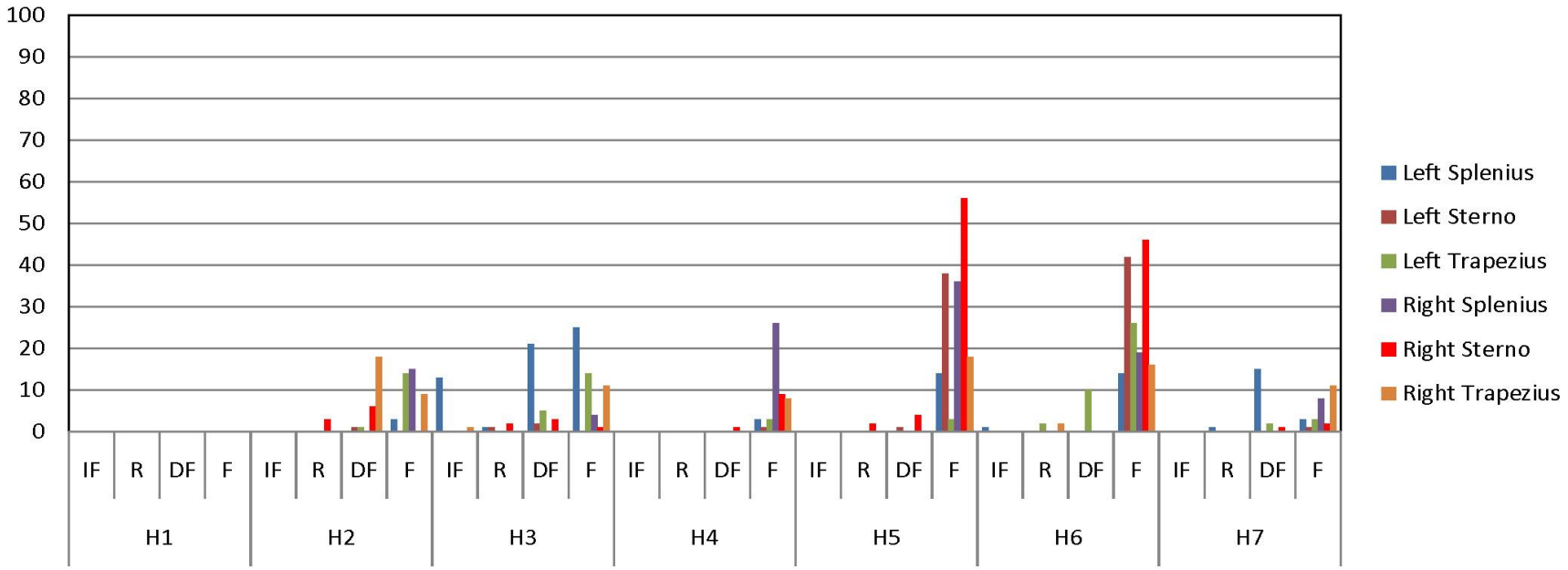

Figure 3.12 Analysis of muscle fatigue when the subject wore helmet E (6.0 Lb forward head CG). Most of the energy related to fatigue is concentrated in the fifth and sixth hour (32.8% in the fifth hour and 32.5% in the sixth hour). The second and fourth hour show less fatigue (8% in the second hour and 11% in the fourth hour). The right splenius is the most fatigued muscle during the fifth and sixth hour.

4
Conclusion

This project proposes a technique for estimating the instantaneous frequency (IF) and the instantaneous amplitude (IA) of a surface electromyographic (SEMG) signal by decomposing it using a 32-channel filter bank. Both the IF and IA should be used for the assessment of muscle fatigue, since in muscle fatigue the SEMG signal suffers a decrease in the IF and an increase in the IA. Then, by computing the IF and IA slopes, which measure their decrease or increase rate over time, the method of joint analysis of frequency and amplitude is used to classify the muscle activity into one of the following stages: increase force, recovery, decrease force, or fatigue.
The proposed method for the assessment of muscle fatigue has the advantage of being computationally less expensive than other standard techniques, such as the Wigner-Ville distribution (WVD), the spectrogram, the Choi-Williams distribution (CWD), and the smoothed pseudo Wigner-Ville distribution (SPWVD). The filter bank is window independent and provides a better cross term supression than the other evaluated techniques. In addition, the filter bank can be implemented by iterating a two channel filter bank used to compute the wavelet coefficients of the SEMG signal in a scheme also known as wavelet packets. The advantage of using a wavelet decomposition is that the estimation of the IF and IA can be combined with other techniques based on wavelet transforms such as baseline drift removal and signal noise reduction.
In the proposed method, the IF is estimated from the subbands of the filter bank as the first order moment of the time subband representation at a certain point in time. The IA is estimated also from the subbands of the filter bank, according to a proposed technique based on applying the outputs of the filters to successive, overlapping adaptive windows and determining the maximum coefficient from each window. The sum of the maximum coefficients for the different subbands then corresponds to a single IA estimate. From the computed IF and IA estimates, the slopes needed for the classification of muscle activity are then obtained by using a first order linear regression model for intervals of one minute every one second.
For evaluating the IF and IA slopes computed from the filter bank decomposition, two other standard techniques, the spectrogram and the SPWVD, were also implemented since they were shown to provide a better estimation of the IF and IA than the WVD and the CWD. From the spectrogram and the SPWVD, the IF was also estimated as the first order moment of the TF distribution, and the IA was estimated as the squared root of the time marginal.
During the performance tests, the IF and IA slopes were computed from the filter bank decomposition, the spectrogram, and the SPWVD of 3480 SEMG signals provided by the AFRL[1].

[1]The Kynesiology Lab from UTEP recorded SEMG signals from six lower back muscles, 4 hip muscles, and 4 hamstring muscles. The physical routines performed by the subjects in the Kynesiology Lab to analyze muscle fatigue

Slopes obtained from the filter bank decomposition were correlated and compared to the slopes obtained from the spectrogram and the SPWVD. In the case of the IF slopes computed with the filter bank, 94% showed correlation coefficients greater than 0.9 with respect to those slopes given by the spectrogram, and 88% showed correlation coefficients greater than 0.9 with respect to those slopes given by the SPWVD. In the case of the IA slopes computed with the filter bank, 97% showed correlation coefficients greater than 0.9 with respect to those slopes given by the spectrogram, and 100% showed correlation coefficients greater than 0.9 with respect to those slopes given by the SPWVD. These results verify that the slopes obtained from the filter bank show a strong correlation and the same trend as those given by the standard spectrogram and the SPWVD techniques.

The relative quadratic differences, when comparing the IF and IA slopes computed from the filter bank with those slopes computed from the spectrogram and the SPWVD, showed that 89.6% of the differences were less than 0.5%. This means that the slopes obtained from the filter bank not only show the same trend but also close values to those given by the spectrogram and the SPWVD.

For a few number of slopes, 3% of the results obtained from the data provided by the AFRL, neither the filter bank, the spectrogram, or the SPWVD showed equivalent slopes. This was attributed to the fact that the corresponding SEMG signals show high peak values at some samples due to poor placement of the electrodes or bad contact of the electrodes with the skin of the subject.

By using a joint analysis of frequency and amplitude, the IF and IA slopes obtained from the filter bank decomposition are classified into one of the following four stages: increase force, recovery, muscle decrease force or fatigue. The energy of the IF and IA slopes for each stage is proposed as an index to measure the intensity level of increase force, recovery, decrease force, or fatigue. The correlation between the measured energy in the fatigue stage and the perceived levels of discomfort reported by the subjects were then evaluated.

An extensive evaluation of the 3480 SEMG signals showed that the proposed filter bank decomposition is a suitable tool for determining muscle fatigue. In all the cases that the subject reported any discomfort or fatigue for a group of muscles, the proposed filter bank provided an index indicating muscle fatigue. However, this index is not linearly proportional to the intensity of fatigue felt by the subject. For instance, muscle fatigue was analyzed for a subject performing 70% MVC and wearing helmets A, B, C, and E during an eight-hour session. In this analysis was shown for all the analyzed helmets (A, B, C, and E) that the proposed filter bank decomposition always identified muscle fatigue which matched the reported perceived levels of discomfort.

were much lighter than the flight routines performed by the subjects in the AFRL experiment. As a result, perceived levels of discomfort reported by the subjects in the UTEP's Kinesiology Lab experiment reported no cases of muscle fatigue, in contrast to the AFRL experiment that reported cases of muscle fatigue. Therefore, the assessment of muscle fatigue used in this research was applied only to SEMG signals provided by the AFRL.

Higher indices of muscle fatigue were expected when the subject wore helmet E compared to helmet A, since helmet E was heavier. However, the indices of muscle fatigue obtained for helmet E were lower than helmet A.

A limitation of the experimental results is that the levels of discomfort were reported for certain regions (head, upper neck, lower neck, shoulders, upper back, and lower back) related to the analyzed neck muscles but not specifically for each muscle. Moreover, the discomfort levels are characteristic of the subject and can change depending on the mood, time, weather, and other factors that are involved during the collection of the SEMG signals. Therefore, it is important to correlate SEMG signals to other biomedical measurements such as blood sample, heart rate, and electroencephalographic (EEG) signals in order to create a more reliable index to measure the intensity of muscle fatigue felt by the subject.

Bibliography

[1] G. Balestra, S. Frassinelli, M. Knaflitz, and F. Molinari, "Time-frequency analysis of surface myoelectric signals during athletic movement," *Engineering in Medicine and Biology Magazine, IEEE*, vol. 20, pp. 106–115, 2001.

[2] B. Boashash, Ed., *Time-frequency Signal Analysis: Methods and Applications*. Longman Cheshire, 1992.

[3] P. Bonato, G. Giagliati, and M. Knaflitz, Analysis of myoelectric signals recorded during dynamic contractions,*IEEE Engineering in medicine and Biology*, vol. 15, pp. 102–111, 1996.

[4] P. Bonato, S. H. Roy, M. Knaflitz, and C. J. D. Luca, Time-frequency parameters of the surface myoelectric signal for assesing muscle fatigue during cyclic dynamic contractions, *IEEE Transactions on Biomedical Engineering*, vol. 48, pp. 745–753, 2001.

[5] A. Chaudhuri and P. O. Behan, "Fatigue in neurological disorders," *The Lancet*, vol. 363, pp. 978–988, 2004.

[6] L. Cohen, *Time-frequency Analysis*, A. V. Oppenheim, Ed. Prentice Hall Signal Processing Series, 1995.

[7] L. Debnath, Ed., *Wavelets and Signal Processing*. Birkhauser, 2003.

[8] J. Duchene, D. Devedeux, S. Mansour, and C. Marque, Analyzing uterine emg: Tracking instantaneous burst frequency, *IEEE Engineering in Medicine and Biology*, vol. 14, pp. 125–132, 1995.

[9] D. Farina and R. Merletti, Comparison of algorithms for estimation of emg variables during voluntary isometric contractions, *Journal of electromyography and kynesiology*, vol. 10, pp. 337–349, 2000.

[10] A. Georgakis, L. K. Stergioulas, and G. Giakas, "Fatigue analysis of the surface emg signal in isometric constant force contractions using the averaged instantaneous frequency," *IEEE Transactions on Biomedical Engineering*, vol. 50, pp. 262–265, 2003.

[11] J. S. Karlsson, B. Gerdle, and M. akay, Analyzing surface myoelectric signals recorded during isokinetic contractions, *IEEE Engineering in Medicine and Biology*, vol. 20, pp. 97–105, 2001.

[12] S. Karlsson, J. Yu, and M. Akay, "Spectral analysis of myoelectric signals by wavelet methods," *2nd International Conference on Bioelectromagnetism*, pp. 33–34, 1998.

[13] S. Karlsson, J. Yu, and M. Akay, Time-frequency analysis of myoelectric signals during dynamic contractions: A comparative study, *IEEE Transactions on Biomedical Engineering*, vol. 47, pp. 228–238, 2000.

[14] J. Kilby and H. Gholam, "Wavelet analysis of surface electromyography signals," *Proceedings of the 26th annual international conference of the IEEE EMBS*, pp. 384–387, 2004.

[15] G. Kim, M. A. Ahad, M. Ferdjallah, and G. F. Harris, "Correlation of muscle fatigue indices between intramuscular and surface emg signals," *SoutheastCon, 2007. Proceedings. IEEE*, pp. 378–382, 2007.

[16] P. Konrad, "The abc of emg," 2005.

[17] S. Krishnan, "Instantaneous mean frequency estimation using adaptive time-frequency distributions," *IEEE*, vol. 1, pp. 141–146, 2001.

[18] D. K. Kumar, N. D. Pah, and A. Bradley, "Wavelet analysis of surface electromyography to determine muscle fatigue," *IEEE Transactions on neural systems and rehabilitation engineering*, vol. 11, pp. 400–406, 2003.

[19] A. Luttmann, M. Jager, and W. Laurig, Electromyographical indication of muscular fatigue in occupational field studies, *International journal of Industrial ergonomics*, vol. 25, pp. 645–660, 2000.

[20] A. Luttmann, M. Jager, J. Sokeland, and W. Laurig, Electromyographical study on surgeons in urology. ii. determination of muscular fatigue, *Ergonomics*, vol. 39, pp. 298–313, 1996.

[21] R. Merletti and P. A. Parker, *Electromyography: Physiology, Engineering, and Noninvasive Applications*, M. Akay, Ed. IEEE Press Series in Biomedical Engineering, 2004.

[22] P. Oliveira and V. Barroso, "Definitions of instantaneous frequency under physical constraints," *Journal of the Franklin Institute*, vol. 37, pp. 303–316, 2000.

[23] A. Papandreou-Suppappola, Ed., *Applications in time-frequency signal processing*. CRC Press, 2003.

[24] S. Pola, A. Macerata, M. Emdin, and C. Marchesi, "Estimation of the power spectral density in nonstationary cardiovascular time series: Assesing the role of the time-frequency representations (tfr)," *IEEE Transactions on Biomedical Engineering*, vol. 43, pp. 46–59, 1996.

[25] C. U. Ranniger and D. L. Akin, "EMG mean power frequency determination using wavelet analysis," *Proceedings of the 19th IEEE/EMBS*, pp. 1589–1592, 1997.

[26] M. B. I. Reaz, M. Hussain, and F. Mohd-Yasin, "Techniques of emg signal analysis: detection, processing, classification and applications," *Biological procedures online*, pp. 11–35, 2006.

[27] P. J. Sparto, M. Parnianpour, E. A. Barria, and J. M. Jagadeesh, "Wavelet and short-time fourier transform analysis of electromyography for detection of back muscle fatigue," *IEEE Transactions on Rehabilitation Engineering*, pp. 433–436, 2000.

[28] T. Thayaparan, "Decomposition of time-varying multicomponent signals using time-frequency based method," *IEEE CCECE/CCGEI*, pp. 60–63, 2003.

[29] V. Tscharner, "Intensity analysis in time-frequency space of surface myoelectric signals by wavelets of specified resolution," *Journal of electromyography and kynesiology*, pp. 433–445, 2000.

[30] H. Xie and Z. Wang, Mean frequency derived via hilbert-huang transform with application to fatigue emg signal analysis, *Computer methods and programs in biomedicine*, vol. 82, pp. 114–120, 2006.

[31] A. A. zaman and M. A. Ahad, "A new approach for muscle fatigue analysis in young adults at different mvc levels," *IEEE*, vol. 1, pp. 499 – 502, 2005.

[32] A. Al zaman, M. Khan, T. Sharmin, and M. Ferdjallah, "Muscle fatigue analysis in young adults at different mvc levels using emg metrics," *SoutheastCon, 2007. Proceedings. IEEE*, pp. 390–394, 2007.

[33] A. A. zaman, M. Ferdjallah, and A. Khamayseh, "Muscle fatigue analysis for healthy adults using tvar model with instantaneous frequency estimation," *Proceedings of the 38th Southeastern symposium on system theory*, pp. 44–47, 2006.

[34] Z. Zhidong, M. Pam, and Y. Chen, "Instantaneous frequency estimate for non-stationary signal," *Proceedings of the 5th World Congress on Intelligent Control and Automation*, pp. 3641–3643, 2004.

Appendix A
Toolbox

Algorithm 1 Compute the instantaneous frequency and the instantaneous amplitude

Input:

- Define the signal $x[n]$, $\forall\, n = 0, 1, 2, 3, \ldots, L-1$, where L is the length of the signal
- Define a filter bank $h[f, n]$, $\forall\, n = 0, 1, 2, 3, \ldots, M-1$ and $f = 0, 1, 2, 3 \ldots, F-1$, where M is the length of each filter and F is the number of subbands. The filter f_0 is a low pass filter and the filter f_{F-1} is a high pass filter. In this tool box all the filters have the same length

Output:

- Instantaneous frequency $\hat{f}[n]$
- Instantaneous amplitude $i_a[n]$

Compute the subband coefficients $\hat{y}[f, n]$ convolving the input $x[n]$ with the filter bank $h[f, n]$; $\hat{y}[f, n] = x[n] * h[f, n]$. The resulting output $\hat{y}[f, n]$ is defined $\forall\, n = 0, 1, 2, 3, \ldots, L + M - 2$ and $f = [0, 1, 2, 3, \ldots, F-1]\frac{1}{2F}$

Define the output $y[f, n]$ as
$y[f, n] = \hat{y}[f, n + \frac{M}{2}]$, $\forall\, n = 0, 1, 2, 3, \ldots, L-1$

Compute the time subband representation as
$y[f, n] = (y[f, n])^2$

Compute the time marginal $m[n]$ as

$$m[n] = \sum_{f=0}^{F-1} y[f, n]$$

Compute the instantaneous frequency $\hat{f}[n]$ as

$$\hat{f}[n] = \frac{\sum_{f=0}^{F-1} f y[f, n]}{m[n]}$$

Compute the instantaneous amplitude $i_a[n]$ as

for $f = 0$ to $F - 1$ **do**
  $\tau = \text{ceil}(\frac{2F}{f+1})$, $k = 0$, flag$= 1$
  while flag$\neq 0$ **do**
    $s_{f,k}[n] = y[f, n + k]$; $\forall\, n = 0, 1, 2, 3, \ldots, \tau - 1$
    $\psi[f, k] = \max(s_{f,k}[n])$
    $r = L + M - 1 - k$
    if $r = 0$ **then**
      $flag = 0$
    else
      $k = k + 1$
    end if
  end while
end for

$$i_a[n = k] = \sum_{f=0}^{F-1} \psi[f, k]$$

Matlab Functions Content

The following functions shown in Table A.1 are implemented in Matlab. These functions are used in this research to assess muscle fatigue.

Table A.1 Matlab functions used in the assessment of muscle fatigue.

Matlab Function	Purpose
gfb	Generate the analysis filter bank
f_filter_bank_ana	Compute the subband outputs of the filter bank
tsub	Arrange all the computed subband coefficients in a matrix form
inst_freq	Compute the instantaneous frequency of a given signal
inst_amp	Compute the instantaneous amplitude of a given signal
windowing	Compute the start and end indexes of the location of a rectangular moving window
linear_regression	Estimate the slopes and points of interception
jasa_analysis	Compute the JASA method to an electromyography signal

gfb

Purpose

Generate the analysis filter bank.

Synopsis

```
[fltana, indfltana]=gfb(n_sb)
```

Description

`gfb` generates the analysis filterbank. For this toolbox the number of subbands `n_sb` can be $16, 32$ or 64. We can represent the filterbank in matrix form by $h[f,n]$=`fltana`$(fM_f + n + 1)$ for f=$0, 1, 2, 3, \ldots, F-1$ and n=$0, 1, 2, 3, \ldots, M_f - 1$ where F is the number of subbands `n_sb` and M_f is the length of the filter in subband f. The length of the filter f can be computed from `indfltana` using M_f=`indfltana`$(f+1)-$`indfltana`(f) for $f > 0$, and `indfltana`$(f+1)$ for f=0. The output `indfltana` is required only when the filters have different length. In this project all the filters used had length equal to 128 coefficients.

Name	Description	Default value
`n_sb`	number of subbands	32
`fltana`	column vector with the coefficients of the analysis filter bank	
`indfltana`	column vector with the index of the end of each filter	

Example

```
[fltana, indfltana]=gfb(32);
hn=reshape(fltana,128,32);
Hw=fft(hn,512);
w=linspace(0,1,256);
plot(w,abs(Hw(256:511,:)));
xlabel('$\frac{\omega}{\pi}$', 'fontsize',14,...
'interpreter', 'latex');
ylabel('$|H(\omega)|$', 'fontsize', 14,...
'interpreter', 'latex'); grid on
```

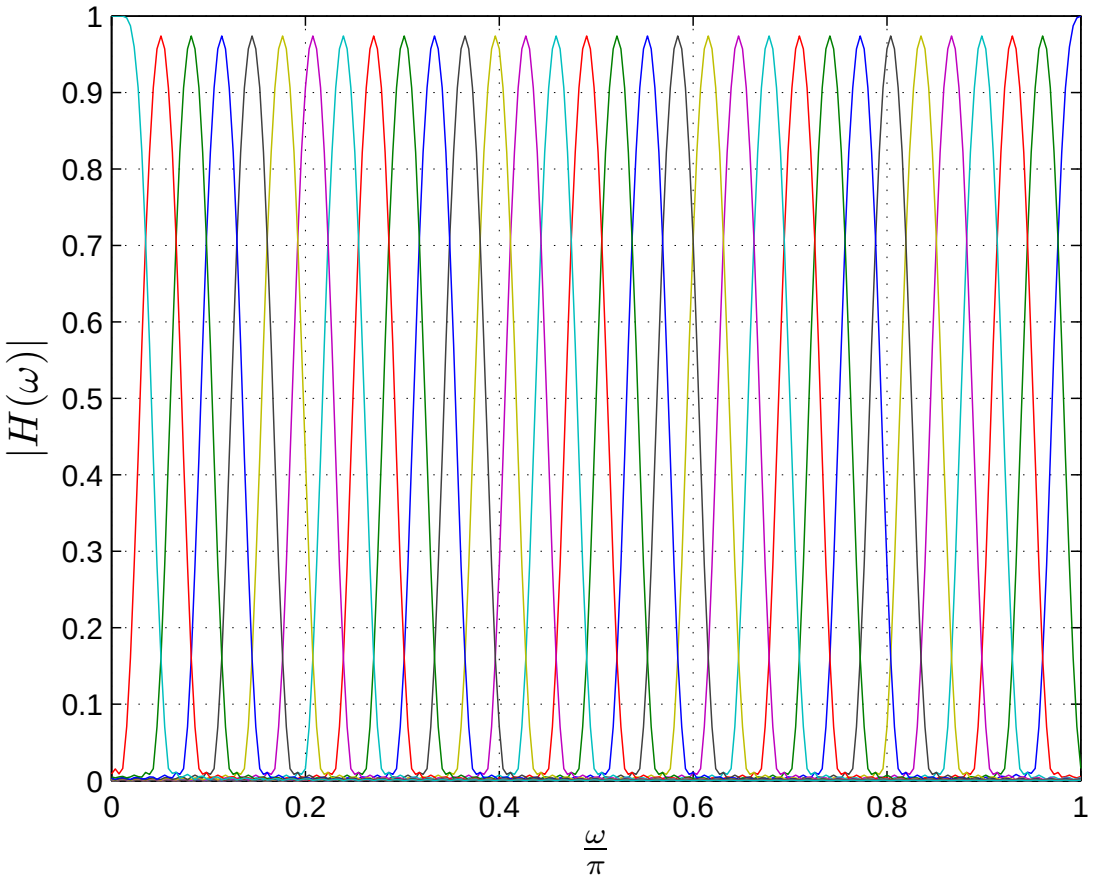

Figure A.1 Frequency response of the analysis filterbank (32 subbands) used in the estimation of the IF and the IA of the SEMG signal.

f_filter_bank_ana

Purpose

Compute the subband outputs of the filter bank.

Synopsis

```
[s0, is0]=f_filter_bank_ana(sig,fltana,indfltana)
```

Description

`f_filter_bank_ana` computes the subband coefficients `s0` by convolving the signal `sig` with the filter coefficients `fltana`. Representing the input signal as $x[n]$, for n=$0, 1, 2, 3, \ldots, L-1$ where L is the length of the signal, then we have $x[n]$=`sig`$(n+1)$. The output $y[f, n]$, for f=$0, 1, 2, 3, \ldots, F-1$ and n=$0, 1, 2, 3, \ldots, L+M_f-2$ where F is the number of subbands `n_sb` and M_f is the length of the filter in subband f, is given by $y[f, n]$=`s0`$($`is0`$(f)+n+1)$, for $f > 0$ and `s0`$(n+1)$, for f=0.

Name	Description	Default value
`sig`	column vector of size $L \times 1$ with the coefficients of the input signal	
`fltana`	column vector of size $F\,M_f \times 1$ with the coefficients of the analysis filter bank	
`indfltana`	column vector of size $F \times 1$ with the index of the end of each filter	
`s0`	column vector of size $\sum_{f=0}^{F-1}(L+M_f-1) \times 1$ with the coefficients of each subband	
`is0`	column vector of size $F \times 1$ with the index of the end of each subband	

Example

```
load 'NFF0001_H1_70_EMG'

[sig]=data(:,2);

[fltana, indfltana]=gfb(32);

[s0, is0]=f_filter_bank_ana(sig,fltana,indfltana);
```

See Also

`gfb`.

tsub

Purpose

Arrange all the computed subband coefficients in a matrix form of size $F \times L$.

Synopsis

```
[tfr]=tsub(s0, is0, shift);
```

Description

`tsub` arranges in a time subband matrix representation all the subband coefficients. This function assumes that all the filters have equal length. The time subband coefficients $y[f,n]$ for f=$0,1,2,3,\ldots,F-1$ and n=$0,1,2,3,\ldots,L+M_f-2$ where F is the number of subbands `n_sb`, L is the length of the signal `sig` and M_f is the length of the filter in subband f is given by $y[f,n]$=`tfr`$(f+1,n+1)$.

Name	Description	Default value
`s0`	column vector of size $\sum_{f=0}^{F-1}(L+M_f-1)\times 1$ with the coefficients of each subband	
`is0`	column vector of size $F \times 1$ with the index of the end of each subband	
`shift`	vector of length two with the number of coefficients to remove from the output `s0` to compensate the increase in the length of the subbands produced by the convolution operation	
`tfr`	time subband matrix representation	

Example

```
load 'NFF0001_H1_70_EMG'

[sig]=data(:,2);

[fltana, indfltana]=gfb(32);

N=length(fltana)/length(indfltana);

shift=[round(N/2),round(N/2)];

[s0, is0]=f_filter_bank_ana(sig,fltana,indfltana);

[tfr]=tsub(s0, is0, shift);
```

See Also

`gfb`, `f_filter_bank_ana`.

inst_freq

Purpose

Compute the instantaneous frequency of a given signal.

Synopsis

```
[fm]=inst_freq(tfr);
```

Description

`inst_freq` computes the instantaneous frequency `fm` from the time subband matrix representation `tfr`. The instantaneous frequency $\hat{f}[n]$ at time n=$0, 1, 2, 3, \ldots, L-1$ is given by $\hat{f}[n]$=`fm`$(n+1)$.

$$\hat{f}[n] = \frac{\sum_{f=0}^{F-1} fy[f,n]}{\sum_{f=0}^{F-1} y[f,n]}$$

Name	Description	Default value
`tfr`	time subband matrix representation of size $F \times L$	
`fm`	column vector of size $L \times 1$ with the instantaneous frequency components	

Example

```
load 'NFF0001_H1_70_EMG'
[sig]=data(:,2);
[fltana, indfltana]=gfb(32);
N=length(fltana)/length(indfltana);
shift=[round(N/2),round(N/2)];
[s0, is0]=f_filter_bank_ana(sig,fltana,indfltana);
[tfr]=tsub(s0, is0, shift);
[fm]=inst_freq(tfr);
t=(1:length(sig))/(60*1024); plot(t, fm.*1024);
axis([1 3 0 511]); grid on;
xlabel('Time (min)', 'fontsize', 14, ...
'interpreter', 'latex');
ylabel('Frequency (Hz)', 'fontsize', 14, ...
'interpreter', 'latex');
```

See Also

gfb, f_filter_bank_ana, tsub.

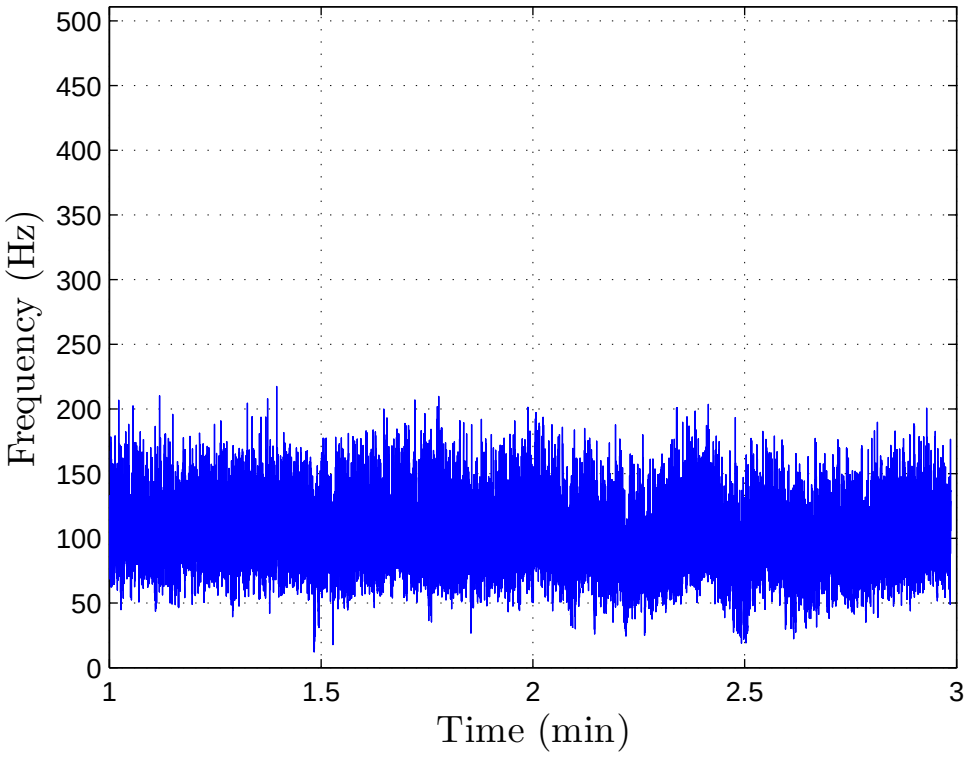

Figure A.2 Computed instantaneous frequency of the input signal `sig` by using 32 channels filter bank.

inst_amp

Purpose

Compute the instantaneous amplitude of a given signal.

Synopsis

```
[i_amp]=inst_amp(tfr);
```

Description

`inst_amp` computes the instantaneous amplitude `i_amp` from the time subband matrix representation `tfr`. The instantaneous amplitude $i_a[n]$ at time n=$0, 1, 2, 3, \ldots, L-1$ is given by $i_a[n]$=`i_amp`$(n+1)$.

Name	Description	Default value
`tfr`	time subband matrix representation of size $F \times L$	
`i_amp`	column vector of size $L \times 1$ with the instantaneous amplitude components	

Example

```
load 'NFF0001_H1_70_EMG'
[sig]=data(:,2);
[fltana, indfltana]=gfb(32);
N=length(fltana)/length(indfltana);
shift=[round(N/2),round(N/2)];
[s0, is0]=f_filter_bank_ana(sig,fltana,indfltana);
[tfr]=tsub(s0, is0, shift);
[i_amp]=inst_amp(tfr);
t=(1:length(sig))/(60*1024);  plot(t, i_amp);
axis([1 3 0 max(i_amp)]); grid on;
xlabel('Time (min)', 'fontsize', 14, ...
'interpreter', 'latex');
ylabel('Amplitude', 'fontsize', 14, ...
'interpreter', 'latex');
```

See Also

gfb, f_filter_bank_ana, tsub.

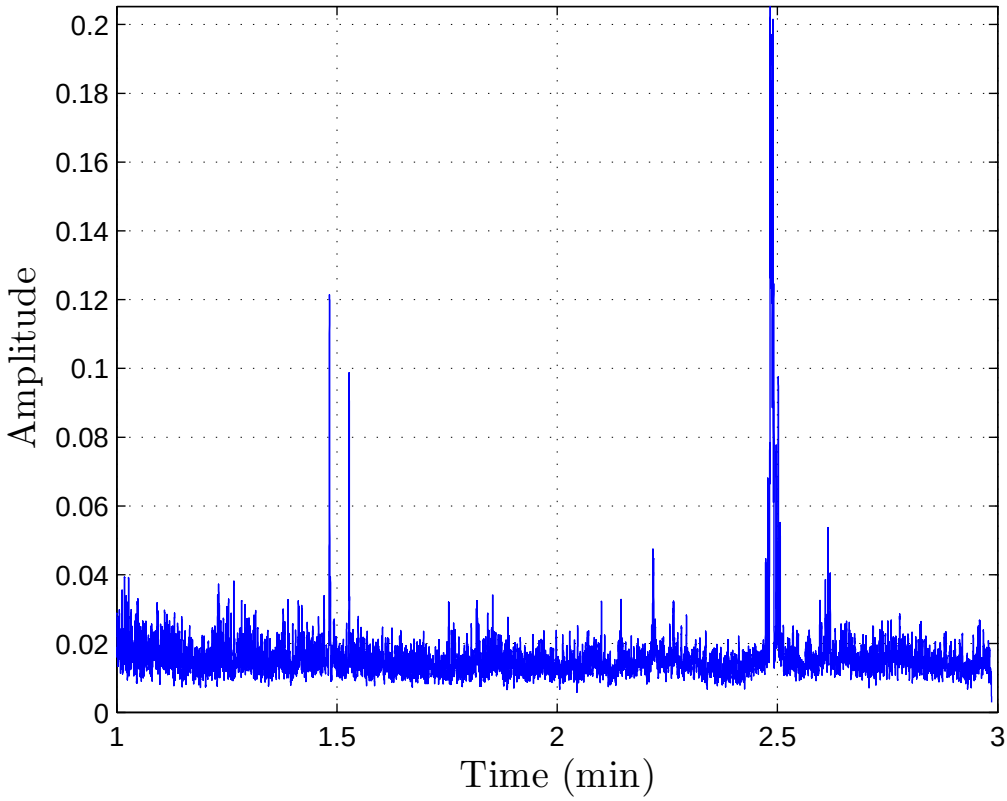

Figure A.3 Computed instantaneous amplitude of the input signal `sig` by using 32 channels filter bank.

windowing

Purpose

Compute the start and end indexes of the location of a rectangular moving window for a specified shift amount.

Synopsis

```
[index_start, index_end]=windowing(nc, L, shift, option)
[index_start, index_end]=windowing(nc, L, shift)
[index_start, index_end]=windowing(nc, L)
```

Description

`windowing` computes the start and end indexes of the location of a rectangular moving window for a specified shift amount. This function is useful when we want to apply a rectangular window to a signal of length `L`.

Name	Description	Default value
`nc`	size of the rectangular window, for $1 \leq$ `nc` $\leq$ `L`	
`L`	length of the signal	
`option`	if $\rightarrow 1$ (`index_end` $-$ `index_start`) is always `nc`. The rectangular window is not zero padded at the end of the signal.	1
	if $\rightarrow 0$ (`index_end` $-$ `index_start`) is not always `nc`. The rectangular window is zero padded at the end of the signal.	
`shift`	shifted window, for $1 \leq$ `shift` $\leq$ nc	`nc`
`index_start`	column vector with the start indexes	
`index_end`	column vector with the end indexes	

Example

```
% Let us suppose that we want to apply a rectangular
% window of 5 points with a shift of  3 to a signal of
% length 15
nc=5; L=15; shift=3;
% when option=1
option=1;
[index_start_1,index_end_1]=windowing(nc, L, shift, option);
% when option=0
option=0;
[index_start_0,index_end_0]=windowing(nc, L, shift, option);

% Output of the code above when option=1
display('index_start_1');

index_start_1 =

     1     4     7    10

display('index_end_1');

index_end_1 =

     5     8    11    14

% Output of the code above when option=0
display('index_start_0');

index_start_0 =

     1     4     7    10    13

display('index_end_0');

index_end_0 =

     5     8    11    14    15
```

linear_regression

Purpose

Estimate the slopes and points of interception.

Synopsis

```
[p]=linear_regression(s, Fs, ns, shift)
```

```
[p]=linear_regression(s, Fs, ns)
```

Description

`linear_regression` estimates the slopes (a_i) and points of interception (b_i) of a piecewise approximation $a_i t + b_i$, for the time interval $t \in [t_{i0}, t_{i1}]$ of the input data.

Name	Description	Default value
`s`	input data	
`Fs`	sampling frequency	
`ns`	size of the interval $[t_{i0}, t_{i1}]$	
`shift`	shifted window, for $1 \leq$ `shift` $\leq$ `length(s)`. The intervals of the linear approximation may overlap	`1`
`p`	matrix where the first column corresponds to the slopes and the second column to the points of interceptions	

Example

```
  load lt_splenius
  % to compute the instantaneous frequency slopes
  s=fm; % the instantaneous frequency fm is the output
  % of the function inst_freq.m
  Fs=1024;
  ns=60*1024; %1 sec = 1024 samples; then 60*1024 = 1 minute
  shift=1024; %shift every minute
  [p]=linear_regression(s, Fs, ns, shift);
  t=linspace(1,3,size(p,1));
  plot(t, p(:,1),'r-','linewidth',3); grid on
  xlabel('Time (min)', 'fontsize', 14, ...
  'interpreter', 'latex');
  ylabel('Slope (Hz/min)', 'fontsize', 14, ...
  'interpreter', 'latex');
% to compute the instantaneous amplitude
s=i_amp; % the instantaneous amplitude i_amp is
% the output of the function inst_amp.m
Fs=1024;
ns=60*1024; %1 sec = 1024 samples; then 60*1024 = 1 minute
shift=1024; %shift every minute
[p]=linear_regression(s, Fs, ns, shift);
t=linspace(1,3,size(p,1));
plot(t, p(:,1)*60*100,'r-','linewidth',3); grid on
xlabel('Time (min)', 'fontsize', 14, ...
'interpreter', 'latex');
ylabel('Slope(\%/min)', 'fontsize', 14, ...
'interpreter', 'latex');
```

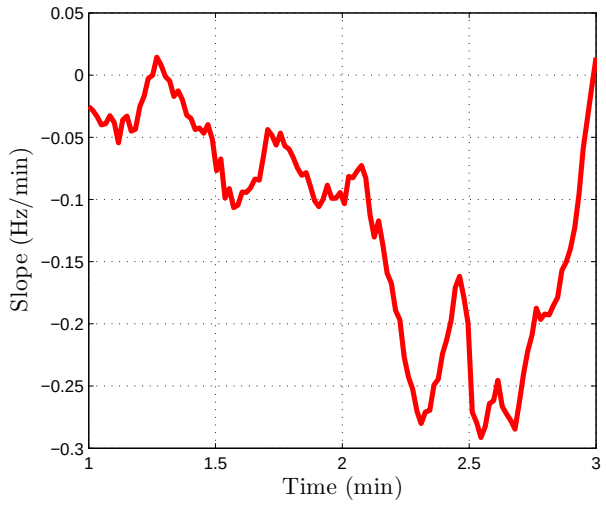

Figure A.4 Instantaneous frequency slopes from the estimated IF.

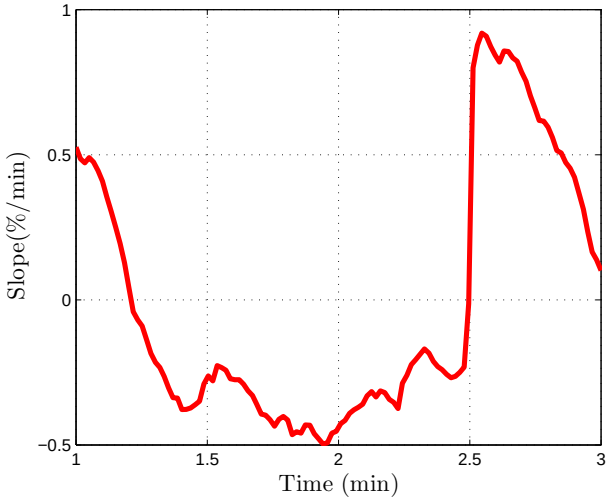

Figure A.5 Instantaneous amplitude slopes from the estimated IA.

jasa_analysis

Purpose

Compute a joint analysis of the spectrum and the amplitude (JASA) of a electromyography signal.

Synopsis

```
[i_f, r, d_f, f]=jasa_analysis(s_inst_amp, s_inst_freq)
```

Description

`jasa_analysis` computes a joint analysis of the spectrum and the amplitude of a electromyography signal (JASA) from the instantaneous frequency and the instantaneous amplitude slopes to compute indexes of muscle increase force, recovery, muscle decrease force and fatigue.

Name	Description	Default value
`s_inst_amp`	instantaneous amplitude slopes	
`s_inst_freq`	instantaneous frequency slopes	
`i_f`	Index corresponding to the energy of muscle increase force	
`r`	Index corresponding to the energy of recovery	
`d_f`	Index corresponding to the energy of muscle decrease force	
`f`	Index corresponding to the energy of fatigue	

Example

```
load lt_splenius
% to compute the instantaneous frequency and the
% instantaneous amplitude slopes
Fs=1024;
sample_interval=60*1024;
%1 sec = 1024 samples; then 60*1024 = 1 minute
shift=1024; %shift every second
[p]=linear_regression(fm, Fs, sample_interval, shift);
lr_f=p(:,1);
[p]=linear_regression(i_amp, Fs, sample_interval, shift);
lr_ia=p(:,1);
[increase_force, recovery, decrease_force, fatigue]=...
jasa_analysis(lr_i, lr_f);

% Output of the code above

increase_force =

    0.8333

recovery =

    1.6667

decrease_force =

   62.5000

fatigue =

    35
```

Appendix B
Questionnaire

Questionnaire to report the perceived levels of discomfort reported by the subject (source — AFRL)

Q1 Have you performed any of the stretching techniques in the last two hours ? (Yes=0, No=6)

Q2 According to the scale, select a number that corresponds to your physical state. (0=No Discomfort, 2=Discomfort, 4=Soreness, 6=Pain)

a Head

b Upper Neck

c Lower Neck

d Shoulders

e Upper Back

f Lower Back

Q3 According to the scale, select a number that corresponds to hot spots or accumulation of perspiration (No Hot Spots, Moderate Hot Spots, Severe Hot Spots).

a Head

b Upper Neck

c Lower Neck

d Shoulders

e Upper Back

f Lower Back

Q4 According to the scale, select a number that corresponds to any numbness or loss of sensation. (0=Normal, 3=Abnormal Sensation, 6=Numbness)

a Head

b Upper Neck

c Lower Neck

d Shoulders

e Upper Back

f Lower Back

Q5 According to the scale, select a number that corresponds to a penetrating ache in your head. (0=No Headache, 3=Minimal Headache, 6=Severe Headache)

Q6 According to the scale, select a number that corresponds to your mental state. (0=Relaxed, 3=Slightly Tense, 6=Restless)

Q7 According to the scale, select a number that corresponds to your mental frame of mind. (0=Alert, 3=Tired, 6=Exhausted)

Q8 According to the scale, select a number that corresponds to your concentration level. (0=Attentive, 3=Distracted, 6=Loss of Focus)

Q9 According to the scale, select a number that corresponds to the effort exerted to perform the MVC at 70%. (0=No Effort, 3=Minimal Effort, 6=Maximal Effort)

Appendix C
Matlab Code

```
% function [fltana, indfltana]= gfb(n_sb);
% Purpose:
% Generate the analysis filterbank. For this toolbox the number of subbands
% n_sb can be 16, 32 or 64. We can represent the filter bank in matrix form
% by h[f,n]=fltana(f*Mf+n+1)for f=0,1,2,...F-1 and n=0,1,2,...Mf-1 where F
% is the number of subbands n_sb and Mf is the length of the filter in
% subband f. The length of the filter f can be computed from indfltana
% using Mf=indfltana(f+1)-indfltana(f) for f>0, and indfltana(f+1) for f=0.
% The output indfltana is required only when the filters have different
% length. In this project all the filters used had length equal to 128
% coefficients.
% Synopsis:
% [fltana, indfltana]= gfb(n_sb);
% input vector:
% n_sb:number of subbands
% output vector:
% fltana: column vector with the coefficients of the analysis filter bank
% indfltana: column vector with the index of the end of each filter
% Example:
% fltana, indfltana]=gfb(32);
% hn=reshape(fltana,128,32);
% Hw=fft(hn,512);
% w=(-1:2/511:1);
% plot(w,abs(Hw)); xlabel('$\frac{\omega}{\pi}$','interpreter','latex');
% ylabel('$|H(\omega)|$','interpreter','latex'); grid on
% #Author: Cristhian Potes
% #Date:   May 23, 2007

function [fltana, indfltana]= gfb(n_sb);
if n_sb==16 | n_sb==32 | n_sb==64
filter{1,1}=['filterbank_' num2str(n_sb) 'subbands'];
load(filter{1,1});
filterbank=filterbank';
[N,M]=size(filterbank);
fltana=filterbank(:);
indfltana=(N:N:M*N)';
else
disp('Number of subbands has to be 16, 32, or 64');
fltana=[];
indfltana=[];
end
```

```
% function [s0,is0]=f_filter_bank_ana(sig,fltana,indfltana)
% Purpose:
% Compute the subband coefficients s0 by convolving the signal sig with the
% filter coefficients fltana. Representing the input signal as x[n], for
% n=0,1,2,...,L-1 where L is the length of the signal, then we have
% x[n]=sig(n+1). The output y[f,n],for f=0,1,2,...,F-1 and
% n=0,1,2,...,L+Mf-2 where F is the number of subbands n_sb and Mf is the
% length of the filter in subband f is given by y[f,n]=s0(is0(f)+n+1),
% for f>0 and s0(n+1), for f=0.
% Synopsis:
% [s0,is0]=f_filter_bank_ana(sig,fltana,indfltana)
% input vector:
% sig: column vector of size LX1 with the coefficients of the input signal
% fltana: column vector of size F*MfX1 with the coefficients of the
% analysis filter
% bank
% indfltana: column vector of size FX1 with the index of the end of each
% filter
% output vector:
% s0: column vector of size sum(L+Mf-1) for 0<=f<=F+1 with the coefficients
% of each subband
% is0: column vector of size FX1 with the index of the end of each subband
% Example:
% load 'NFF0001_H1_70_EMG'
% [sig]=data(:,2);
% [fltana, indfltana]=gfb(32);
% [s0, is0]=f_filter_bank_ana(sig,fltana,indfltana);
% #Author: Ricardo von Borries, Cristhian Potes
% #Date:   November 13, 2007
function [s0,is0]=f_filter_bank_ana(sig,fltana,indfltana)
sig=sig(:);
down_samp=1;
indsig=length(sig);
indsig=[0;indsig];
indfltana=[0;indfltana];
lisig=length(indsig);
i0=indsig(lisig-1);
i1=indsig(lisig);
x=sig(i0+1:i1);
sig=sig(1:i0);
indsig=indsig(1:(lisig-1));
lisig=lisig-1;
for i=0:(length(indfltana)-2)
  f=conv(x,fltana((indfltana(i+1)+1):indfltana(i+2)));
  f=f(1:down_samp:length(f));
  sig=[sig;f];
  indsig=[indsig;indsig(lisig)+length(f)];
  lisig=lisig+1;
end
indsig=indsig(2:length(indsig));
is0=indsig;
s0=sig;
```

```
% function [tfr]=tsub(s0, is0, shift);
% Purpose:
% Arrange in a time subband matrix representation all the subband
% coefficients. This function assumes that all the filters have equal
% length. The time subband coefficients y[f,n] for f=0,1,2,...,F-1 and
% n=0,1,2,...,L+Mf-2 where F is the number of subbands n_sb and Mf is the
% length of the filter in subband f is given by y[f,n]=tfr(f+1,n+1.
% Synopsis:
% [tfr]=tsub(s0, is0, shift);
% input vector:
% s0: column vector of size sum(L+Mf-1) for 0<=f<=F+1 with the coefficients
% of each subband
% is0: column vector of size FX1 with the index of the end of each subband
% shift: vector of length two with the number of coefficients to remove
% from the output s0 to compensate the increase in the length of the
% subbands by the convolution operation
% output vector:
% tfr: time subband matrix representation
% Example:
% load 'NFF0001_H1_70_EMG'
% [sig]=data(:,2);
% [fltana, indfltana]=gfb(32);
% N=length(fltana)/length(indfltana);
% shift=[round(N/2),round(N/2)];
% [s0, is0]=f_filter_bank_ana(sig,fltana,indfltana);
% [tfr]=tsub(s0, is0, shift);
% #Author: Cristhian Potes
% #Date:   July 10, 2007

function [tfr]=tsub(s0, is0, shift);
s0=s0(:);
is0=is0(:);
M=length(is0);
L=is0(1);
tfr=reshape(s0,L,M)';
tfr=tfr.^2;
tfr=tfr(:,shift(1):L-shift); % Compensation of the delay
```

```
% function [fm]=inst_freq(tfr);
% Purpose:
% Compute the instantaneous frequency fm of a given signal from the time
% subband matrix representation tfr. The instantaneous frequency f[n] at
% time n=0,1,2,...,L-1 is given by f[n]=fm(n+1).
% Synopsis:
% [fm]=inst_freq(tfr);
% input vector:
% tfr: time subband matrix representation
% output vector:
% fm: column vector of size LX1 with the instantaneous frequency components
% Example:
% load 'NFF0001_H1_70_EMG'
% [sig]=data(:,2);
% [fltana, indfltana]=gfb(32);
% N=length(fltana)/length(indfltana);
% shift=[round(N/2),round(N/2)];
% [s0, is0]=f_filter_bank_ana(sig,fltana,indfltana);
% [tfr]=tsub(s0, is0, shift);
% [fm]=inst_freq(tsub);
% t=(1:length(sig))/1024; fm=fm*1024; plot(t, fm);
% axis([1 max(t) 0 511]); grid on;
% xlabel('Time[s]', 'interpreter', 'latex');
% ylabel('Frequency[Hz]', 'interpreter', 'latex');
% #Author: Cristhian Potes
% #Date:   Mayo 22, 2007

function [fm]=inst_freq(tfr);
[N,M]=size(tfr);
freqs=(0:N-1)*1/(2*N);
E=sum(tfr);
fm=(freqs*tfr)./E;
fm=fm(:);
```

```
% function [i_amp]=inst_amp(tfr);
% Purpose:
% Compute the instantaneous amplitude i_amp of a given signal from the
% time subband matrix representation tfr. The instantaneous amplitude ia[n]
% at time n=0,1,2,...,L-1 is given by ia[n]=i_amp(n+1).
% Synopsis:
% [i_amp]=inst_amp(tfr);
% input vector:
% tfr: time subband matrix representation of size FXL
% output vector:
% i_amp: column vector of size LX1 with the instantaneous amplitude
% components
% Example:
% load 'NFF0001_H1_70_EMG'
% [sig]=data(:,2);
% [fltana, indfltana]=gfb(32);
% N=length(fltana)/length(indfltana);
% shift=[round(N/2),round(N/2)];
% [s0, is0]=f_filter_bank_ana(sig,fltana,indfltana);
% [tfr]=tsub(s0, is0, shift);
% [i_amp]=inst_amp(tsub);
% t=(1:length(sig))/1024;  plot(t, i_amp);
% axis([1 max(t) 0 max(i_amp)]); grid on;
% xlabel('Time[s]', 'interpreter', 'latex');
% ylabel('Amplitude', 'interpreter', 'latex');
% #Author: Cristhian Potes
% #Date:   Mayo 25, 2007

function [i_amp]=inst_amp(tfr);
ws=1;
ss=1;
[N,M]=size(tfr);
ia=zeros(M,1);
i_amp=ia;
for i=1:N
    nc=ceil(2*N/ss);
    ss=ss+1;
    [is, ie]=windowing(nc,M,ws,0);
    ana_sig=tfr(i,:);
    for j=1:length(is)
ww=abs(ana_sig(is(j):ie(j)));
ia(is(j))=max(ww);
    end
    ia=ia(:);
    i_amp=i_amp+ia;
    ia=zeros(M,1);
end
i_amp=sqrt(i_amp);
```

```
% function [index_start, index_end]=windowing(nc, L, ,shift, option)
% Purpose:
% Compute the start and end indexes of the location of a rectangular window
% for a specified shift amount. This function is useful when we want to apply
% a rectangular window to a signal of length L
% Synopsis:
% [index_start, index_end]=windowing(nc, L, shift, option); %option default = 1;
% [index_start, index_end]=windowing(nc, L, shift); %shift default =1
% [index_start, index_end]=windowing(nc, L);
% input vector:
% nc: size of the rectangular window, for 1<=nc<=L
% L: length of the signal
% option: if 1 -> (index_end-index_start) is always nc. The rectangular
%   window is not zero padded at the end of the signal
%         if 0 -> (index_end-index_start) is not always nc. The rectangular
%   window is zero padded at the end of the signal
% shift: shifted window, for 1<=shift<=nc;
% output vector:
% index_start: column vector with the start indexes;
% index_end: column vector with the end indexes;
% Example:
% % Let us suppose that we want to apply a rectangular window of 5 points with
% a shift of  3 to a signal of length 15
% nc=5; L=15; shift=3;
% when option=1
% option=1;
% [index_start,index_end]=windowing(nc, L, option, shift)
% when option=0
% option=0;
% [index_start,index_end]=windowing(nc, L, option, shift)
% #Author: Cristhian Potes
% #Date:   Feb 16, 2007

function [index_start, index_end]=windowing(nc, L, shift, option)

if nargin==3
option=1;
end
if nargin==2
shift=nc;
option=1;
end

if nc>L
disp('Length of the rectangular window nc has to be 1<=nc<=L');
end
if shift>nc | shift==0
disp('Shift of the window has to be 1<=shift<=nc');
end

index_start=1:shift:L;
index_end=nc:shift:L;
dif=abs(length(index_end)-length(index_start));
if dif ~=0
```

```
    index_end=[index_end, ones(1, dif).*L];
end
if option ==1
c=find(index_end-index_start+1==nc);
index_start=index_start(c);
index_end=index_end(c);
end
index_start=index_start(:);
index_end=index_end(:);
```

```
% function [p]=linear_regression(s, Fs, ns, shift)
% Purpose:
% Estimate the slopes (a_i) and points of interception (b_i) of a piecewise
% approximation a_i*t+b_i, for the time interval t_i0<=t<=t_i1 of the input
% data.
% Synopsis:
% [p]=linear_regression(s, Fs, ns, shift); shift default=1;
% [p]=linear_regression(s, Fs, ns);
% input vector:
% s:input data
% Fs: sampling frequency
% ns: size of the interval t_i0<=t<=t_i1
% shift: shifted window, for 1<=shift<=length(s); The intervals of the linear
% approximation may overlap
% output vector:
% p: matrix where the first column corresponds to the slopes and the second
% column to the points of interception
% Example:
% load lt_splenius to compute the instantaneous frequency slopes
% s=fm; % the instantaneous frequency fm is the output of the function inst_freq.m
% Fs=1024;
% ns=60*1024; %1 sec = 1024 samples; then 60*1024 = 1 minute
% shift=1024; %shift every minute
% [p]=linear_regression(s, Fs, ns, shift);
% t=round(int_time/2)+(0:size(p,1)-1)*shift;
% t=t./(60*1024);
% plot(t, p(:,1),'r.','MarkerSize',15); grid on
% xlabel('Time[min]','interpreter', 'latex', 'fontweight', 'bold',...
% 'fontsize', 11);
% ylabel('Slope(Hz/min)', 'interpreter', 'latex', 'fontweight', 'bold',...
% 'fontsize', 11);
% #Author: Cristhian Potes
% #Date:   Aug 31, 2007

function [p]=linear_regression(s, Fs, ns, shift)

if nargin==3
shift=ns;
end
s = s(:);
N = length(s);
time=(1:N)./Fs; time=time(:);
[n, m]=windowing(ns, N, shift);

for i = 1:length(n)
x = s(n(i):m(i));
t = time(n(i):m(i));
p(i,:) = polyfit(t, x, 1);
end
```

```
% function [increase_force, recovery, decrease_force, fatigue]=
% jasa_analysis(s_inst_amp, s_inst_freq)
% Purpose:
% computes a joint analysis of the spectrum and the amplitude of the
% electromyography signals (JASA)from the instantaneous frequency  and the
% instantaneous amplitude slopes to compute indexes of muscle increase force,
% recovery, muscle decrease force and fatigue.
% Synopsis:
% [increase_force, recovery, decrease_force, fatigue]=
% jasa_analysis(s_inst_amp, s_inst_freq)
% input vector:
% s_inst_amp: instantaneous amplitude slopes
% s_inst_freq: instantaneous frequency slopes
% output vector:
% if: index corresponding to the energy of muscle increase force
% r: index corresponding to the energy of recovery
% df: index corresponding to the energy of muscle decrease force
% f: index corresponding to the energy of fatigue
% Example:
% load lt_splenius to compute the instantaneous frequency and the
% instantaneous amplitude slopes
% Fs=1024;
% sample_interval=60*1024; %1 sec = 1024 samples; then 60*1024 = 1 minute
% shift=1024; %shift every minute
% [p]=linear_regression(fm, Fs, sample_interval, shift); lr_fm=p(:,1);
% [p]=linear_regression(i_amp, Fs, sample_interval, shift); lr_inst_am[=p(:,1);
% [increase_force, recovery, decrease_force, fatigue] =
% jasa_analysis(lr_inst_amp, lr_fm)
% #Author: Cristhian Potes
% #Date:   Nov 13, 2007
% #Date modified: March 10, 2008

function [increase_force, recovery, decrease_force, fatigue]=...
    jasa_analysis(s_inst_amp, s_inst_freq)

if length(s_inst_freq)>0 & length(s_inst_amp)>0
if_ia=find(s_inst_amp>0);
increase_force_ia=s_inst_amp(if_ia);
increase_force_if=s_inst_freq(if_ia);
if_if=find(increase_force_if>0);
increase_force_if=increase_force_if(if_if);
increase_force_ia=increase_force_ia(if_if);
increase_force=increase_force_ia.^2+increase_force_if.^2;
increase_force=sum(increase_force);

if_ia=find(s_inst_amp<0);
recovery_ia=s_inst_amp(if_ia);
recovery_if=s_inst_freq(if_ia);
if_if=find(recovery_if>0);
recovery_if=recovery_if(if_if);
recovery_ia=recovery_ia(if_if);
recovery=recovery_ia.^2+recovery_if.^2;
recovery=sum(recovery);
```

```
if_ia=find(s_inst_amp<0);
decrease_force_ia=s_inst_amp(if_ia);
decrease_force_if=s_inst_freq(if_ia);
if_if=find(decrease_force_if<0);
decrease_force_if=decrease_force_if(if_if);
decrease_force_ia=decrease_force_ia(if_if);
decrease_force=decrease_force_ia.^2+decrease_force_if.^2;
decrease_force=sum(decrease_force);

if_ia=find(s_inst_amp>0);
fatigue_ia=s_inst_amp(if_ia);
fatigue_if=s_inst_freq(if_ia);
if_if=find(fatigue_if<0);
fatigue_if=fatigue_if(if_if);
fatigue_ia=fatigue_ia(if_if);
fatigue=fatigue_ia.^2+fatigue_if.^2;
fatigue=sum(fatigue);

else
increase_force=0;
recovery=0;
decrease_force=0;
fatigue=0;
end
```